Biorthonormal Expansion Formulas for Signal Spaces Composed of Fluency Functions and Their Applications

March 1994

Mamoru IWAKI

Biorthonormal Expansion Formulas for Signal Spaces Composed of Fluency Functions and Their Applications

(フルーエンシ関数から成る信号空間における双直交展開とその応用)

by

Mamoru IWAKI, B.E., M.E.

Dissertation

Presented to

the Doctoral Program in Engineering

University of Tsukuba Graduate School

In Partial Fulfillment

of the Requirement

for the Degree of

Doctor of Engineering

University of Tsukuba

March 1994

Table of Contents

List of Figures

List of Tables

Part I

Introduction

Electric circuits, which are considered as a typical example of a conventional signal processing model, are composed of inductors, capacitors, and resistors. Each component corresponds to a differential operator, integral operator, and multiplication, respectively. The conventional mathematical model for signal processing has been based on these operators. This means that conventional signal processing is characterized by exponential functions which are the eigenfunctions of differential operator and integral operator. This is why exponential functions have been used for representation of signals, and the conventional mathematical model for digital signal processing consists of a differential operator, integral operator, and multiplication in band-limited signal space. In band-limited signal space, the mutual relation between continuous time signal and discrete time signal is expressed by the sampling theorem of Whittaker[101]-Someya[102]- Shannon[103]. This theorem is an orthonormal expansion formula using sinc function, and the expansion coefficients are identical to the sample values of signals.

Since band-limited signals are continuously differentiable at any time, their waveforms can be determined in all domains by using only a function value and all higher derivatives at one point. However, in general, signals in nature do not satisfy those conditions, then band-limited signal space is not always suited for the modeling of signals.

Modeling of signals by finite times continuously differentiable functions was studied in the Wisdom Systems Laboratory, of which the author is a member. The functions of n-times continuously differentiable, and not $(n+1)$-times, has been considered as an approach to the problem. Suppose that those functions belonging to the above class are

named D^n, then the convolution of two functions $a \in D^n$ and $b \in D^m$ becomes a function in D^{n+m}:

$$c(t) = \int_{-\infty}^{\infty} a(\tau)b(t-\tau)d\tau.$$

And functions in D^n, $(n = -1, 0, 1, 2, \cdots)$ are systematically generated by repeating the convolution operation with starting from a function in D^{-1} of discontinuous functions. It has been decided to call these *fluency functions*. They are not rational functions. The non-rational property makes it possible to approximate some non-rational functions well. This is one of approaches to provide effective methods for the analysis of some complex systems with non-rational transfer functions. When D^{-1} is stepwise functions, the generated functions become piecewise polynomials with finite times continuous differentiability [105]. In this case, the generated functions are identical with spline functions. Members of the Wisdom Systems Laboratory have derived a sampling basis for spline function spaces to characterize them[111, 112, 114]. Signal spaces composed of spline functions generalize band-limited signal space because band-limited signals can be represented by spline functions when convolution is performed infinitely [116]. So the most suitable signal space for the purpose can be picked out from those flexible signal spaces. Members of the Wisdom Systems Laboratory have also derived an orthonormal basis to characterize operators[113, 115]. This corresponds to the exponential functions in band-limited signal space. The operator whose eigenfunctions are the exponential functions is a difference operator. Integral operation has the role of increasing the degree of functions.

The aim of the present dissertation is to characterize fluency signal spaces which connect the signal space of stepwise functions with Fourier's band limited signal space by a sampling theorem, and apply them to the flexible signal processing and analysis of complex systems. With this aim, the present thesis deals with the theoretical analysis of signal spaces composed of fluency functions, especially spline functions, in the aspect of sampling formulas and experimental investigation applying the theoretical results to real fields.

The theoretical analysis is composed of four kinds of discussion. The first is derivation and analysis of the sampling theorem for periodic spline signal spaces. The class of spline functions is limited to the finite closed domain with periodic condition. One of the spline functions is a quadratic one, quadratic spline function being the least degree to retain smoothness. Then the class of periodic spline functions is extended to arbitrary degrees to generalize Cahn's sampling theorem. The derived sampling theorem is identical with Cahn's sampling theorem when the degree tends to infinity.

The second aspect of the theoretical analysis is the derivation and analysis of the sampling theorem for non-periodic spline signal spaces. The class of spline functions is limited to the infinite open domain. The degree of spline functions is arbitrary. The derived sampling theorem is identical with Whittaker-Someya-Shannon's sampling theorem when the degree tends to infinity.

The third aspect of the theoretical discussion consists of the derivation of the reproducing kernel for spline functions. The class of spline functions is limited to the infinite

open domain.

The fourth aspect of the theoretical analysis proposes the real-time approximation method and its numerical analysis. The class of spline functions is limited to the infinite open domain.

Experimental investigation is composed of an immediate spline approximation method and FIR filter design method.

In Chapter 1, a sampling theorem for the quadratic spline signal space in the finite closed domain is derived and analyzed[118]. The impulse and frequency responses are derived to characterize quadratic spline approximation for a finite closed domain. It is clarified that quadratic spline approximation has strong locality in the time domain.

In Chapter 2, a sampling theorem for spline signal space of arbitrary degree in the finite closed domain is derived and analyzed[1] in a manner similar to that in Chapter 1. The degree of spline functions are extended to arbitrary degree to generalize Cahn's sampling theorem.

In Chapter 3, a problem of the generalization of bandlimited signal space and the signal space of stepwise functions is accomplished by deriving the sampling theorem for spline signal space of arbitrary degree in the infinite open domain[5]. It is proven that the spline signal space is identical with the space of stepwise functions when the degree is zero, and that it converges to the bandlimited signal space when the degree tends to infinity. The derived sampling theorem is considered to be a generalization of Whittaker-Someya-Shannon's sampling theorem.

In Chapter 4, the reproducing kernel for spline signal space is derived. The reproducing kernel is considered to be delta function with some continuous differentiability in spline signal space. The uniform convergence of spline approximation is easily proven by using the reproducing kernel.

In Chapter 5, the real-time spline approximation with biorthonormal expansion formula is derived. The approximation error is estimated in the practical use of spline approximation for digital signal processing. An example of the real-time approximation shows the effectiveness of the approximation method for the implementation of flexible signal processing with spline functions.

In Chapter 6, a design technique of linear phase FIR filters using spline functions is presented. The filters are represented by C-spline functions. The method is based on Remez exchange method to approximate frequency characteristics in the sense of equi-ripple error.

In Chapter 7, computational complexity of polynomial interpolation for Remez exchange method is evaluated[4, 9]. The Remez exchange method is widely utilized to design digital filters in the sense of equi-ripple approximation. For the Remez exchange method, Newton's polynomial interpolation is two times faster than the conventional polynomial interpolation.

Finally, scientific and technical points derived from the theoretical considerations in Chapter 1 through 4 and the applications in Chapter 5 through 7 are summarized . Problems beyond the scope of the present study are also pointed out.

Part II

Biorthonormal Expansion Formulas for Periodic Fluency Signal Spaces

In Part II, the sampling theorem for periodic spline signal spaces is completed by deriving biorthonormal expansion formula. The class of spline functions are limited to the finite closed domain with periodic condition.

In Chapter 1, a sampling theorem for the quadratic spline signal space in the finite closed domain is completed by deriving biorthonormal expansion formulas. The impulse and frequency responses are derived to characterize quadratic spline approximation for the finite closed domain. It is clarified that quadratic spline approximation has strong locality in the time domain.

Next, in Chapter 2, the class of periodic spline functions is extended to arbitrary degree. The sampling theorem for spline signal space of arbitrary degree in the finite closed domain is completed in the similar manner in Chapter 1. It is identical with the Cahn's sampling theorem [104] when the degree tends to infinity, and the sampling theorem fir the space of staircase functions when the degree is zero.

Chapter 1

Biorthonormal Expansion Formula for Quadratic Spline Signal Space in Finite Closed Domain

1.1 Introduction

In this chapter, we shall complete a Fourier-like expansion formula in the signal space composed of spline functions, with the sample value sequence of the signal as the expansion coefficients, where the domain is a finite closed interval and the boundary condition is periodic. It is empirically known that quadratic spline functions achieve short as well as smooth interpolation. We shall adopt the quadratic ones in this chapter.

One of the signal representations, which is useful for signal processing, is the Fourier-like expansion formula with the sample value sequence as the expansion coefficients[122]. This expansion formula is composed of the pair of the following formulas.

(i) The representation of the signal in the form of linear combination of the sampling basis with the sample value sequence of the signal as the coefficients.

(ii) The integral transform expression to obtain the sample value sequence, which is the expansion coefficients, from the signal.

In the spline signal space, the sampling basis has already derived [112]. However the sampling basis is not a system of orthonormal functions. Then, he Fourier-like expansion formula with the sample value sequence as the expansion coefficient is not complete. In order to derive the complete expansion formula, the integral kernel to specify the integral transform expression must newly be derived.

In this chapter, we shall derive the integral kernel of the integral transform which obtain sample values from periodic quadratic spline functions on the finite closed domain, and complete a sampling theorem for the signal space spanned by periodic quadratic spline functions with equidistantly spaced knots.

This expression formula is the simplest signal representation, providing the basis for utilizing the periodic quadratic spline signal space in the signal processing.

1.2 Preliminaries

This section prepares the signal space composed of the periodic quadratic spline functions which is the object of the analysis in this paper.

In general, the signal waveform, which is actually handled as the object of signal processing, is considered to be defined on a finite observation interval. The energy is assumed as finite. Let the observation interval be $[0, T]$, the set of all such signals can be considered as a typical Hilbert space[111]

$$L_2[0,T] = \left\{ u \middle| \int_0^T |u(t)|^2 dt < +\infty \right\}$$

with the inner product

$$(u,v) = \frac{1}{T}\int_0^T u(t)\overline{v(t)}dt$$

Based on this formulation, the signal space composed of periodic quadratic spline functions[108] shall be considered in this paper as a subspace of above $L_2[0,T]$. This signal space is called the periodic quadratic spline signal space, and is written as ${}^3S_N$. It is defined as[108]

$${}^3S_N \triangleq \left[{}^3_{[B]}\psi_k^N\right]_{k=0}^{N-1}$$

using the system of periodic quadratic B-spline functions

$${}^3_{[B]}\psi_k^N(t) \triangleq \frac{1}{N}\sum_{p=-\infty}^{\infty}\left\{\frac{\sin \pi p/N}{\pi p/N}\right\}^3 e^{j2\pi p(t/T-k/N)}, \quad k=0,1,\cdots,N-1 \tag{1.1}$$

as the basis.

The periodic quadratic B-spline function is the piecewise polynomial give by

$$\begin{aligned} {}^3_{[B]}\psi_k^N &= 3h^{-2}\sum_{p=-\infty}^{\infty}\sum_{r=0}^{3}(t-((r+k-3/2)/N+p)T)_+^2\frac{(-1)^r}{r!(3-r)!}, \\ (t-a)_+^2 &\triangleq \begin{cases} (t-a)^2, & t>a \\ 0, & t\le a \end{cases} \end{aligned}$$

where h is the interval ($h = T/N$) between knots. The system of functions $\left\{{}^3_{[B]}\psi_k^N\right\}_{k=0}^{N-1}$ is called the periodic quadratic B-spline function. Figure 1.1 shows an example of the functions composed of the periodic quadratic B-spline function.

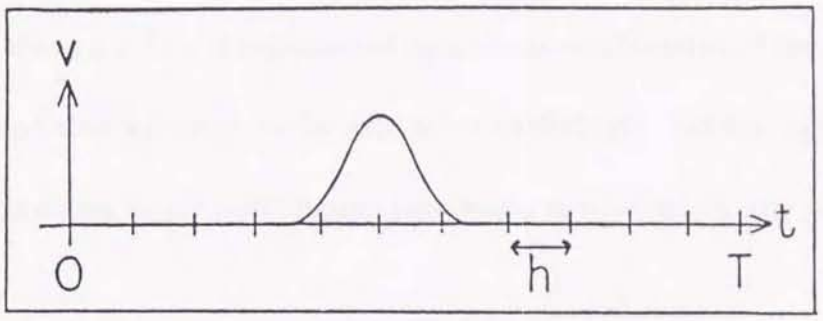

Figure 1.1: An example of periodic quadratic B-spline function $\left(v = {}^{3}_{[B]}\psi^{11}_{5}(t)\right)$.

The coordinate system ${}^{3}\varphi_{[B]}$ defined as follows is introduced in ${}^{3}S_N$. The set of all vectors, composed of the expansion coefficients of $s \in {}^{3}S_N$ by the periodic quadratic B-spline basis

$$ {}^{3}K_{[B]} \triangleq \left\{ \boldsymbol{\lambda} \middle| \boldsymbol{\lambda} = {}^{t}[\lambda_0, \lambda_1, \cdots, \lambda_{N-1}], \quad s = \sum_{k=0}^{N-1} \lambda_k {}^{3}_{[B]}\psi^{N}_{k}, \quad s \in {}^{3}S_N \right\} $$

forms the N dimensional Hilbert space with the inner product

$$ (\boldsymbol{\lambda}, \boldsymbol{\mu}) \triangleq \frac{1}{N} \sum_{k=0}^{N-1} \lambda_k \overline{\mu_k}. $$

Then, the coordinate system ${}^{3}\varphi_{[B]}$ is defined as the mapping to derive the expansion coefficient vector $\boldsymbol{\lambda}$ from an arbitrary $s \in {}^{3}S_N$. The coordinate system ${}^{3}\varphi_{[B]}$ is a bijection, with the domain ${}^{3}S_N$ and the range and the range ${}^{3}K_{[B]}$.

This section constructed the periodic quadratic spline signal space ${}^{3}S_N$.

1.3 Formulation

This section formulates the Fourier-like expansion formula to be derived in this paper.

When there exists a sampling basis in the periodic quadratic spline signal space ${}^3S_N$, any signal waveform $s \in {}^3S_N$ is represented by a linear combination of the sampling basis with the sample value sequence as the expansion coefficients. Let the sampling basis be $\left\{ {}^3_{[S]}\psi_k^N \right\}_{k=0}^{N-1}$, the above linear combination expression is written, for any signal waveform $s \in {}^3S_N$, as

$$s = \sum_{k=0}^{N-1} \mu_k {}^3_{[S]}\psi_k^N, \quad \mu_k = s(t_k), \quad t_k = kh. \tag{1.2}$$

The sampling basis has the feature that the result of interpolation is directly given by the linear combination expression, using the given sample value sequence as the coefficients. This means that sampling basis represents the impulse response of the data interpolation operator. If there exists a sampling basis in the signal space, it is unique.

The linear combination expression of the sampling basis is to construct the signal waveform, under the premises that the sample value sequence as the expansion coefficients has already given. The inverse operation is to derive the sample value sequence from the signal waveform. This operation has been considered as a technical problem in A-D conversion circuits such as sample-and-hold. Consequently, no formula has been derived for this operation. If, however, there is no formula to derive the sample value sequence from the signal waveform, the isomorphism between the signal waveform and the sample value sequence can not be discussed.

From such a viewpoint, a fundamental equation is needed, which represents the correspondence between the continuous time signal and the sample value sequence. Representing this fundamental equation is the form of the integral equation, as in the case of the Fourier series expansion of the function, it is given

$$\begin{aligned} \mu_k &= \left(s, {}^{3}_{[S^{\bullet}]}\psi^{N}_{k}\right) \\ &= \frac{1}{T}\int_0^T s(t)\overline{{}^{3}_{[S^{\bullet}]}\psi^{N}_{k}}dt, \quad \mu_k = s(t_k), \\ & \quad k = 0, 1, \cdots, N-1. \end{aligned} \tag{1.3}$$

This integral kernel is determined when its integral kernel $\left\{{}^{3}_{[S^{\bullet}]}\psi^{N}_{k}\right\}_{k=0}^{N-1}$ is determined. If this integral kernel is an element of the signal space ${}^{3}S_N$, the integral kernel is called the biorthonormal basis for the sampling basis[122, 123]. Thus, the biorthonormal basis is the characterization of the sampling operation, which derives the sample value sequence from the signal, as the impulse response.

Consider

(i) The linear combination expression of the sampling basis, which derives the signal waveform from the sampled value sequence, and

(ii) The integral transform expression, which derives the sample value sequence as the inner product of the signal waveform and the biorthonormal basis.

They form the Fourier-like expansion formula with the sample value sequence as the expansion coefficients[122, 123]. Especially, when a signal waveform u is given, which

does not belong to the signal space ${}^3S_N$, the signal s obtained by

$$\begin{aligned} \mu_k &= \left(u, {}^3_{[S\bullet]}\psi^N_k\right) \\ s &= \sum_{k=0}^{N-1} \mu_k {}^3_{[S]}\psi^N_k \end{aligned}$$

has the engineering implication that it is the least-square approximation of u in ${}^3S_N$[123].

This section formulated the Fourier-like expansion formula to be derived in this paper. In the following, The sampling basis is derived in section 1.4. Section 1.5 derives the biorthonormal basis, concluding the derivation of the Fourier-like expansion formula.

1.4 Derivation of sampling basis

This section derives the sampling basis in the signal space ${}^3S_N$ composed of periodic quadratic spline functions. This basis characterizes the correspondence from the sampled value sequence to the signal waveform.

As the first step, the coordinate system corresponding to the sampling basis is introduced into ${}^3S_N$ for deriving the sampling basis. Let the vector composed of the sample value sequence of the signal waveform $s \in {}^3S_N$ be

$$\boldsymbol{\mu} = {}^t[\mu_0, \mu_1, \cdots, \mu_{N-1}], \quad \mu_k = s(t_k).$$

The set of all such vector $\boldsymbol{\mu}$ is written as ${}^3K_{[S]}$. Then, the coordinate system ${}^3\varphi_{[S]} : {}^3S_N \rightarrow {}^3K_{[S]}$ for the sampling basis is defined as the mapping which satisfies

$${}^3\varphi_{[S]}(s) = \boldsymbol{\mu}$$

for any $s \in {}^3S_N$.

As the next step, the coordinate transformation matrix ${}^3A$ from ${}^3\varphi_{[B]}$ to ${}^3\varphi_{[S]}$ is introduced, in order to represent the relation between ${}^3\varphi_{[B]}$ and ${}^3\varphi_{[S]}$.

As in the case of eq.(A.1) of proposition 1 in [111], it is defined as the coordinate transformation matrix from ${}^3K_{[B]}$ to ${}^3K_{[S]}$,

$$ {}^3A = {}^3\varphi_{[S]}{}^3\varphi_{[B]}{}^{-1}. $$

It is an N-th order square matrix

$$ \begin{aligned} {}^3A &= \left[{}^3\varphi_{[S]}({}^3_{[B]}\psi^N_0), {}^3\varphi_{[S]}({}^3_{[B]}\psi^N_1), \cdots, {}^3\varphi_{[S]}({}^3_{[B]}\psi^N_{N-1}) \right] \\ &= \begin{bmatrix} {}^3_{[B]}\psi^N_0(t_0) & {}^3_{[B]}\psi^N_1(t_0) & \cdots & {}^3_{[B]}\psi^N_{N-1}(t_0) \\ {}^3_{[B]}\psi^N_0(t_1) & {}^3_{[B]}\psi^N_1(t_1) & \cdots & {}^3_{[B]}\psi^N_{N-1}(t_1) \\ \vdots & \vdots & & \vdots \\ {}^3_{[B]}\psi^N_0(t_{N-1}) & {}^3_{[B]}\psi^N_1(t_{N-1}) & \cdots & {}^3_{[B]}\psi^N_{N-1}(t_{N-1}) \end{bmatrix}. \end{aligned} $$

Figure 1.2 shows the relations among ${}^3\varphi_{[B]}$, ${}^3\varphi_{[S]}$, and ${}^3A$.

The following proposition is to utilize coordinate systems ${}^3\varphi_{[B]}$, ${}^3\varphi_{[S]}$, and matrix ${}^3A$, to derive the sampling basis in the periodic quadratic spline signal space ${}^3S_N$ as a linear combination of the periodic quadratic spline basis.

Proposition 1 *The sampling basis ${}^3S_N$ in the periodic quadratic spline signal space $\left\{ {}^3_{[S]}\psi^N_k \right\}_{k=0}^{N-1}$ is given by*

$$ {}^3_{[S]}\psi^N_k = \sum_{\ell=0}^{N-1} {}^3\alpha_{|l-k|}\, {}^3_{[B]}\psi^N_\ell, \tag{1.4} $$

where the coefficients $\{{}^3\alpha_\ell\}_{\ell=0}^{N-1}$ are given by

$$ {}^3\alpha_\ell = \frac{1}{N^2} \sum_{p=0}^{N-1} \frac{1}{{}^3\xi_p} e^{j2\pi\ell p/N} $$

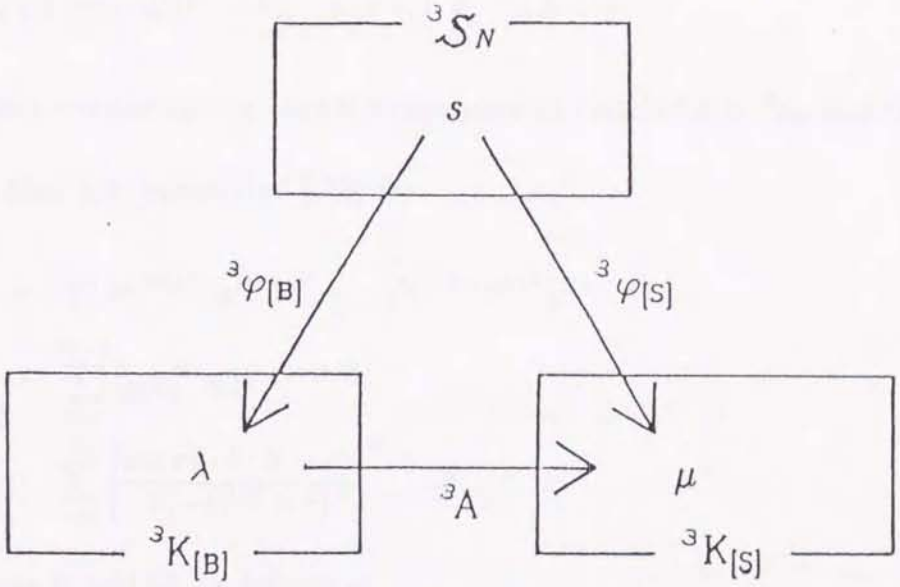

Figure 1.2: Mutual relations between ${}^3\varphi_{[B]}$, ${}^3\varphi_{[S]}$ and ${}^3A$.

$$
{}^3\xi_p = \sum_{r=-\infty}^{\infty} \left[\frac{\sin(\pi(-p/N + r))}{\pi(-p/N + r)} \right]^3 .
$$

(Proof)

From eq.(1.1), the system of B-spline functions has the invariance against the shift

$$
{}^3_{[B]}\psi^N_k(t) = {}^3_{[B]}\psi^N_0(t - kh), \quad k = 0, 1, 2, \cdots, N-1.
$$

Then, ${}^3A$ is a circular matrix. Let the eigenvalue of matrix ${}^3A$ be ${}^3\xi_k$, and the eigenvector be X_k/N, they are represented [135] as

$$
\begin{aligned}
X_k &= {}^t[1, e^{j2\pi k/N}, e^{j4\pi k/N}, \cdots, e^{j2\pi(N-1)k/N}], \\
{}^3\xi_k &= \sum_{\ell=0}^{N-1} {}^3_{[B]}\psi^N_\ell(t_0) e^{-j2\pi\ell k/N} \\
&= \sum_{-\infty}^{\infty} \left[\frac{\sin \pi(-k/N + r)}{\pi(-k/N + r)} \right]^3 .
\end{aligned}
$$

Let matrix V and ${}^3\Xi$ be defined as

$$
\begin{aligned}
V &= \frac{1}{N}[X_0, X_1, \cdots, X_{N-1}], \\
{}^3\Xi &= diag({}^3\Xi_0, {}^3\Xi_1, \cdots, {}^3\Xi_{N-1}).
\end{aligned}
$$

Then, ${}^3A$ is decomposed as

$$
{}^3A = V {}^3\Xi V^*.
$$

The eigenvalue of matrix ${}^3A$ is calculated as

$$
{}^3\Xi_k = \sum_{\ell=0}^{N-1} {}^3_{[B]}\psi^N_\ell(t_0) e^{-j2\pi\ell k/N}
$$

$$= \sum_{\ell=0}^{N-1} \frac{1}{N} \sum_{p=-\infty}^{\infty} \left[\left\{ \frac{\sin \pi p/N}{\pi p/N} \right\}^3 e^{-j2\pi p\ell/N} \right] e^{-j2\pi \ell k/N}$$
$$= \sum_{r=-\infty}^{\infty} N \left[\frac{\sin \pi(-k/N + r)}{\pi(-k/N + r)} \right]^3 .$$

Thus,

$$^3\Xi_k > 0, \quad k = 0, 1, \cdots, N-1$$

is derived. Consequently, matrix ^3A is regular.

By the definitions for the coordinate systems $^3\varphi_{[S]}$ and $^3\varphi_{[B]}$ as well as the coordinate transformation matrix ^3A

$$^3\varphi_{[S]} = {}^3A\,{}^3\varphi_{[B]}, \quad {}^3\varphi_{[S]}{}^{-1} = {}^3\varphi_{[B]}\,{}^3A^{-1}.$$

Then $^3\varphi_{[S]}$ is a bijection. Thus, there exists the sampling basis.

In the same way as in the derivation of eq.(A.5) in the proof of Proposition 1 of Ref. [111], the sampling basis $\left\{ {}^3_{[S]}\psi^N_k \right\}_{k=0}^{N-1}$ in the periodic quadratic spline signal space ^3S_N is represented as

$$ {}^3_{[S]}\psi^N_k = {}^3\varphi_{[S]}{}^{-1}(\boldsymbol{e}_k) = {}^3\varphi_{[B]}{}^{-1}\,{}^3A^{-1}\boldsymbol{e}_k. \tag{1.5}$$

Since matrix ^3A is regular, $^3A^{-1}$ is represented, using V and $^3\Xi$, as

$$^3A^{-1} = V\,{}^3\Xi^{-1}V^*.$$

Then,

$$^3A^{-1} = V\,{}^3\Xi^{-1}V^*$$

$$
\begin{aligned}
&= \frac{1}{N^2}[X_0, X_1, \cdots, X_{N-1}] \\
&\quad diag({}^3\Xi_0^{-1}, {}^3\Xi_1^{-1}, \cdots, {}^3\Xi_{N-1}^{-1}) \\
&\quad [X_0, X_1, \cdots, X_{N-1}]^* \\
&= \frac{1}{N^2}[X_0 {}^3\Xi_0^{-1}, X_1 {}^3\Xi_1^{-1}, \cdots, X_{N-1} {}^3\Xi_{N-1}^{-1}] \begin{bmatrix} X_0^* \\ X_1^* \\ \vdots \\ X_{N-1}^* \end{bmatrix} \\
&= \frac{1}{N^2}\left[\sum_{k=0}^{N-1} X_k X_k^{*3}\Xi_k^{-1}\boldsymbol{e}_0, \sum_{k=0}^{N-1} X_k X_k^{*3}\Xi_k^{-1}\boldsymbol{e}_1, \cdots, \sum_{k=0}^{N-1} X_k X_k^{*3}\Xi_k^{-1}\boldsymbol{e}_{N-1}\right].
\end{aligned}
$$

The $(\ell,\ k)$ element of ${}^3A^{-1}$ is given by

$$
\frac{1}{N^2}\sum_{p=0}^{N-1} {}^t\boldsymbol{e}_\ell(X_p X_p^{*3}\Xi_p^{-1}\boldsymbol{e}_k) = \frac{1}{N^2}\sum_{p=0}^{N-1}\frac{1}{{}^3\Xi_p}e^{j2\pi(\ell-k)p/N}.
$$

Thus ${}^3A^{-1}$ is represented by the symmetrical matrix

$$
{}^3A^{-1} = \begin{bmatrix} {}^3\alpha_0 & {}^3\alpha_1 & \cdots & {}^3\alpha_{N-1} \\ {}^3\alpha_1 & {}^3\alpha_0 & \cdots & {}^3\alpha_{N-2} \\ \vdots & \vdots & & \vdots \\ {}^3\alpha_{N-1} & {}^3\alpha_{N-2} & \cdots & {}^3\alpha_0 \end{bmatrix} \tag{1.6}
$$

with

$$
{}^3\alpha_{|\ell-k|} = \frac{1}{N^2}\sum_{p=0}^{N-1}\frac{1}{{}^3\Xi_p}e^{j2\pi(\ell-k)p/N}
$$

as the element. By substituting eq.(1.6)into eq.(1.5), eq.(1.4) is obtained. ■

Figure 1.3 shows the example of the functions ${}^3_{[S]}\psi_k^N$ composing the sampling basis.

This section derived the sampling basis in the signal space ${}^3S_N$ composed of the periodic quadratic spline functions, which constructs the linear combination expression to represent the signal waveform from the sample value sequence. The expression characterizes the

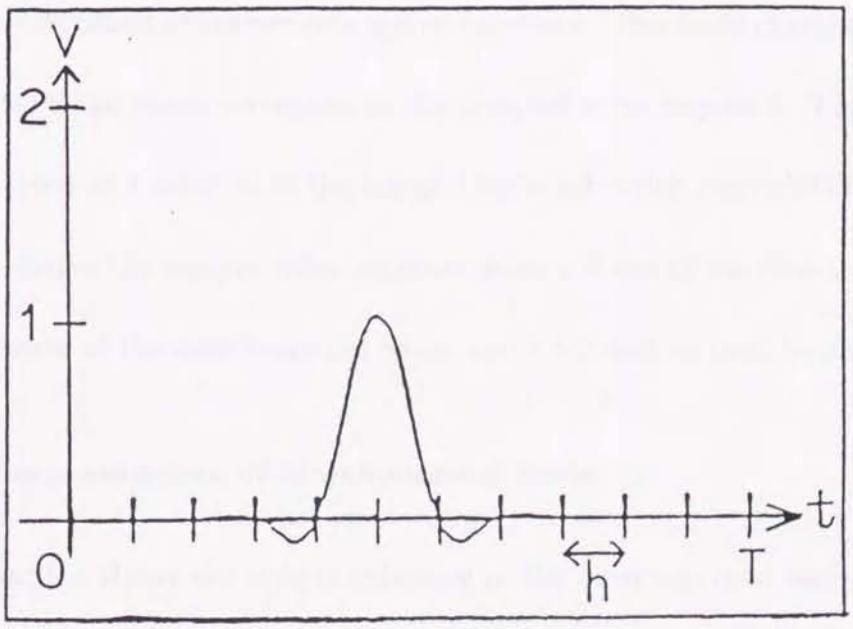

Figure 1.3: An example of functions composing the sampling basis for ${}^3S_N$ $\left(v = {}^3_{[S]}\psi^{11}_5(t)\right)$.

operation to derive the periodic quadratic spline functions that interpolate the sample value sequence. The inverse operation is to derive the sample value sequence from the given periodic quadratic spline functions. This operation is not characterized by the sampling basis. In order to characterize the both operations, the biorthonormal basis is required. This problem is discussed in the next section.

1.5 Derivation of biorthonormal basis

This section derives the biorthonormal basis corresponding to the sampling basis, in the signal space composed of the periodic spline functions. This basis characterizes the correspondence from the signal waveform to the sampled value sequence. The biorthonormal basis is obtained as a solution of the integral equation which represents the fundamental equation to derive the sample value sequence from the signal waveform. 1.5.1 shows the unique existence of the biorthonormal basis, and 1.5.2 derives the biorthonormal basis.

1.5.1 Unique existence of biorthonormal basis

This subsection shows the unique existence of the biorthonormal basis $\{{}^{3}_{[S\bullet]}\psi^{N}_{k}\}^{N-1}_{k=0}$ in ${}^{3}S_{N}$. As the first step, as a means to show the unique existence of the biorthonormal basis, a mapping ${}^{3}\varphi_{[S\bullet]}$ and a matrix ${}^{3}G$ are introduced. Then, by showing the regularity of the matrix ${}^{3}G$, the unique existence of the biorthonormal basis is shown.

A mapping ${}^{3}\varphi_{[S\bullet]}$ is introduced, which obtains the inner product of the signal s and the sampling basis $\left\{{}^{3}_{[S]}\psi^{N}_{k}\right\}^{N-1}_{k=0}$ for an arbitrary $s \in {}^{3}S_{N}$. Let the vector composed of the

inner product of the signal s and the sampling basis $\left\{ {}^{3}_{[S]}\psi^{N}_{k} \right\}_{k=0}^{N-1}$ as

$$\begin{aligned} \eta_k &= \left(s, {}^{3}_{[S]}\psi^{N}_{k} \right) \\ &= \frac{1}{T} \int_0^T s(t) \overline{{}^{3}_{[S]}\psi^{N}_{k}(t)} dt, \quad k = 0, 1, \cdots, N-1, \end{aligned}$$

where each component is written as

$$\boldsymbol{\eta} = {}^{t}[\eta_0, \eta_1, \cdots, \eta_{N-1}].$$

The set of all such vector $\boldsymbol{\eta}$ is written as ${}^{3}K_{[S\bullet]}$. Then, ${}^{3}\varphi_{[S\bullet]} : {}^{3}S_N \rightarrow {}^{3}K_{[S\bullet]}$ defined as the mapping satisfying

$${}^{3}\varphi_{[S\bullet]}(s) = \boldsymbol{\eta}$$

for any $s \in {}^{3}S_N$.

As the next step, the transformation matrix ${}^{3}G$ from ${}^{3}\varphi_{[S]}$ to ${}^{3}\varphi_{[S\bullet]}$ is introduced. It is defined as the transformation matrix from ${}^{3}K_{[S]}$ to ${}^{3}K_{[S\bullet]}$

$${}^{3}G = {}^{3}\varphi_{[S\bullet]} {}^{3}\varphi_{[S]}{}^{-1}.$$

It is an N-th order square matrix

$$\begin{aligned} {}^{3}G &= \left[{}^{s}\varphi_{[S\bullet]}({}^{3}_{[S]}\psi^{N}_{0}), {}^{3}\varphi_{[S\bullet]}({}^{3}_{[S]}\psi^{N}_{1}), \cdots, {}^{3}\varphi_{[S\bullet]}({}^{3}_{[S]}\psi^{N}_{N-1}) \right] \\ &= \begin{bmatrix} \left({}^{3}_{[S]}\psi^{N}_{0}, {}^{3}_{[S]}\psi^{N}_{0} \right) & \left({}^{3}_{[S]}\psi^{N}_{1}, {}^{3}_{[S]}\psi^{N}_{0} \right) & \cdots & \left({}^{3}_{[S]}\psi^{N}_{N-1}, {}^{3}_{[S]}\psi^{N}_{0} \right) \\ \left({}^{3}_{[S]}\psi^{N}_{0}, {}^{3}_{[S]}\psi^{N}_{1} \right) & \left({}^{3}_{[S]}\psi^{N}_{1}, {}^{3}_{[S]}\psi^{N}_{1} \right) & \cdots & \left({}^{3}_{[S]}\psi^{N}_{N-1}, {}^{3}_{[S]}\psi^{N}_{1} \right) \\ \vdots & \vdots & & \vdots \\ \left({}^{3}_{[S]}\psi^{N}_{0}, {}^{3}_{[S]}\psi^{N}_{N-1} \right) & \left({}^{3}_{[S]}\psi^{N}_{1}, {}^{3}_{[S]}\psi^{N}_{N-1} \right) & \cdots & \left({}^{3}_{[S]}\psi^{N}_{N-1}, {}^{3}_{[S]}\psi^{N}_{N-1} \right) \end{bmatrix}. \end{aligned} \tag{1.7}$$

Figure 1.4 shows the relations among ${}^{3}\varphi_{[S]}$, ${}^{3}\varphi_{[S\bullet]}$, and ${}^{3}G$.

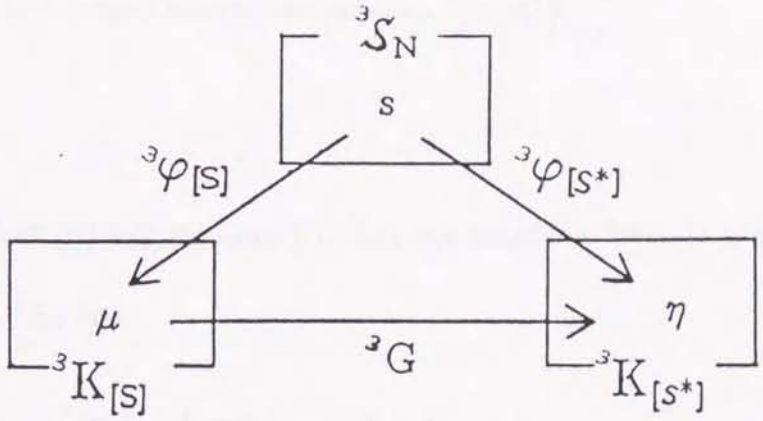

Figure 1.4: Mutual relations between ${}^3\varphi_{[S]}$, ${}^3\varphi_{[S^*]}$ and ${}^3G$.

In the following, the relations among ${}^3\varphi_{[S]}$, ${}^3\varphi_{[S^\bullet]}$, and ${}^3G$ are used to discuss the unique existence of the biorthonormal basis. The following lemma gives the relation between the mapping ${}^3\varphi_{[S^\bullet]}$ and the unique existence of the biorthonormal basis.

Lemma 1 *The following two conditions are equivalent.*

(i) *The mapping* ${}^3\varphi_{[S^\bullet]}$ *is a bijection.*

(ii) *There exists unique biorthonormal basis* $\left\{{}^3_{[S^\bullet]}\psi^N_k\right\}_{k=0}^{N-1}$.

(Proof)

It is shown first (ii) follows from (i). Let the mapping ${}^3\varphi_{[S^\bullet]}$ is a bijection. Define the function $u_k \in {}^3S_N$ by

$$u_k = {}^3\varphi_{[S^\bullet]}{}^{-1}(\boldsymbol{e}_k), \quad k = 0, 1, \cdots, N-1$$

where $\boldsymbol{e}_k$ is a vector with the k-th components being 1 and others being zero. Then, function u_k satisfies the following relation for any signal $s \in {}^3S_N$

$$\begin{aligned}
(s, u_k) &= \left(\sum_{\ell=0}^{N-1} \mu_\ell {}^3_{[S]}\psi^N_\ell, {}^3\varphi_{[S^\bullet]}{}^{-1}(\boldsymbol{e}_k)\right) \\
&= \sum_{\ell=0}^{N-1} \mu_\ell \left({}^3_{[S]}\psi^N_\ell, {}^3\varphi_{[S^\bullet]}{}^{-1}(\boldsymbol{e}_k)\right) \\
&= \sum_{\ell=0}^{N-1} \mu_\ell \overline{\left({}^3\varphi_{[S^\bullet]}{}^{-1}(\boldsymbol{e}_k), {}^3_{[S]}\psi^N_\ell\right)} \\
&= \sum_{\ell=0}^{N-1} \mu_\ell \overline{{\boldsymbol{e}_\ell}^t \left({}^3\varphi_{[S^\bullet]}{}^3\varphi_{[S^\bullet]}{}^{-1}(\boldsymbol{e}_k)\right)} \\
&= \sum_{\ell=0}^{N-1} \mu_\ell \overline{\delta_{k\ell}}
\end{aligned}$$

$$= \sum_{\ell=0}^{N-1} \mu_\ell \delta_{k\ell}$$

$$= \mu_k, \quad k = 0, 1, 2, \cdots, N-1.$$

Consequently, it is the function in ${}^3S_N$ satisfying the condition for the biorthonormal basis. The symbol $\delta_{k\ell}$ is Kronecker's delta.

Assume that a function $v_k \in {}^3S_N$ which is different from u_k also satisfies the condition of the biorthonormal basis. Then, by the definition, functions u_k and v_k satisfy

$$(s, u_k) = u(t_k),$$

$$(s, v_k) = u(t_k), \quad k = 0, 1, \cdots, N-1$$

for any $s \in {}^3S_N$. Consequently,

$$\begin{aligned}(s, v_k - u_k) &= (s, v_k) - (s, u_k) \\ &= u(t_k) - u(t_k) \\ &= 0\end{aligned}$$

and

$$v_k = u_k, \quad k = 0, 1, \cdots, N-1.$$

Thus, there exists the unique biorthonormal basis.

Next, it is shown that (i) follows from (ii). Assume that there exists unique biorthonormal basis. By definition, the mapping ${}^3\varphi_{[S^\bullet]}$ is a bijection. By assumption, any signal $s \in {}^3S_N$ can be represented in the form

$$s = \sum_{k=0}^{N-1} \mu_{k\,{}^3_{[S]}} \psi_k^N,$$

$$\mu_k \;=\; \left(s, {}^3_{[S\bullet]}\psi^N_k\right), \quad k = 0, 1, \cdots, N-1.$$

Consequently, for the signals $s1, s2 \in {}^3S_N$ satisfying the relation

$${}^3\varphi_{[S\bullet]}(s1) = {}^3\varphi_{[S\bullet]}(s2),$$

there must hold

$$\left(\sum_{k=0}^{N-1}\left(s1, {}^3_{[S\bullet]}\psi^N_k\right){}^3_{[S]}\psi^N_k, {}^3_{[S]}\psi^N_\ell\right) = \left(\sum_{k=0}^{N-1}\left(s2, {}^3_{[S\bullet]}\psi^N_k\right){}^3_{[S]}\psi^N_k, {}^3_{[S]}\psi^N_\ell\right)$$

$$\sum_{k=0}^{N-1}\left(s1 - s2, {}^3_{[S\bullet]}\psi^N_k\right)\left({}^3_{[S]}\psi^N_k, {}^3_{[S]}\psi^N_\ell\right) = 0, \quad \ell = 0, 1, \cdots, N-1.$$

Since functions ${}^3_{[S\bullet]}\psi^N_k$, $(k = 0, 1, 2, \cdots, N-1)$ are not identically zero, there holds

$$s1 = s2.$$

Consequently, ${}^3\varphi_{[S\bullet]}$ is a bijection.

Therefore, Lemma 1 holds good. ■

By Lemma 1, there exists unique biorthonormal basis if and only if ${}^3\varphi_{[S\bullet]}$ is a bijection.

The following lemma indicates the relation between ${}^3\varphi_{[S\bullet]}$ and ${}^3G$.

Lemma 2 *The following two conditions are equivalent.*

(i) *The mapping* ${}^3\varphi_{[S\bullet]}$ *is a bijection.*

(ii) *The matrix* ${}^3G$ *is regular.*

(Proof)

It is shown first (ii) follows from (i). By the definitions of mapping ${}^3\varphi_{[S\bullet]}$ and matrix ${}^3G$, ${}^3G$ and ${}^3G^{-1}$ are represented as

$$ {}^3G = {}^3\varphi_{[S^\bullet]}{}^3\varphi_{[S]}{}^{-1}, \quad {}^3G^{-1} = {}^3\varphi_{[S]}{}^3\varphi_{[S^\bullet]}{}^{-1}, $$

respectively. Since mapping ${}^3\varphi_{[S]}$ is a bijection, ${}^3G$ is regular if ${}^3\varphi_{[S^\bullet]}$ is a bijection.

Next, it is shown that (i) follows from (ii). By the definition of mapping ${}^3\varphi_{[S^\bullet]}$ and matrix ${}^3G$, ${}^3\varphi_{[S^\bullet]}$ and ${}^3\varphi_{[S^\bullet]}{}^{-1}$ are , respectively, as

$$ {}^3\varphi_{[S^\bullet]} = {}^3G{}^3\varphi_{[S]}, \quad {}^3\varphi_{[S^\bullet]}{}^{-1} = {}^3\varphi_{[S]}{}^{-1}{}^3G^{-1}. $$

Since ${}^3\varphi_{[S]}$ is a bijection, ${}^3\varphi_{[S^\bullet]}$ is a bijection if ${}^3G$ is regular.

Therefore, Lemma 2 holds good. ■

By Lemma 2, the bijection property of ${}^3\varphi_{[S^\bullet]}$ and the regularity of ${}^3G$ are equivalent. The following property indicates the relation between the unique existence of the biorthonormal basis and the regularity of ${}^3G$.

Proposition 2 *The following two conditions are equivalent.*

(i) *The matrix* ${}^3G$ *is regular.*

(ii) *There exists the unique biorthonormal basis* $\left\{ {}^3_{[S^\bullet]}\psi_k^N \right\}_{k=0}^{N-1}$.

(Proof)

By Lemma 1 and Lemma 2, the regularity of ${}^3G$ and the unique existence of the biorthonormal basis are equivalent.

Therefore Proposition 2 holds good. ■

By Proposition 2, the biorthonormal basis uniquely exists if and only if ${}^3G$ is regular. The following lemma indicates the regularity of ${}^3G$.

Lemma 3 *The matrix* ${}^3G$ *is regular.*

(Proof)

As it seen from eq.(1.4), the sampling basis has the invariance against the shift.

$$ {}^3_{[S]}\psi^N_k(t) = {}^3_{[S]}\psi^N_0(t-kh), \quad k = 0,1,2,\cdots,N-1 $$

Then, the matrix ${}^3G$ represented by eq.(1.7) is a circular matrix. Consequently, the eigenvalue ${}^3\theta_k$ of ${}^3G$ is given [135] by

$$ {}^3\theta_k = \sum_{\ell=0}^{N-1} \left({}^3_{[S]}\psi^N_\ell, {}^3_{[S]}\psi^N_0 \right) e^{-j2\pi\ell k/N}, \quad k = 0,1,\cdots,N-1. $$

The inner product in the right-hand side of the above expression is calculated as

$$ \begin{aligned} \left({}^3_{[S]}\psi^N_\ell, {}^3_{[S]}\psi^N_0 \right) &= \left(\sum_{p=0}^{N-1} {}^3\alpha_{|p-\ell|} {}^3_{[B]}\psi^N_p, \sum_{q=0}^{N-1} {}^3\alpha_{|q|} {}^3_{[B]}\psi^N_q \right) \\ &= \sum_{p=0}^{N-1}\sum_{q=0}^{N-1} {}^3\alpha_{|p-\ell|} {}^3\alpha_{|q|} \left({}^3_{[B]}\psi^N_p, {}^3_{[B]}\psi^N_q \right). \end{aligned} $$

Consequently, the eigenvalue ${}^3\theta_k$ is given by

$$ \begin{aligned} {}^3\theta_k &= \sum_{\ell=0}^{N-1} \left\{ \sum_{p=0}^{N-1}\sum_{q=0}^{N-1} {}^3\alpha_{|p-l|} {}^3\alpha_{|q|} \left({}^3_{[B]}\psi^N_p, {}^3_{[B]}\psi^N_q \right) e^{-j2\pi\ell k/N} \right\} \\ &= \sum_{p=0}^{N-1}\sum_{q=0}^{N-1} {}^3\alpha_{|q|} \left({}^3_{[B]}\psi^N_p, {}^3_{[B]}\psi^N_q \right) \left\{ \sum_{\ell=0}^{N-1} {}^3\alpha_{|p-\ell|} e^{-j2\pi\ell k/N} \right\} \\ &= \sum_{q=0}^{N-1} {}^3\alpha_{|q|} \sum_{p=0}^{N-1} \left({}^3_{[B]}\psi^N_p, {}^3_{[B]}\psi^N_q \right) \frac{1}{\sum_{r=-\infty}^{\infty} N^2 \left[\frac{\sin\pi(-k/N+r)}{\pi(-k/N+r)} \right]^3} e^{-j2\pi pk/N} \\ &= \frac{1}{\sum_{r=-\infty}^{\infty} N^2 \left[\frac{\sin\pi(-k/N+r)}{\pi(-k/N+r)} \right]^3} \sum_{q=0}^{N-1} {}^3\alpha_{|q|} \sum_{p=0}^{N-1} \left({}^3_{[B]}\psi^N_p, {}^3_{[B]}\psi^N_q \right) e^{-j2\pi pk/N} \\ &= \frac{1}{\sum_{r=-\infty}^{\infty} N^2 \left[\frac{\sin\pi(-k/N+r)}{\pi(-k/N+r)} \right]^3} \frac{1}{N} \sum_{p=-\infty}^{\infty} \left[\frac{\sin\pi p/N}{\pi p/N} \right]^6 \sum_{q=0}^{N-1} {}^3\alpha_{|q|} e^{-j2\pi pk/N} \end{aligned} $$

$$= \sum_{p=-\infty}^{\infty} \left[\frac{\sin \pi p/N}{\pi p/N} \right]^6 / N^5 \left\{ \sum_{r=-\infty}^{\infty} \left[\frac{\sin \pi(-k/N+r)}{\pi(-k/N+r)} \right]^3 \right\}^2 .$$

Thus

$$^3\theta_k > 0, \quad k = 0, 1, \cdots, N-1$$

is derived. Therefore, all eigenvalues are positive, and the matrix ^3G is regular. ■

By Lemma 3, ^3G is regular. By Proposition 2 and Lemma 3, the unique existence of the biorthonormal basis is given by the following theorem.

Theorem 1 *In the signal space* ^3S_N *composed of periodic quadratic spline functions, there exists the unique biorthonormal basis* $\left\{ {}^3_{[S^\bullet]}\psi_k^N \right\}_{k=0}^{N-1}$.

(Proof)

By Lemma 3, ^3G is regular. Consequently, there exists the unique biorthonormal basis, by Proposition 2. Therefore, theorem 1 holds good. ■

Theorem 1 indicates that there exists the unique biorthonormal basis. This subsection showed the unique existence of the biorthonormal basis in the periodic quadratic spline signal space ^3S_N. The next subsection derives the biorthonormal basis using the matrix ^3G.

1.5.2 Derivation of biorthonormal basis

This subsection derives the biorthonormal basis in ^3S_N.

The following proposition indicates that the biorthonormal basis $\left\{ {}^3_{[S^\bullet]}\psi_k^N \right\}_{k=0}^{N-1}$ can be represented by matrix $^3G^{-1}$ and the sampling basis.

Proposition 3 *The biorthonormal basis* $\left\{{}^{3}_{[S^{\bullet}]}\psi^{N}_{k}\right\}_{k=0}^{N-1}$ *is represented, using* ${}^{3}G^{-1}$, *as*

$$ {}^{3}_{[S^{\bullet}]}\psi^{N}_{k} = \sum_{\ell=0}^{N-1} {}^{t}\boldsymbol{e}_{\ell}\,{}^{3}G^{-1}\boldsymbol{e}_{k}\,{}^{3}_{[S]}\psi^{N}_{\ell} $$

where $\boldsymbol{e}_k$ *is the* N*-dimensional vector, with only the* k*-th component being 1 and other components being zero.*

(Proof)

By Lemma 1 and Lemma 2, ${}^{3}\varphi_{[S^{\bullet}]}$ is a bijection. Consequently, for any signal $s \in {}^{3}S_{N}$, there holds

$$\begin{aligned}
\left(s, {}^{3}\varphi_{[S^{\bullet}]}{}^{-1}(\boldsymbol{e}_k)\right) &= \left(\sum_{\ell=0}^{N-1} \mu_{\ell}\,{}^{3}_{[S]}\psi^{N}_{\ell}, {}^{3}\varphi_{[S^{\bullet}]}{}^{-1}(\boldsymbol{e}_k)\right) \\
&= \sum_{\ell=0}^{N-1} \mu_{\ell}\,{}^{t}\boldsymbol{e}_{\ell}\left({}^{3}\varphi_{[S^{\bullet}]}\,{}^{3}\varphi_{[S^{\bullet}]}{}^{-1}(\boldsymbol{e}_k)\right) \\
&= \sum_{\ell=0}^{N-1} \mu_{\ell}\delta_{k\ell} \\
&= \mu_k, \quad k = 0, 1, \cdots, N-1.
\end{aligned}$$

Then the biorthonormal basis $\left\{{}^{3}_{[S^{\bullet}]}\psi^{N}_{k}\right\}_{k=0}^{N-1}$ is represented as

$$\begin{aligned}
{}^{3}_{[S^{\bullet}]}\psi^{N}_{k} &= {}^{3}\varphi_{[S^{\bullet}]}{}^{-1}(\boldsymbol{e}_k) \\
&= \left({}^{3}\varphi_{[S]}{}^{-1}\,{}^{3}G^{-1}\right)(\boldsymbol{e}_k) \\
&= \sum_{\ell=0}^{N-1} {}^{t}\boldsymbol{e}_{\ell}\,{}^{3}G^{-1}\boldsymbol{e}_{k}\,{}^{3}_{[S]}\psi^{N}_{\ell}, \quad k = 0, 1, \cdots, N-1.
\end{aligned}$$

■

Proposition 3 provides the representation for the biorthonormal basis, using matrix ${}^{3}G^{-1}$. The following lemma gives detailed form of the matrix ${}^{3}G^{-1}$.

Lemma 4 *The matrix* ${}^3G^{-1}$ *is represented as*

$$
{}^3G^{-1} = \begin{bmatrix} {}^3g_0 & {}^3g_1 & \cdots & {}^3g_{N-1} \\ {}^3g_1 & {}^3g_0 & \cdots & {}^3g_{N-2} \\ \vdots & \vdots & & \vdots \\ {}^3g_{N-1} & {}^3g_{N-2} & \cdots & {}^3g_0 \end{bmatrix}
$$

where the coefficients $\{{}^3g_\ell\}_{\ell=0}^{N-1}$ *are given by*

$$
\begin{aligned}
{}^3g_\ell &= \frac{1}{N^2} \sum_{p=0}^{N-1} \frac{1}{{}^3\theta_p} e^{j2\pi\ell p/N} \\
{}^3\theta_p &= \sum_{k=-\infty}^{\infty} \left\{ \frac{\sin \pi k/N}{\pi k/N} \right\}^6 / N^5 \left\{ \sum_{r=-\infty}^{\infty} \left[\frac{\sin \pi(-p/N+r)}{\pi(-p/N+r)} \right]^3 \right\}^2 .
\end{aligned}
$$

(Proof)

Since the sampling basis is shift-invariant, the matrix ${}^3G$ is a circular matrix. Then diagonal matrix ${}^3\Theta$ composed of the eigenvalues of ${}^3G$ and the matrix U composed of the eigenvectors of ${}^3G$ are given by

$$
\begin{aligned}
{}^3\Theta &= diag({}^3\Theta_0, {}^3\Theta_1, \cdots, {}^3\Theta_{N-1}), \\
U &= \frac{1}{N}[X_0, X_1, \cdots, X_{N-1}], \\
X_k &= {}^t[1, e^{j2\pi k/N}, e^{j4\pi k/N}, \cdots, e^{j2\pi(N-1)k/N}], \\
{}^3\Theta_k &= \sum_{\ell=0}^{N-1} \left({}^3_{[S]}\psi_\ell^N, {}^3_{[S]}\psi_0^N \right) e^{-j2\pi\ell k/N} \\
&= \sum_{p=-\infty}^{N-1} \left\{ \frac{\sin \pi p/N}{\pi p/N} \right\}^6 \\
&\quad / N^5 \left\{ \sum_{r=-\infty}^{\infty} \left[\frac{\sin \pi(-k/N+r)}{\pi(-k/N+r)} \right]^3 \right\}^2 .
\end{aligned}
$$

Using those expressions, ${}^3G$ is represented by

$$^3G = U\,^3\Theta^{-1}U^*.$$

Then, $^3G^{-1}$ is given by

$$\begin{aligned}
^3G^{-1} &= U\,^3\Theta^{-1}U^* \\
&= \frac{1}{N^2}[X_0, X_1, \cdots, X_{N-1}] \\
&\quad diag(^3\Theta_0^{-1}, {}^3\Theta_1^{-1}, \cdots, {}^3\Theta_{N-1}^{-1}) \\
&\quad [X_0, X_1, \cdots, X_{N-1}]^* \\
&= \frac{1}{N^2}[X_0\,{}^3\Theta_0^{-1}, X_1\,{}^3\Theta_1^{-1}, \cdots, X_{N-1}\,{}^3\Theta_{N-1}^{-1}] \begin{bmatrix} X_0^* \\ X_1^* \\ \vdots \\ X_{N-1}^* \end{bmatrix} \\
&= \frac{1}{N^2}\left[\sum_{k=0}^{N-1} X_k X_k^{*3}\Theta_k^{-1}\boldsymbol{e}_0, \sum_{k=0}^{N-1} X_k X_k^{*3}\Theta_k^{-1}\boldsymbol{e}_1, \cdots, \sum_{k=0}^{N-1} X_k X_k^{*3}\Theta_k^{-1}\boldsymbol{e}_{N-1}\right].
\end{aligned}$$

The $(\ell,\ k)$ element of $^3G^{-1}$ is calculated as

$$\frac{1}{N^2}\sum_{p=0}^{N-1} {}^t\boldsymbol{e}_\ell(X_p X_p^{*3}\Theta_p^{-1}\boldsymbol{e}_k) = \frac{1}{N^2}\sum_{p=0}^{N-1}\frac{1}{^3\Theta_p}e^{j2\pi(\ell-k)p/N}.$$

Let coefficients ^3g_k be

$$^3g_k = \frac{1}{N^2}\sum_{p=0}^{N-1}\frac{1}{^3\Theta_p}e^{j2\pi kp/N}, k = 0, 1, 2, \cdots, N-1,$$

the $(\ell,\ k)$ element of $^3G^{-1}$ is represented by $^3g_{|\ell-k|}$.

Therefore, Lemma 4 holds good. ■

Using $^3G^{-1}$ obtained by Lemma 4, the biorthonormal basis in the periodic quadratic spline signal space is derived by the following theorem.

Theorem 2 *The biorthonormal basis* $\left\{ {}^{3}_{[S^{\bullet}]}\psi^{N}_{k} \right\}_{k=0}^{N-1}$ *in the signal space* ${}^{3}S_{N}$ *composed of periodic quadratic spline functions is represented as*

$$ {}^{3}_{[S^{\bullet}]}\psi^{N}_{k} = \sum_{\ell=0}^{N-1} {}^{3}g_{|\ell-k|} {}^{3}_{[S]}\psi^{N}_{\ell} \tag{1.8} $$

where the coefficients $\{ {}^{3}g_{\ell} \}_{\ell=0}^{N-1}$ *are given by*

$$ \begin{aligned} {}^{3}g_{\ell} &= \frac{1}{N^2} \sum_{p=0}^{N-1} \frac{1}{{}^{3}\theta_{p}} e^{j2\pi\ell p/N} \\ {}^{3}\theta_{p} &= \sum_{k=-\infty}^{\infty} \left\{ \frac{\sin \pi k/N}{\pi k/N} \right\}^{6} / N^{5} \left\{ \sum_{r=-\infty}^{\infty} \left[\frac{\sin \pi(-p/N+r)}{\pi(-p/N+r)} \right]^{3} \right\}^{2}. \end{aligned} $$

(Proof)

By substituting ${}^{3}\varphi_{[S^{\bullet}]}{}^{-1}$ derived by Lemma 4 for ${}^{3}G^{-1}$ in Proposition 3, the biorthonormal basis ${}^{3}_{[S^{\bullet}]}\psi^{N}_{k}$ is represented as

$$ \begin{aligned} {}^{3}_{[S^{\bullet}]}\psi^{N}_{k} &= \sum_{\ell=0}^{N-1} {}^{t}\boldsymbol{e}_{\ell} {}^{3}G^{-1} \boldsymbol{e}_{k} {}^{3}_{[S]}\psi^{N}_{\ell}, \quad k = 0, 1, \cdots, N-1 \\ &= \sum_{\ell=0}^{N-1} {}^{t}g_{|\ell-k|} {}^{3}_{[S]}\psi^{N}_{\ell}. \end{aligned} $$

where the coefficients $\{ {}^{3}g_{\ell} \}_{\ell=0}^{N-1}$ are given by

$$ \begin{aligned} {}^{3}g_{\ell} &= \frac{1}{N^2} \sum_{p=0}^{N-1} \frac{1}{{}^{3}\theta_{p}} e^{j2\pi\ell p/N} \\ {}^{3}\theta_{p} &= \sum_{k=-\infty}^{\infty} \left\{ \frac{\sin \pi k/N}{\pi k/N} \right\}^{6} / N^{5} \left\{ \sum_{r=-\infty}^{\infty} \left[\frac{\sin \pi(-p/N+r)}{\pi(-p/N+r)} \right]^{3} \right\}^{2}. \end{aligned} $$

Therefore, Theorem 2 holds good. ■

Figure 1.5 shows an example of the function ${}^{3}_{[S^{\bullet}]}\psi^{N}_{k}$ composing the biorthonormal basis.

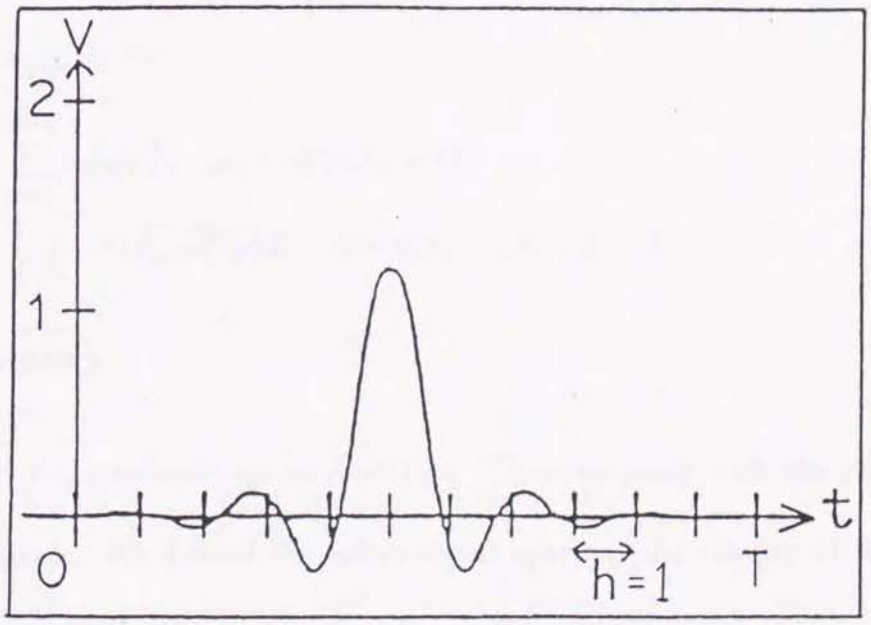

Figure 1.5: An example of functions composing the biorthonormal basis for ${}^3S_N$ $\left(v = {}^3_{[S^\bullet]}\psi^{11}_5(t)\right)$.

This subsection derived the biorthonormal basis, which composes the integral transform expression to derive the sample value sequence from the signal waveform, in the spline signal space ${}^3S_N$.

This section derived the biorthonormal basis for the sampling basis in the spline signal space ${}^3S_N$. The operation to derive the sample value sequence from the signal in the spline signal space is characterized. By this biorthonormal basis and the sampling basis derived in section 1.4, the Fourier-like expansion formula for the sampling basis in the periodic quadratic spline signal space ${}^3S_N$ is completed.

The derived Fourier-like expansion formula is summarized as follows.

$$\begin{aligned} \forall s \in {}^3S_N; \\ s &= \sum_{k=0}^{N-1} \mu_k {}^3_{[S]}\psi_k^N, \quad \mu_k = s(t_k), t_k = kh \\ \mu_k &= \frac{1}{T}\int_0^T s(t)\overline{{}^3_{[S^\bullet]}\psi_k^N(t)}dt, \quad k = 0, 1, \cdots, N-1. \end{aligned}$$

1.6 Summary

We adopted the quadratic spline functions. Then we dealt with the representation problem of signals. We defined the spline signal space as the totality of the quadratic spline functions with equidistantly spaced knots. Then the sampling theorem for periodic quadratic spline functions was derived. The sampling theorem was characterizes spline approximation. By the sampling basis and its biorthonormal basis, it was shown that the approximation is a uniform operation to every point and that it achieves a local approximation.

Chapter 2

Biorthonormal Expansion Formulas for Spline Signal Spaces of Arbitrary Degree in Finite Closed Domain

2.1 Introduction

In this chapter, we shall complete Fourier-like expansion formulas in the signal spaces composed of periodic spline functions, with the sample value sequence of the signal as the expansion coefficients, where the domain is a finite closed interval.

The signal space composed of spline functions has the following features [115, 113]:

1 The continuous differentiability changes with the order.

2 When the order is zero, the space agree with the discontinuous staircase signal space.

3 In the limit where the order tends to infinity, the space agree with the bandlimited signal space with infinite differentiability.

In this sense, the spline signal space is a generalization of the band-limited signal space with the continuous differentiability as the parameter. The Fourier-like expansion formula

derived in this paper is a generalization of the Cahn's sampling theorem in the band-limited signal spaces.

This expansion formula is composed of the pair of the following formulas.

(i) The representation of the signal in the form of linear combination of the sampling basis with the sample value sequence of the signal as the coefficients.

(ii) The integral transform expression to obtain the sample value sequence, which is the expansion coefficients, from the signal.

Since the band limited signal space can be considered as the limit of the spline signal space where the order tends to infinity, the expansion formulas in the bandlimited signal space have already given as follows:

(a) Cahn's sampling theorem[104], for the case where the domain of the signal is a finite closed interval and the periodicity is posed as the boundary condition.

(b) Whittaker[101]-Someya[102]- Shannon's[103] sampling theorem, for the case where the domain of the signal is the infinite open interval.

In those two kind of sampling theorems, the sampling basis forms a system of orthonormal functions. Then, the integral transform expression to derive the sample value sequence from the signal is identical with the sampling basis.

In the spline signal space, the sampling basis has already derived [112]. However the sampling basis is not a system of orthonormal functions. Then, he Fourier-like expansion

formula with the sample value sequence as the expansion coefficient is not complete. In order to derive the complete expansion formula, the integral kernel to specify the integral transform expression must newly be derived.

The integral kernel derived in this paper completes the Fourier-like expansion formula with the sample values sequence as the expansion coefficients, in the spline signal space, with the domain as the finite closed interval and the periodicity as the boundary condition. This expression formula is the simplest signal representation, providing the basis for utilizing the spline signal space in the signal processing.

2.2 Preliminaries

This section prepares the signal space composed of the periodic spline functions which is the object of the analysis in this paper.

In general, the signal waveform, which is actually handled as the object of signal processing, is considered to be defined on a finite observation interval. The energy is assumed as finite. Let the observation interval be $[0, T]$, the set of all such signals can be considered as a typical Hilbert space[111]

$$L_2[0,T] = \left\{ u \middle| \int_0^T |u(t)|^2 dt < +\infty \right\}$$

with the inner product

$$(u, v) = \frac{1}{T} \int_0^T u(t)\overline{v(t)} dt$$

Based on this formulation, the signal space composed of periodic spline functions of

degree $(m-1)$[108] shall be considered in this paper as a subspace of above $L_2[0,T]$. This signal space is called the periodic spline signal space of degree $(m-1)$, and is written as ${}^mS_N$. It is defined as[108]

$$ {}^mS_N \triangleq \left[{}^m_{[B]}\psi^N_k \right]_{k=0}^{N-1} $$

using the system of periodic B-spline functions

$$ {}^m_{[B]}\psi^N_k(t) \triangleq \frac{1}{N} \sum_{p=-\infty}^{\infty} \left\{ \frac{\sin \pi p/N}{\pi p/N} \right\}^m e^{j2\pi p(t/T - k/N)}, \quad k = 0, 1, \cdots, N-1 \tag{2.1} $$

as the basis.

The periodic B-spline function is the piecewise polynomial give by

$$ {}^m_{[B]}\psi^N_k = mh^{-m+1} \sum_{p=-\infty}^{\infty} \sum_{r=0}^{m} (t - ((r+k-m/2)/N + p)T)_+^{m-1} \frac{(-1)^r}{r!(m-r)!}, $$

$$ (t-a)_+^{m-1} \triangleq \begin{cases} (t-a)^{m-1}, & t > a \\ 0, & t \le a \end{cases} $$

where h is the interval $(h = T/N)$ between knots. The system of functions $\left\{ {}^m_{[B]}\psi^N_k \right\}_{k=0}^{N-1}$ is called the periodic B-spline function. Figure 2.1 shows an example of the functions composed of the periodic B-spline function.

The coordinate system ${}^m\varphi_{[B]}$ defined as follows is introduced in ${}^mS_N$. The set of all vectors, composed of the expansion coefficients of $s \in {}^mS_N$ by the periodic B-spline basis

$$ {}^mK_{[B]} \triangleq \left\{ \boldsymbol{\lambda} \middle| \boldsymbol{\lambda} = {}^t[\lambda_0, \lambda_1, \cdots, \lambda_{N-1}], \quad s = \sum_{k=0}^{N-1} \lambda_k {}^m_{[B]}\psi^N_k, \quad s \in {}^mS_N \right\} $$

forms the N dimensional Hilbert space with the inner product

$$ (\boldsymbol{\lambda}, \boldsymbol{\mu}) \triangleq \frac{1}{N} \sum_{k=0}^{N-1} \lambda_k \overline{\mu_k}. $$

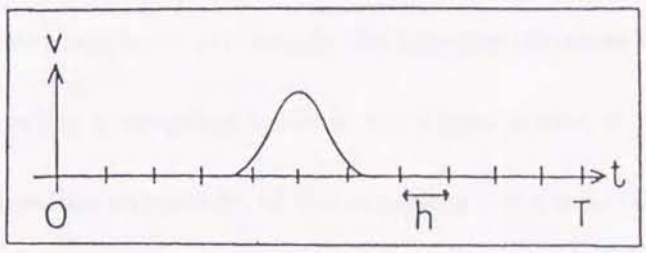

Figure 2.1: An example of periodic B-spline function $\left(v = {}^{3}_{[B]}\psi^{11}_{5}(t)\right)$.

Then, the coordinate system ${}^{m}\varphi_{[B]}$ is defined as the mapping to derive the expansion coefficient vector $\boldsymbol{\lambda}$ from an arbitrary $s \in {}^{m}S_N$. The coordinate system ${}^{m}\varphi_{[B]}$ is a bijection, with the domain ${}^{m}S_N$ and the range and the range ${}^{m}K_{[B]}$.

This section constructed the periodic spline signal space ${}^{m}S_N$.

2.3 Formulation

This section formulates the Fourier-like expansion formula to be derived in this paper.

When there exists a sampling basis in the periodic spline signal space ${}^{m}S_N$, any signal waveform $s \in {}^{m}S_N$ is represented by a linear combination of the sampling basis with the sample value sequence as the expansion coefficients. Let the sampling basis be $\left\{ {}^{m}_{[S]}\psi^{N}_{k} \right\}_{k=0}^{N-1}$, the above linear combination expression is written, for any signal waveform $s \in {}^{m}S_N$, as

$$s = \sum_{k=0}^{N-1} \mu_k {}^{m}_{[S]}\psi^{N}_{k}, \quad \mu_k = s(t_k), \quad t_k = kh. \tag{2.2}$$

The sampling basis has the feature that the result of interpolation is directly given by the linear combination expression, using the given sample value sequence as the coefficients. This means that sampling basis represents the impulse response of the data interpolation operator. If there exists a sampling basis in the signal space, it is unique.

The linear combination expression of the sampling basis is to construct the signal waveform, under the premises that the sample value sequence as the expansion coefficients has already given. The inverse operation is to derive the sample value sequence from the signal waveform. This operation has been considered as a technical problem in A-D conversion circuits such as sample-and-hold. Consequently, no formula has been derived for this operation. If, however, there is no formula to derive the sample value sequence from the signal waveform, the isomorphism between the signal waveform and the sample value sequence can not be discussed.

From such a viewpoint, a fundamental equation is needed, which represents the correspondence between the continuous time signal and the sample value sequence. Representing this fundamental equation is the form of the integral equation, as in the case of the Fourier series expansion of the function, it is given

$$\begin{aligned} \mu_k &= \left(s, {}^{m}_{[S\bullet]}\psi^{N}_{k}\right) \\ &= \frac{1}{T}\int_0^T s(t)\overline{{}^{m}_{[S\bullet]}\psi^{N}_{k}}\,dt, \quad \mu_k = s(t_k), \\ &\quad k = 0, 1, \cdots, N-1. \end{aligned} \tag{2.3}$$

This integral kernel is determined when its integral kernel $\left\{ {}^{m}_{[S^{\bullet}]}\psi^{N}_{k} \right\}_{k=0}^{N-1}$ is determined. If this integral kernel is an element of the signal space ${}^{m}S_N$, the integral kernel is called the biorthonormal basis for the sampling basis[122, 123]. Thus, the biorthonormal basis is the characterization of the sampling operation, which derives the sample value sequence from the signal, as the impulse response.

Consider

(i) The linear combination expression of the sampling basis, which derives the signal waveform from the sampled value sequence, and

(ii) The integral transform expression, which derives the sample value sequence as the inner product of the signal waveform and the biorthonormal basis.

They form the Fourier-like expansion formula with the sample value sequence as the expansion coefficients[122, 123]. Especially, when a signal waveform u is given, which does not belong to the signal space ${}^{m}S_N$, the signal s obtained by

$$\begin{aligned} \mu_k &= \left(u, {}^{m}_{[S^{\bullet}]}\psi^{N}_{k} \right) \\ s &= \sum_{k=0}^{N-1} \mu_k {}^{m}_{[S]}\psi^{N}_{k} \end{aligned}$$

has the engineering implication that it is the least-square approximation of u in ${}^{m}S_N$[123].

This section formulated the Fourier-like expansion formula to be derived in this paper. In the following, The sampling basis is derived in section 2.4. Section 2.5 derives the biorthonormal basis, concluding the derivation of the Fourier-like expansion formula.

2.4 Derivation of sampling basis

This section derives the sampling basis in the signal space ${}^{m}S_N$ composed of periodic spline functions. This basis characterizes the correspondence from the sampled value sequence to the signal waveform.

As the first step, the coordinate system corresponding to the sampling basis is introduced into ${}^{m}S_N$ for deriving the sampling basis. Let the vector composed of the sample value sequence of the signal waveform $s \in {}^{m}S_N$ be

$$\boldsymbol{\mu} = {}^{t}[\mu_0, \mu_1, \cdots, \mu_{N-1}], \quad \mu_k = s(t_k).$$

The set of all such vector $\boldsymbol{\mu}$ is written as ${}^{m}K_{[S]}$. Then, the coordinate system ${}^{m}\varphi_{[S]} : {}^{m}S_N \rightarrow {}^{m}K_{[S]}$ for the sampling basis is defined as the mapping which satisfies

$${}^{m}\varphi_{[S]}(s) = \boldsymbol{\mu}$$

for any $s \in {}^{m}S_N$.

As the next step, the coordinate transformation matrix ${}^{m}A$ from ${}^{m}\varphi_{[B]}$ to ${}^{m}\varphi_{[S]}$ is introduced, in order to represent the relation between ${}^{m}\varphi_{[B]}$ and ${}^{m}\varphi_{[S]}$.

As in the case of eq.(A.1) of proposition 1 in [111], it is defined as the coordinate transformation matrix from ${}^{m}K_{[B]}$ to ${}^{m}K_{[S]}$,

$${}^{m}A = {}^{m}\varphi_{[S]}{}^{m}\varphi_{[B]}{}^{-1}.$$

It is an N-th order square matrix

$${}^{m}A = \left[{}^{m}\varphi_{[S]}({}^{m}_{[B]}\psi^{N}_{0}), {}^{m}\varphi_{[S]}({}^{m}_{[B]}\psi^{N}_{1}), \cdots, {}^{m}\varphi_{[S]}({}^{m}_{[B]}\psi^{N}_{N-1})\right]$$

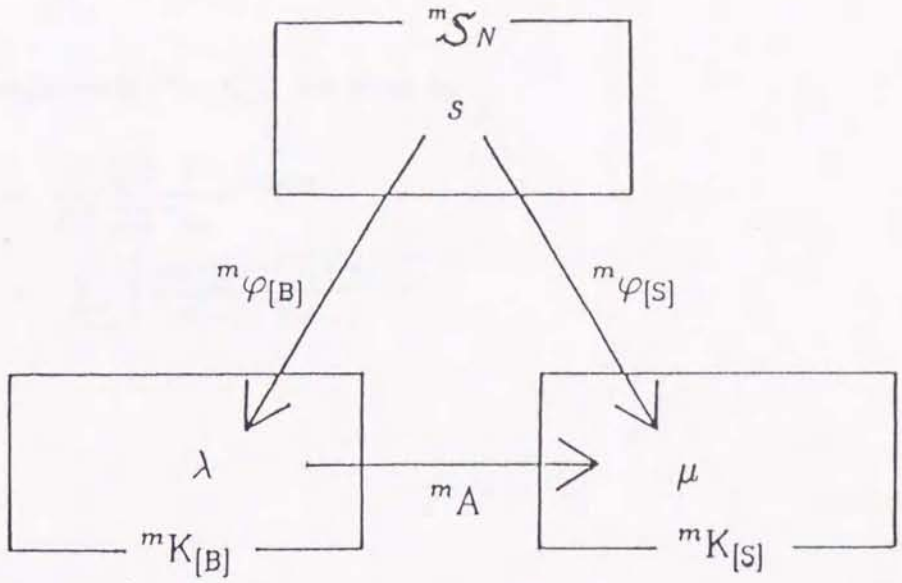

Figure 2.2: Mutual relations between $^{m}\varphi_{[B]}$, $^{m}\varphi_{[S]}$ and ^{m}A.

$$= \begin{bmatrix} {}^{m}_{[B]}\psi^{N}_{0}(t_0) & {}^{m}_{[B]}\psi^{N}_{1}(t_0) & \cdots & {}^{m}_{[B]}\psi^{N}_{N-1}(t_0) \\ {}^{m}_{[B]}\psi^{N}_{0}(t_1) & {}^{m}_{[B]}\psi^{N}_{1}(t_1) & \cdots & {}^{m}_{[B]}\psi^{N}_{N-1}(t_1) \\ \vdots & \vdots & & \vdots \\ {}^{m}_{[B]}\psi^{N}_{0}(t_{N-1}) & {}^{m}_{[B]}\psi^{N}_{1}(t_{N-1}) & \cdots & {}^{m}_{[B]}\psi^{N}_{N-1}(t_{N-1}) \end{bmatrix}.$$

Figure 2.2 shows the relations among $^{m}\varphi_{[B]}$, $^{m}\varphi_{[S]}$, and ^{m}A.

The following proposition is to utilize coordinate systems $^{m}\varphi_{[B]}$, $^{m}\varphi_{[S]}$, and matrix ^{m}A, to derive the sampling basis in the periodic spline signal space $^{m}S_N$ as a linear combination of the periodic spline basis.

Proposition 4 *The sampling basis $^{m}S_N$ in the periodic spline signal space $\left\{{}^{m}_{[S]}\psi^{N}_{k}\right\}_{k=0}^{N-1}$ is given by*

$$ {}^{m}_{[S]}\psi^{N}_{k} = \sum_{\ell=0}^{N-1} {}^{m}\alpha_{|l-k|} {}^{m}_{[B]}\psi^{N}_{\ell}, \tag{2.4} $$

where the coefficients $\{{}^{m}\alpha_{\ell}\}_{\ell=0}^{N-1}$ *are given by*

$$ \begin{aligned} {}^{m}\alpha_{\ell} &= \frac{1}{N^2} \sum_{p=0}^{N-1} \frac{1}{{}^{m}\xi_{p}} e^{j2\pi\ell p/N} \\ {}^{m}\xi_{p} &= \sum_{r=-\infty}^{\infty} \left[\frac{\sin(\pi(-p/N+r))}{\pi(-p/N+r)} \right]^{m}. \end{aligned} $$

(Proof)

From eq.(2.1), the system of B-spline functions has the invariance against the shift

$$ {}^{m}_{[B]}\psi^{N}_{k}(t) = {}^{m}_{[B]}\psi^{N}_{0}(t-kh), \quad k = 0, 1, 2, \cdots, N-1. $$

Then, ${}^{m}A$ is a circular matrix. Let the eigenvalue of matrix ${}^{m}A$ be ${}^{m}\xi_{k}$, and the eigenvector be X_k/N, they are represented [135] as

$$ \begin{aligned} X_k &= {}^{t}[1, e^{j2\pi k/N}, e^{j4\pi k/N}, \cdots, e^{j2\pi(N-1)k/N}], \\ {}^{m}\xi_{k} &= \sum_{\ell=0}^{N-1} {}^{m}_{[B]}\psi^{N}_{\ell}(t_0) e^{-j2\pi\ell k/N} \\ &= \sum_{-\infty}^{\infty} \left[\frac{\sin\pi(-k/N+r)}{\pi(-k/N+r)} \right]^{m}. \end{aligned} $$

Let matrix V and ${}^{m}\Xi$ be defined as

$$ \begin{aligned} V &= \frac{1}{N}[X_0, X_1, \cdots, X_{N-1}], \\ {}^{m}\Xi &= diag({}^{m}\Xi_0, {}^{m}\Xi_1, \cdots, {}^{m}\Xi_{N-1}). \end{aligned} $$

Then, ${}^{m}A$ is decomposed as

$$ {}^{m}A = V\,{}^{m}\Xi V^{*}. $$

The eigenvalue of matrix ${}^{m}A$ is calculated as

$$ \begin{aligned} {}^{m}\Xi_k &= \sum_{\ell=0}^{N-1} {}^{m}_{[B]}\psi_{\ell}^{N}(t_0)e^{-j2\pi\ell k/N} \\ &= \sum_{\ell=0}^{N-1}\frac{1}{N}\sum_{p=-\infty}^{\infty}\left[\left\{\frac{\sin\pi p/N}{\pi p/N}\right\}^{m} e^{-j2\pi p\ell/N}\right] e^{-j2\pi\ell k/N} \\ &= \sum_{r=-\infty}^{\infty} N\left[\frac{\sin\pi(-k/N+r)}{\pi(-k/N+r)}\right]^{m}. \end{aligned} $$

Thus,

$$ {}^{m}\Xi_k > 0, \quad k = 0, 1, \cdots, N-1 $$

is derived. Consequently, matrix ${}^{m}A$ is regular.

By the definitions for the coordinate systems ${}^{m}\varphi_{[S]}$ and ${}^{m}\varphi_{[B]}$ as well as the coordinate transformation matrix ${}^{m}A$

$$ {}^{m}\varphi_{[S]} = {}^{m}A\,{}^{m}\varphi_{[B]}, \quad {}^{m}\varphi_{[S]}{}^{-1} = {}^{m}\varphi_{[B]}\,{}^{m}A^{-1}. $$

Then ${}^{m}\varphi_{[S]}$ is a bijection. Thus, there exists the sampling basis.

In the same way as in the derivation of eq.(A.5) in the proof of Proposition 1 of Ref. [111], the sampling basis $\left\{{}^{m}_{[S]}\psi_k^N\right\}_{k=0}^{N-1}$ in the periodic spline signal space ${}^{m}S_N$ is represented as

$$ {}^{m}_{[S]}\psi_k^N = {}^{m}\varphi_{[S]}{}^{-1}(\boldsymbol{e}_k) = {}^{m}\varphi_{[B]}{}^{-1}\,{}^{m}A^{-1}\boldsymbol{e}_k. \tag{2.5} $$

Since matrix ${}^{m}A$ is regular, ${}^{m}A^{-1}$ is represented, using V and ${}^{m}\Xi$, as

$$ {}^{m}A^{-1} = V\,{}^{m}\Xi^{-1}V^{*}. $$

Then,

$$
\begin{aligned}
{}^{m}A^{-1} &= V\,{}^{m}\Xi^{-1}V^{*} \\
&= \frac{1}{N^2}[X_0, X_1, \cdots, X_{N-1}] \\
&\quad diag({}^{m}\Xi_0^{-1}, {}^{m}\Xi_1^{-1}, \cdots, {}^{m}\Xi_{N-1}^{-1}) \\
&\quad [X_0, X_1, \cdots, X_{N-1}]^{*} \\
&= \frac{1}{N^2}[X_0\,{}^{m}\Xi_0^{-1}, X_1\,{}^{m}\Xi_1^{-1}, \cdots, X_{N-1}\,{}^{m}\Xi_{N-1}^{-1}] \begin{bmatrix} X_0^{*} \\ X_1^{*} \\ \vdots \\ X_{N-1}^{*} \end{bmatrix} \\
&= \frac{1}{N^2}\left[\sum_{k=0}^{N-1} X_k X_k^{*\,m}\Xi_k^{-1}\boldsymbol{e}_0, \sum_{k=0}^{N-1} X_k X_k^{*\,m}\Xi_k^{-1}\boldsymbol{e}_2, \cdots, \sum_{k=0}^{N-1} X_k X_k^{*\,m}\Xi_k^{-1}\boldsymbol{e}_{N-1}\right].
\end{aligned}
$$

The $(\ell,\ k)$ element of ${}^{m}A^{-1}$ is given by

$$
\frac{1}{N^2}\sum_{p=0}^{N-1} {}^{t}\boldsymbol{e}_\ell(X_p X_p^{*\,m}\Xi_p^{-1}\boldsymbol{e}_k) = \frac{1}{N^2}\sum_{p=0}^{N-1}\frac{1}{{}_{m}\Xi_p}e^{j2\pi(\ell-k)p/N}.
$$

Thus ${}^{m}A^{-1}$ is represented by the symmetrical matrix

$$
{}^{m}A^{-1} = \begin{bmatrix} {}^{m}\alpha_0 & {}^{m}\alpha_1 & \cdots & {}^{m}\alpha_{N-1} \\ {}^{m}\alpha_1 & {}^{m}\alpha_0 & \cdots & {}^{m}\alpha_{N-2} \\ \vdots & \vdots & & \vdots \\ {}^{m}\alpha_{N-1} & {}^{m}\alpha_{N-2} & \cdots & {}^{m}\alpha_0 \end{bmatrix} \tag{2.6}
$$

with

$$
{}^{m}\alpha_{|\ell-k|} = \frac{1}{N^2}\sum_{p=0}^{N-1}\frac{1}{{}_{m}\Xi_p}e^{(j2\pi(\ell-k)p/N}
$$

as the element. By substituting eq.(2.6)into eq.(2.5), eq.(2.4) is obtained. ■

Figure 2.3 shows the example of the functions ${}^{m}_{[S]}\psi_k^N$ composing the sampling basis.

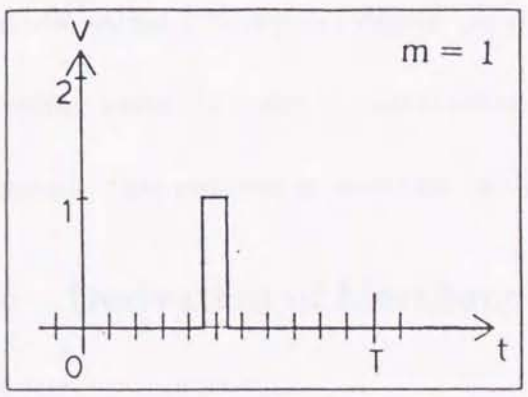

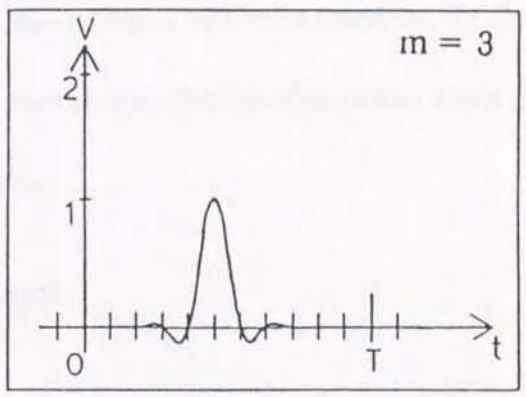

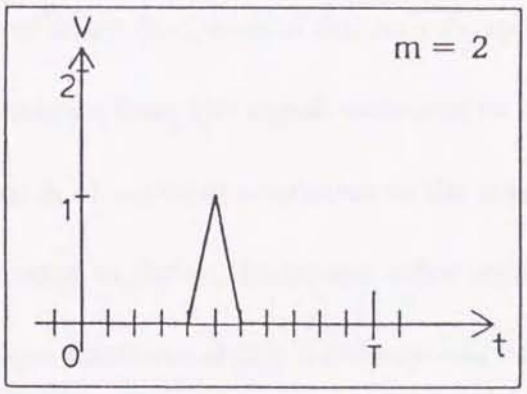

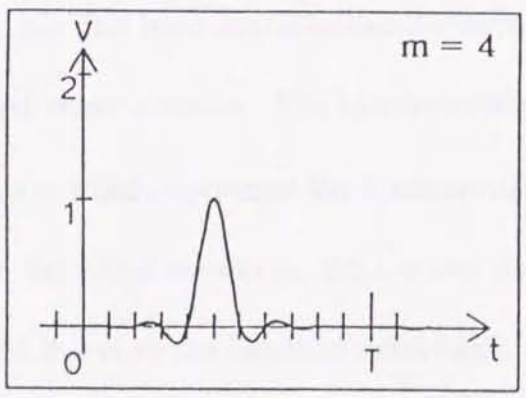

Figure 2.3: Examples of functions composing the sampling basis for ${}^{m}S_{N}$ $\left(v = {}^{m}_{[S]}\psi^{11}_{5}(t)\right)$.

This section derived the sampling basis in the signal space ${}^{m}S_N$ composed of the periodic spline functions, which constructs the linear combination expression to represent the signal waveform from the sample value sequence. The expression characterizes the operation to derive the periodic spline functions of order $(m-1)$ that interpolate the sample value sequence. The inverse operation is to derive the sample value sequence from the given periodic spline functions of degree $(m-1)$. This operation is not characterized by the sampling basis. In order to characterize the both operations, the biorthonormal basis is required. This problem is discussed in the next section.

2.5 Derivation of biorthonormal basis

This section derives the biorthonormal basis corresponding to the sampling basis, in the signal space composed of the periodic spline functions. This basis characterizes the correspondence from the signal waveform to the sampled value sequence. The biorthonormal basis is obtained as a solution of the integral equation which represents the fundamental equation to derive the sample value sequence from the signal waveform. 2.5.1 shows the unique existence of the biorthonormal basis, and 2.5.2 derives the biorthonormal basis.

2.5.1 Unique existence of biorthonormal basis

This subsection shows the unique existence of the biorthonormal basis $\{{}^{m}_{[S^{\bullet}]}\psi^{N}_{k}\}_{k=0}^{N-1}$ in ${}^{m}S_N$. As the first step, as a means to show the unique existence of the biorthonormal basis, a mapping ${}^{m}\varphi_{[S^{\bullet}]}$ and a matrix ${}^{m}G$ are introduced. Then, by showing the regularity

of the matrix ${}^{m}G$, the unique existence of the biorthonormal basis is shown.

A mapping ${}^{m}\varphi_{[S^{\bullet}]}$ is introduced, which obtains the inner product of the signal s and the sampling basis $\left\{ {}^{m}_{[S]}\psi^{N}_{k} \right\}_{k=0}^{N-1}$ for an arbitrary $s \in {}^{m}S_{N}$. Let the vector composed of the inner product of the signal s and the sampling basis $\left\{ {}^{m}_{[S]}\psi^{N}_{k} \right\}_{k=0}^{N-1}$ as

$$\begin{aligned} \eta_{k} &= \left(s, {}^{m}_{[S]}\psi^{N}_{k} \right) \\ &= \frac{1}{T} \int_{0}^{T} s(t) \overline{{}^{m}_{[S]}\psi^{N}_{k}(t)} dt, \quad k = 0, 1, \cdots, N-1, \end{aligned}$$

where each component is written as

$$\boldsymbol{\eta} = {}^{t}[\eta_{0}, \eta_{1}, \cdots, \eta_{N-1}].$$

The set of all such vector $\boldsymbol{\eta}$ is written as ${}^{m}K_{[S^{\bullet}]}$. Then, ${}^{m}\varphi_{[S^{\bullet}]} : {}^{m}S_{N} \to {}^{m}K_{[S^{\bullet}]}$ defined as the mapping satisfying

$${}^{m}\varphi_{[S^{\bullet}]}(s) = \boldsymbol{\eta}$$

for any $s \in {}^{m}S_{N}$.

As the next step, the transformation matrix ${}^{m}G$ from ${}^{m}\varphi_{[S]}$ to ${}^{m}\varphi_{[S^{\bullet}]}$ is introduced. It is defined as the transformation matrix from ${}^{m}K_{[S]}$ to ${}^{m}K_{[S^{\bullet}]}$

$${}^{m}G = {}^{m}\varphi_{[S^{\bullet}]} {}^{m}\varphi_{[S]}{}^{-1}.$$

It is an N-th order square matrix

$$\begin{aligned} {}^{m}G &= \left[{}^{m}\varphi_{[S^{\bullet}]}({}^{m}_{[S]}\psi^{N}_{0}), {}^{m}\varphi_{[S^{\bullet}]}({}^{m}_{[S]}\psi^{N}_{1}), \cdots, {}^{m}\varphi_{[S^{\bullet}]}({}^{m}_{[S]}\psi^{N}_{N-1}) \right] \\ &= \begin{bmatrix} \left({}^{m}_{[S]}\psi^{N}_{0}, {}^{m}_{[S]}\psi^{N}_{0} \right) & \left({}^{m}_{[S]}\psi^{N}_{1}, {}^{m}_{[S]}\psi^{N}_{0} \right) & \cdots & \left({}^{m}_{[S]}\psi^{N}_{N-1}, {}^{m}_{[S]}\psi^{N}_{0} \right) \\ \left({}^{m}_{[S]}\psi^{N}_{0}, {}^{m}_{[S]}\psi^{N}_{1} \right) & \left({}^{m}_{[S]}\psi^{N}_{1}, {}^{m}_{[S]}\psi^{N}_{1} \right) & \cdots & \left({}^{m}_{[S]}\psi^{N}_{N-1}, {}^{m}_{[S]}\psi^{N}_{1} \right) \\ \vdots & \vdots & & \vdots \\ \left({}^{m}_{[S]}\psi^{N}_{0}, {}^{m}_{[S]}\psi^{N}_{N-1} \right) & \left({}^{m}_{[S]}\psi^{N}_{1}, {}^{m}_{[S]}\psi^{N}_{N-1} \right) & \cdots & \left({}^{m}_{[S]}\psi^{N}_{N-1}, {}^{m}_{[S]}\psi^{N}_{N-1} \right) \end{bmatrix}. \end{aligned} \tag{2.7}$$

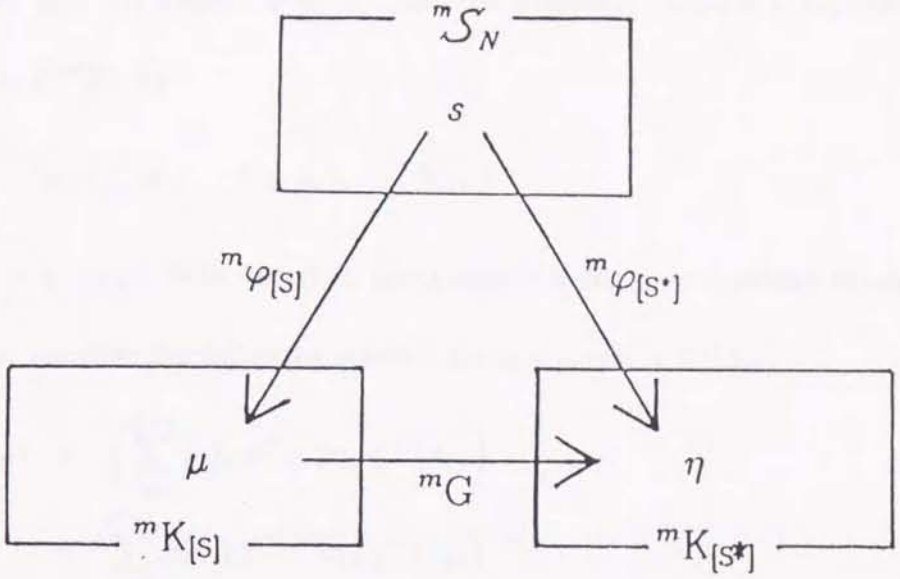

Figure 2.4: Mutual relations between $^{m}\varphi_{[S]}$, $^{m}\varphi_{[S^\bullet]}$ and ^{m}G.

Figure 2.4 shows the relations among $^{m}\varphi_{[S]}$, $^{m}\varphi_{[S^\bullet]}$, and ^{m}G.

In the following, the relations among $^{m}\varphi_{[S]}$, $^{m}\varphi_{[S^\bullet]}$, and ^{m}G are used to discuss the unique existence of the biorthonormal basis. The following lemma gives the relation between the mapping $^{m}\varphi_{[S^\bullet]}$ and the unique existence of the biorthonormal basis.

Lemma 5 *The following two conditions are equivalent.*

(i) *The mapping* $^{m}\varphi_{[S^\bullet]}$ *is a bijection.*

(ii) *There exists unique biorthonormal basis* $\left\{ {}^{m}_{[S^\bullet]}\psi^{N}_{k} \right\}_{k=0}^{N-1}$.

(Proof)

It is shown first (ii) follows from (i). Let the mapping ${}^m\varphi_{[S^\bullet]}$ is a bijection. Define the function $u_k \in {}^mS_N$ by

$$u_k = {}^m\varphi_{[S^\bullet]}{}^{-1}(\boldsymbol{e}_k), \quad k = 0, 1, \cdots, N-1$$

where $\boldsymbol{e}_k$ is a vector with the k-th components being 1 and others being zero. Then, function u_k satisfies the following relation for any signal $s \in {}^mS_N$

$$\begin{aligned}
(s, u_k) &= \left(\sum_{\ell=0}^{N-1} \mu_\ell {}^m_{[S]}\psi^N_\ell, {}^m\varphi_{[S^\bullet]}{}^{-1}(\boldsymbol{e}_k) \right) \\
&= \sum_{\ell=0}^{N-1} \mu_\ell \left({}^m_{[S]}\psi^N_\ell, {}^m\varphi_{[S^\bullet]}{}^{-1}(\boldsymbol{e}_k) \right) \\
&= \sum_{\ell=0}^{N-1} \mu_\ell \overline{\left({}^m\varphi_{[S^\bullet]}{}^{-1}(\boldsymbol{e}_k), {}^m_{[S]}\psi^N_\ell \right)} \\
&= \sum_{\ell=0}^{N-1} \mu_\ell \overline{{}^t\boldsymbol{e}_l \left({}^m\varphi_{[S^\bullet]}{}^m\varphi_{[S^\bullet]}{}^{-1}(\boldsymbol{e}_k) \right)} \\
&= \sum_{\ell=0}^{N-1} \mu_\ell \overline{\delta_{k\ell}} \\
&= \sum_{\ell=0}^{N-1} \mu_\ell \delta_{k\ell} \\
&= \mu_k, \quad k = 0, 1, 2, \cdots, N-1.
\end{aligned}$$

Consequently, it is the function in ${}^mS_N$ satisfying the condition for the biorthonormal basis. The symbol $\delta_{k\ell}$ is Kronecker's delta.

Assume that a function $v_k \in {}^mS_N$ which is different from u_k also satisfies the condition of the biorthonormal basis. Then, by the definition, functions u_k and v_k satisfy

$$\begin{aligned}
(s, u_k) &= u(t_k), \\
(s, v_k) &= u(t_k), \quad k = 0, 1, \cdots, N-1
\end{aligned}$$

for any $s \in {}^{m}S_N$. Consequently,

$$\begin{aligned}(s, v_k - u_k) &= (s, v_k) - (s, u_k) \\ &= u(t_k) - u(t_k) \\ &= 0\end{aligned}$$

and

$$v_k = u_k, \quad k = 0, 1, \cdots, N-1.$$

Thus, there exists the unique biorthonormal basis.

Next, it is shown that (i) follows from (ii). Assume that there exists unique biorthonormal basis. By definition, the mapping ${}^{m}\varphi_{[S\bullet]}$ is a bijection. By assumption, any signal $s \in {}^{m}S_N$ can be represented in the form

$$\begin{aligned}s &= \sum_{k=0}^{N-1} \mu_k {}^{m}_{[S]}\psi^{N}_{k}, \\ \mu_k &= \left(s, {}^{m}_{[S\bullet]}\psi^{N}_{k}\right), \quad k = 0, 1, \cdots, N-1.\end{aligned}$$

Consequently, for the signals $s1, s2 \in {}^{m}S_N$ satisfying the relation

$${}^{m}\varphi_{[S\bullet]}(s1) = {}^{m}\varphi_{[S\bullet]}(s2),$$

there must hold

$$\left(\sum_{k=0}^{N-1} \left(s1, {}^{m}_{[S\bullet]}\psi^{N}_{k}\right) {}^{m}_{[S]}\psi^{N}_{k}, {}^{m}_{[S]}\psi^{N}_{\ell}\right) = \left(\sum_{k=0}^{N-1} \left(s2, {}^{m}_{[S\bullet]}\psi^{N}_{k}\right) {}^{m}_{[S]}\psi^{N}_{k}, {}^{m}_{[S]}\psi^{N}_{\ell}\right)$$

$$\sum_{k=0}^{N-1} \left(s1 - s2, {}^{m}_{[S\bullet]}\psi^{N}_{k}\right) \left({}^{m}_{[S]}\psi^{N}_{k}, {}^{m}_{[S]}\psi^{N}_{\ell}\right) = 0, \quad \ell = 0, 1, \cdots, N-1.$$

Since functions ${}^{m}_{[S^{\bullet}]}\psi^{N}_{k}$, $(k = 0, 1, 2, \cdots, N-1)$ are not identically zero, there holds

$$s1 = s2.$$

Consequently, ${}^{m}\varphi_{[S^{\bullet}]}$ is a bijection.

Therefore, Lemma 5 holds good. ■

By Lemma 5, there exists unique biorthonormal basis if and only if ${}^{m}\varphi_{[S^{\bullet}]}$ is a bijection.

The following lemma indicates the relation between ${}^{m}\varphi_{[S^{\bullet}]}$ and ${}^{m}G$.

Lemma 6 *The following two conditions are equivalent.*

(i) *The mapping* ${}^{m}\varphi_{[S^{\bullet}]}$ *is a bijection.*

(ii) *The matrix* ${}^{m}G$ *is regular.*

(Proof)

It is shown first (ii) follows from (i). By the definitions of mapping ${}^{m}\varphi_{[S^{\bullet}]}$ and matrix ${}^{m}G$, ${}^{m}G$ and ${}^{m}G^{-1}$ are represented, respectively, as

$${}^{m}G = {}^{m}\varphi_{[S^{\bullet}]}{}^{m}\varphi_{[S]}{}^{-1}, \quad {}^{m}G^{-1} = {}^{m}\varphi_{[S]}{}^{m}\varphi_{[S^{\bullet}]}{}^{-1}.$$

Since mapping ${}^{m}\varphi_{[S]}$ is a bijection, ${}^{m}G$ is regular if ${}^{m}\varphi_{[S^{\bullet}]}$ is a bijection.

Next, it is shown that (i) follows from (ii). By the definition of mapping ${}^{m}\varphi_{[S^{\bullet}]}$ and matrix ${}^{m}G$, ${}^{m}\varphi_{[S^{\bullet}]}$ and ${}^{m}\varphi_{[S^{\bullet}]}{}^{-1}$ are , respectively, as

$${}^{m}\varphi_{[S^{\bullet}]} = {}^{m}G{}^{m}\varphi_{[S]}, \quad {}^{m}\varphi_{[S^{\bullet}]}{}^{-1} = {}^{m}\varphi_{[S]}{}^{-1}{}^{m}G^{-1}.$$

Since ${}^m\varphi_{[S]}$ is a bijection, ${}^m\varphi_{[S^\bullet]}$ is a bijection if ${}^mG$ is regular.

Therefore, Lemma 6 holds good. ■

By Lemma 6, the bijection property of ${}^m\varphi_{[S^\bullet]}$ and the regularity of ${}^mG$ are equivalent. The following property indicates the relation between the unique existence of the biorthonormal basis and the regularity of ${}^mG$.

Proposition 5 *The following two conditions are equivalent.*

(i) *The matrix ${}^mG$ is regular.*

(ii) *There exists the unique biorthonormal basis* $\left\{ {}^m_{[S^\bullet]}\psi^N_k \right\}_{k=0}^{N-1}$.

(Proof)

By Lemma 5 and Lemma 6, the regularity of ${}^mG$ and the unique existence of the biorthonormal basis are equivalent.

Therefore Proposition 5 holds good. ■

By Proposition 5, the biorthonormal basis uniquely exists if and only if ${}^mG$ is regular. The following lemma indicates the regularity of ${}^mG$.

Lemma 7 *The matrix ${}^mG$ is regular.*

(Proof)

As it seen from eq.(2.4), the sampling basis has the invariance against the shift.

$$ {}^m_{[S]}\psi^N_k(t) = {}^m_{[S]}\psi^N_0(t - kh), \quad k = 0, 1, 2, \cdots, N-1 $$

Then, the matrix ${}^{m}G$ represented by eq.(2.7) is a circular matrix. Consequently, the eigenvalue ${}^{m}\theta_k$ of ${}^{m}G$ is given [135] by

$$ {}^{m}\theta_k = \sum_{\ell=0}^{N-1} \left({}^{m}_{[S]}\psi_{\ell}^{N}, {}^{m}_{[S]}\psi_{0}^{N} \right) e^{-j2\pi\ell k/N}, \quad k = 0, 1, \cdots, N-1. $$

The inner product in the right-hand side of the above expression is calculated as

$$ \begin{aligned} \left({}^{m}_{[S]}\psi_{\ell}^{N}, {}^{m}_{[S]}\psi_{0}^{N} \right) &= \left(\sum_{p=0}^{N-1} {}^{m}\alpha_{|p-\ell|} {}^{m}_{[B]}\psi_{p}^{N}, \sum_{q=0}^{N-1} {}^{m}\alpha_{|q|} {}^{m}_{[B]}\psi_{q}^{N} \right) \\ &= \sum_{p=0}^{N-1} \sum_{q=0}^{N-1} {}^{m}\alpha_{|p-\ell|} {}^{m}\alpha_{|q|} \left({}^{m}_{[B]}\psi_{p}^{N}, {}^{m}_{[B]}\psi_{q}^{N} \right). \end{aligned} $$

Consequently, the eigenvalue ${}^{m}\theta_k$ is given by

$$ \begin{aligned} {}^{m}\theta_k &= \sum_{\ell=0}^{N-1} \left\{ \sum_{p=0}^{N-1} \sum_{q=0}^{N-1} {}^{m}\alpha_{|p-l|} {}^{m}\alpha_{|q|} \left({}^{m}_{[B]}\psi_{p}^{N}, {}^{m}_{[B]}\psi_{q}^{N} \right) e^{-j2\pi\ell k/N} \right\} \\ &= \sum_{p=0}^{N-1} \sum_{q=0}^{N-1} {}^{m}\alpha_{|q|} \left({}^{m}_{[B]}\psi_{p}^{N}, {}^{m}_{[B]}\psi_{q}^{N} \right) \left\{ \sum_{\ell=0}^{N-1} {}^{m}\alpha_{|p-\ell|} e^{-j2\pi\ell k/N} \right\} \\ &= \sum_{q=0}^{N-1} {}^{m}\alpha_{|q|} \sum_{p=0}^{N-1} \left({}^{m}_{[B]}\psi_{p}^{N}, {}^{m}_{[B]}\psi_{q}^{N} \right) \frac{1}{\sum_{r=-\infty}^{\infty} N^2 \left[\frac{\sin \pi(-k/N+r)}{\pi(-k/N+r)} \right]^m} e^{-j2\pi pk/N} \\ &= \frac{1}{\sum_{r=-\infty}^{\infty} N^2 \left[\frac{\sin \pi(-k/N+r)}{\pi(-k/N+r)} \right]^m} \sum_{q=0}^{N-1} {}^{m}\alpha_{|q|} \sum_{p=0}^{N-1} \left({}^{m}_{[B]}\psi_{p}^{N}, {}^{m}_{[B]}\psi_{q}^{N} \right) e^{-j2\pi pk/N} \\ &= \frac{1}{\sum_{r=-\infty}^{\infty} N^2 \left[\frac{\sin \pi(-k/N+r)}{\pi(-k/N+r)} \right]^m} \frac{1}{N} \sum_{p=-\infty}^{\infty} \left[\frac{\sin \pi p/N}{\pi p/N} \right]^{2m} \sum_{q=0}^{N-1} {}^{m}\alpha_{|q|} e^{-j2\pi pk/N} \\ &= \sum_{p=-\infty}^{\infty} \left[\frac{\sin \pi p/N}{\pi p/N} \right]^{2m} / N^5 \left\{ \sum_{r=-\infty}^{\infty} \left[\frac{\sin \pi(-k/N+r)}{\pi(-k/N+r)} \right]^m \right\}^2. \end{aligned} $$

Thus

$$ {}^{m}\theta_k > 0, \quad k = 0, 1, \cdots, N-1 $$

is derived. Therefore, all eigenvalues are positive, and the matrix ${}^mG$ is regular. ■

By Lemma 7, ${}^mG$ is regular. By Proposition 5 and Lemma 7, the unique existence of the biorthonormal basis is given by the following theorem.

Theorem 3 *In the signal space ${}^mS_N$ composed of periodic spline functions of degree $(m-1)$, there exists the unique biorthonormal basis $\left\{ {}^m_{[S^\bullet]}\psi_k^N \right\}_{k=0}^{N-1}$.*

(Proof)

By Lemma 7, ${}^mG$ is regular. Consequently, there exists the unique biorthonormal basis, by Proposition 5. Therefore, theorem 3 holds good. ■

Theorem 3 indicates that there exists the unique biorthonormal basis. This subsection showed the unique existence of the biorthonormal basis in the periodic spline signal space ${}^mS_N$. The next subsection derives the biorthonormal basis using the matrix ${}^mG$.

2.5.2 Derivation of biorthonormal basis

This subsection derives the biorthonormal basis in ${}^mS_N$.

The following proposition indicates that the biorthonormal basis $\left\{ {}^m_{[S^\bullet]}\psi_k^N \right\}_{k=0}^{N-1}$ can be represented by matrix ${}^mG^{-1}$ and the sampling basis.

Proposition 6 *The biorthonormal basis $\left\{ {}^m_{[S^\bullet]}\psi_k^N \right\}_{k=0}^{N-1}$ is represented, using ${}^mG^{-1}$, as*

$$ {}^m_{[S^\bullet]}\psi_k^N = \sum_{\ell=0}^{N-1} {}^t\boldsymbol{e}_\ell \, {}^mG^{-1} \boldsymbol{e}_k \, {}^m_{[S]}\psi_\ell^N $$

where $\boldsymbol{e}_k$ is the N-dimensional vector, with only the k-th component being 1 and other components being zero.

(Proof)

By Lemma 5 and Lemma 6, ${}^m\varphi_{[S^\bullet]}$ is a bijection. Consequently, for any signal $s \in {}^mS_N$, there holds

$$\begin{aligned}
\left(s, {}^m\varphi_{[S^\bullet]}{}^{-1}(\boldsymbol{e}_k)\right) &= \left(\sum_{\ell=0}^{N-1} \mu_\ell {}^m_{[S]}\psi^N_\ell, {}^m\varphi_{[S^\bullet]}{}^{-1}(\boldsymbol{e}_k)\right) \\
&= \sum_{\ell=0}^{N-1} \mu_\ell {}^t\boldsymbol{e}_\ell \left({}^m\varphi_{[S^\bullet]}{}^m\varphi_{[S^\bullet]}{}^{-1}(\boldsymbol{e}_k)\right) \\
&= \sum_{\ell=0}^{N-1} \mu_\ell \delta_{k\ell} \\
&= \mu_k, \quad k = 0, 1, \cdots, N-1.
\end{aligned}$$

Then the biorthonormal basis $\left\{{}^m_{[S^\bullet]}\psi^N_k\right\}_{k=0}^{N-1}$ is represented as

$$\begin{aligned}
{}^m_{[S^\bullet]}\psi^N_k &= {}^m\varphi_{[S^\bullet]}{}^{-1}(\boldsymbol{e}_k) \\
&= \left({}^m\varphi_{[S]}{}^{-1}{}^mG^{-1}\right)(\boldsymbol{e}_k) \\
&= \sum_{\ell=0}^{N-1} {}^t\boldsymbol{e}_\ell {}^mG^{-1}\boldsymbol{e}_k {}^m_{[S]}\psi^N_\ell, \quad k = 0, 1, \cdots, N-1.
\end{aligned}$$

■

Proposition 6 provides the representation for the biorthonormal basis, using matrix ${}^mG^{-1}$. The following lemma gives detailed form of the matrix ${}^mG^{-1}$.

Lemma 8 *The matrix ${}^mG^{-1}$ is represented as*

$${}^mG^{-1} = \begin{bmatrix}
{}^mg_0 & {}^mg_1 & \cdots & {}^mg_{N-1} \\
{}^mg_1 & {}^mg_0 & \cdots & {}^mg_{N-2} \\
\vdots & \vdots & & \vdots \\
{}^mg_{N-1} & {}^mg_{N-2} & \cdots & {}^mg_0
\end{bmatrix}$$

where the coefficients $\{{}^m g_\ell\}_{\ell=0}^{N-1}$ *are given by*

$$
\begin{aligned}
{}^m g_\ell &= \frac{1}{N^2} \sum_{p=0}^{N-1} \frac{1}{{}^m\theta_p} e^{j2\pi\ell p/N} \\
{}^m\theta_p &= \sum_{k=-\infty}^{\infty} \left\{ \frac{\sin \pi k/N}{\pi k/N} \right\}^{2m} /N^5 \left\{ \sum_{r=-\infty}^{\infty} \left[\frac{\sin \pi(-p/N+r)}{\pi(-p/N+r)} \right]^m \right\}^2 .
\end{aligned}
$$

(Proof)

Since the sampling basis is shift-invariant, the matrix ${}^m G$ is a circular matrix. Then diagonal matrix ${}^m\Theta$ composed of the eigenvalues of ${}^m G$ and the matrix U composed of the eigenvectors of ${}^m G$ are given by

$$
\begin{aligned}
{}^m\Theta &= diag({}^m\Theta_0, {}^m\Theta_1, \cdots, {}^m\Theta_{N-1}), \\
U &= \frac{1}{N}[X_0, X_1, \cdots, X_{N-1}], \\
X_k &= {}^t[1, e^{j2\pi k/N}, e^{j4\pi k/N}, \cdots, e^{j2\pi(N-1)k/N}], \\
{}^m\Theta_k &= \sum_{\ell=0}^{N-1} \left({}^m_{[S]}\psi_\ell^N, {}^m_{[S]}\psi_0^N \right) e^{-j2\pi\ell k/N} \\
&= \sum_{p=-\infty}^{N-1} \left\{ \frac{\sin \pi p/N}{\pi p/N} \right\}^{2m} \\
&\quad /N^5 \left\{ \sum_{r=-\infty}^{\infty} \left[\frac{\sin \pi(-k/N+r)}{\pi(-k/N+r)} \right]^m \right\}^2 .
\end{aligned}
$$

Using those expressions, ${}^m G$ is represented by

$$
{}^m G = U {}^m\Theta^{-1} U^* .
$$

Then, ${}^m G^{-1}$ is given by

$$
{}^m G^{-1} = U {}^m\Theta^{-1} U^*
$$

$$
\begin{aligned}
&= \frac{1}{N^2}[X_0, X_1, \cdots, X_{N-1}] \\
&\quad diag({}^m\Theta_0^{-1}, {}^m\Theta_1^{-1}, \cdots, {}^m\Theta_{N-1}^{-1}) \\
&\quad [X_0, X_1, \cdots, X_{N-1}]^* \\
&= \frac{1}{N^2}[X_0 {}^m\Theta_0^{-1}, X_1 {}^m\Theta_1^{-1}, \cdots, X_{N-1} {}^m\Theta_{N-1}^{-1}] \begin{bmatrix} X_0^* \\ X_1^* \\ \vdots \\ X_{N-1}^* \end{bmatrix} \\
&= \frac{1}{N^2}\left[\sum_{k=0}^{N-1} X_k X_k^{*m}\Theta_k^{-1}\boldsymbol{e}_0, \sum_{k=0}^{N-1} X_k X_k^{*m}\Theta_k^{-1}\boldsymbol{e}_2, \cdots, \sum_{k=0}^{N-1} X_k X_k^{*m}\Theta_k^{-1}\boldsymbol{e}_{N-1}\right].
\end{aligned}
$$

The $(\ell,\ k)$ element of ${}^mG^{-1}$ is calculated as

$$
\frac{1}{N^2}\sum_{p=0}^{N-1} {}^t\boldsymbol{e}_\ell(X_p X_p^{*m}\Theta_p^{-1}\boldsymbol{e}_k) = \frac{1}{N^2}\sum_{p=0}^{N-1}\frac{1}{{}^m\Theta_p}e^{j2\pi(\ell-k)p/N}.
$$

Let coefficients ${}^mg_k$ be

$$
{}^mg_k = \frac{1}{N^2}\sum_{p=0}^{N-1}\frac{1}{{}^m\Theta_p}e^{j2\pi kp/N}, k = 0, 1, 2, \cdots, N-1,
$$

the $(\ell,\ k)$ element of ${}^mG^{-1}$ is represented by ${}^mg_{|\ell-k|}$.

Therefore, Lemma 8 holds good. ■

Using ${}^mG^{-1}$ obtained by Lemma 8, the biorthonormal basis in the periodic spline signal space of degree $(m-1)$ is derived by the following theorem.

Theorem 4 *The biorthonormal basis* $\left\{{}^m_{[S^\bullet]}\psi_k^N\right\}_{k=0}^{N-1}$ *in the signal space* ${}^mS_N$ *composed of periodic spline functions of degree* $(m-1)$ *is represented as*

$$
{}^m_{[S^\bullet]}\psi_k^N = \sum_{\ell=0}^{N-1} {}^mg_{|\ell-k|}\,{}^m_{[S]}\psi_\ell^N \tag{2.8}
$$

where the coefficients $\{{}^m g_\ell\}_{\ell=0}^{N-1}$ *are given by*

$$
\begin{aligned}
{}^m g_\ell &= \frac{1}{N^2} \sum_{p=0}^{N-1} \frac{1}{{}^m\theta_p} e^{j2\pi\ell p/N} \\
{}^m\theta_p &= \sum_{k=-\infty}^{\infty} \left\{ \frac{\sin \pi k/N}{\pi k/N} \right\}^{2m} / N^5 \left\{ \sum_{r=-\infty}^{\infty} \left[\frac{\sin \pi(-p/N+r)}{\pi(-p/N+r)} \right]^m \right\}^2 .
\end{aligned}
$$

(Proof)

By substituting ${}^m\varphi_{[S\bullet]}{}^{-1}$ derived by Lemma 8 for ${}^m G^{-1}$ in Proposition 6, the biorthonormal basis ${}^m_{[S\bullet]}\psi_k^N$ is represented as

$$
\begin{aligned}
{}^m_{[S\bullet]}\psi_k^N &= \sum_{\ell=0}^{N-1} {}^t\boldsymbol{e}_\ell \, {}^m G^{-1} \boldsymbol{e}_{k[S]} \, {}^m_{[S]}\psi_\ell^N, \quad k = 0, 1, \cdots, N-1 \\
&= \sum_{\ell=0}^{N-1} {}^t g_{|\ell-k|} \, {}^m_{[S]}\psi_\ell^N .
\end{aligned}
$$

where the coefficients $\{{}^m g_\ell\}_{\ell=0}^{N-1}$ are given by

$$
\begin{aligned}
{}^m g_\ell &= \frac{1}{N^2} \sum_{p=0}^{N-1} \frac{1}{{}^m\theta_p} e^{j2\pi\ell p/N} \\
{}^m\theta_p &= \sum_{k=-\infty}^{\infty} \left\{ \frac{\sin \pi k/N}{\pi k/N} \right\}^{2m} / N^5 \left\{ \sum_{r=-\infty}^{\infty} \left[\frac{\sin \pi(-p/N+r)}{\pi(-p/N+r)} \right]^m \right\}^2 .
\end{aligned}
$$

Therefore, Theorem 4 holds good. ■

Figure 2.5 shows an example of the function ${}^m_{[S\bullet]}\psi_k^N$ composing the biorthonormal basis.

This subsection derived the biorthonormal basis, which composes the integral transform expression to derive the sample value sequence from the signal waveform, in the spline signal space ${}^m S_N$.

This section derived the biorthonormal basis for the sampling basis in the spline signal space ${}^m S_N$. The operation to derive the sample value sequence from the signal in the

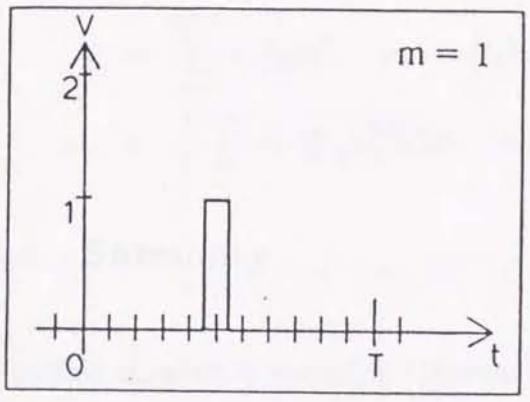

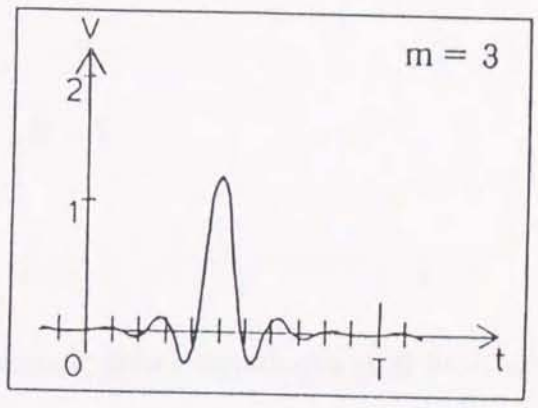

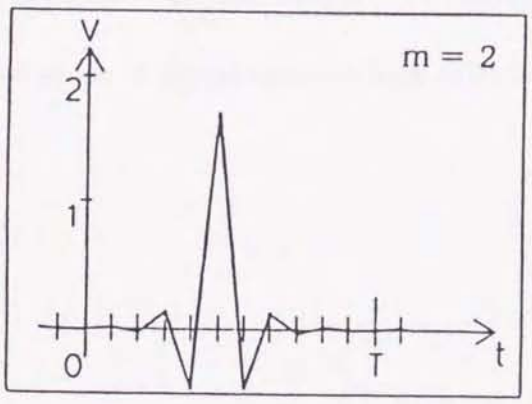

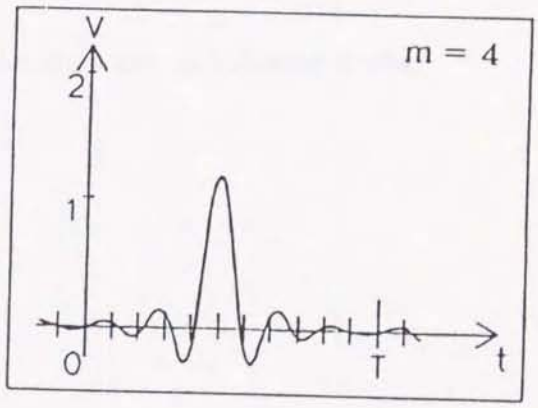

Figure 2.5: Examples of functions composing the biorthonormal basis for ${}^{m}S_N$ $\left(v = {}^{m}_{[S^{\bullet}]}\psi_5^{11}(t)\right)$.

spline signal space is characterized. By this biorthonormal basis and the sampling basis derived in section 2.4, the Fourier-like expansion formula for the sampling basis in the periodic spline signal space ${}^{m}S_N$ is completed.

The derived Fourier-like expansion formula is summarized as follows.

$$\begin{aligned} \forall s &\in {}^{m}S_N; \\ s &= \sum_{k=0}^{N-1} \mu_k {}^{m}_{[S]}\psi^N_k, \quad \mu_k = s(t_k), t_k = kh \\ \mu_k &= \frac{1}{T}\int_0^T s(t)\overline{{}^{m}_{[S^*]}\psi^N_k(t)}dt, \quad k = 0, 1, \cdots, N-1. \end{aligned}$$

2.6 Summary

In this chapter, a sampling theorem for the periodic spline signal spaces of arbitrary degree was derived. The present theory makes it possible to select a signal space out of the series of signal spaces which exist between the staircase and Fourier series.

Part III

Biorthonormal Expansion Formulas for Non-periodic Fluency Signal Spaces

In Part III, the sampling theorem for non-periodic spline signal spaces is completed by deriving biorthonormal expansion formulas. The class of spline functions are limited to the infinite open domain.

In Chapter 3, the spline functions of arbitrary degree are prepared. The sampling theorem for spline signal space of arbitrary degree in the infinite open domain is completed. It generalizes the Whittaker-Someya-Shannon's sampling theorem when the degree tends to infinity and that the spline signal space of degree zero is identical with the space of staircase functions.

Chapter 3

Biorthonormal Expansion Formulas for Spline Signal Spaces of Arbitrary Degree in Infinite Open Domain

3.1 Introduction

In this Chapter, a sampling theorem for spline signal spaces of arbitrary order shall be completed in the infinite open domain by deriving biorthonormal expansion formulas. The sampling theorem in the spline signal space corresponds to Whittaker-Someya-Shannon's sampling theorem in band-limited signal space.

In band-limited signal space, the mutual relation between a continuous time signal and discrete time signal is expressed by the Whittaker-Someya-Shannon's sampling theorem. This theorem consists of an orthonormal expansion formula using sinc function. In that formula, the expansion coefficients are identical to the sample values of signals. In general, however, the band-limited signal space is not always suited to model the signals in nature.

By deriving biorthonormal expansion formulas, the sampling theorem is completed for

the spline signal spaces which are suited to model the signals in nature rather than the band-limited signal space. Since the obtained sampling theorem gives the simplest representation of signals, it is considered to be the most fundamental characterization of spline functions used for signal processing. The biorthonormal basis derived in this chapter is considered to be the delta function at sampling point with some continuous differentiability.

3.2 Preliminaries

In this section, signal spaces composed of spline functions are prepared.

Continuous time signals in signal processing are generally considered to be in the Hilbert space [140, 139]

$$L_2(\boldsymbol{R}) \triangleq \left\{ u \middle| \int_{-\infty}^{\infty} |u(t)|^2 dt < +\infty \right\} \tag{3.1}$$

with the inner product

$$(u, v)_{L_2} \triangleq \int_{-\infty}^{\infty} u(t)\overline{v(t)}dt, \tag{3.2}$$

where $\boldsymbol{R}$ denotes the totality of real numbers.

So we consider a signal space composed of spline functions [105] of degree $(m-1)$ as a subspace of $L_2(\boldsymbol{R})$. Let ${}^mS$ denote the signal space composed of spline functions of degree $(m-1)$ and be called a spline signal space of degree $(m-1)$. Then ${}^mS$ can be defined by

$${}^mS \triangleq \left[{}^m_{[b]}\psi_k \right]_{k=-\infty}^{\infty}, \quad {}^mS \subset L_2(\boldsymbol{R}) \tag{3.3}$$

based on the B-spline functions[105] of degree $(m-1)$

$$ {}^{m}_{[b]}\psi_k(t) \triangleq \int_{-\infty}^{\infty} \left(\frac{\sin \pi f h}{\pi f h} \right)^m e^{j2\pi f(t-kh)} df, \quad k = 0, \pm 1, \pm 2, \cdots. \tag{3.4} $$

The B-spline functions can be represented in the form of piecewise polynomials of degree $(m-1)$ as follows:

$$ {}^{m}_{[b]}\psi_k(t) = mh^{-m} \sum_{r=0}^{m} \frac{(-1)^r}{r!(m-r)!} (t - (r+k-m/2)h)_+^{m-1}, \tag{3.5} $$

$$ (t-a)_+^{m-1} \triangleq \begin{cases} (t-a)^{m-1}, & t > a \\ 0, & t \leq a, \end{cases} \tag{3.6} $$

which are $(m-2)$-times continuously differentiable. Here, h is a positive constant which means knots interval. Functions $\left\{ {}^{m}_{[b]}\psi_k \right\}_{k=-\infty}^{\infty}$ shall be called the B-spline basis of degree $(m-1)$.

In this section, the spline signal space ${}^{m}S$ has been prepared.

3.3 Formulation of Problem

In this section, the sampling theorem for the spline signal spaces is formulated.

The sampling theorem consists of two transforms: (i) the linear combination of the sampling basis weighted by sample values, and (ii) the integral transform to give sample values from signal. The transform (i) was formulated by showing the sampling basis in ${}^{m}S$ [114]. The transform (ii) can be formulated by introducing the concepts of the biorthonormal basis.

First, we formulate the transform (i). In the spline signal space ${}^{m}S$, the linear combination which reconstructs a waveform from sampled values is represented by

$$s(t) = \sum_{k=-\infty}^{\infty} \mu_k {}^m_{[s]}\psi_k(t), \quad (\mu_k = s(t_k), \quad t_k = kh) \tag{3.7}$$

for any $s \in {}^mS$, which is based on the sampling basis [114] $\left\{ {}^m_{[s]}\psi_k \right\}_{k=-\infty}^{\infty}$ for ${}^mS$:

$${}^m_{[s]}\psi_k(t) \triangleq \sum_{\ell=-\infty}^{\infty} {}^m\beta_{|\ell-k|} {}^m_{[b]}\psi_\ell(t). \tag{3.8}$$

Here, the coefficients $\{{}^m\beta_k\}_{k=-\infty}^{\infty}$ are defined as follows:

$${}^m\beta_k \triangleq h \int_{-h/2}^{h/2} {}^m_f B(f) e^{j2\pi fkh} df, \tag{3.9}$$

$${}^m_f B(f) \triangleq \frac{h}{\sum_{p=-\infty}^{\infty} \left\{ \frac{\sin \pi(fh-p)}{\pi(fh-p)} \right\}^m}. \tag{3.10}$$

Since the sampling basis directly gives an interpolant $s(t)$ of sampled values $\{\mu_k\}_{k=-\infty}^{\infty}$ in the form of linear combination (3.7), the sampling basis characterizes spline interpolation as its impulse response.

Next, we formulate the transform (ii) which gives sampled values from a waveform. In the band-limited signal space, the sampling basis $\left\{ \frac{\sin \pi(t/h-k)}{\pi(t/h-k)} \right\}_{k=-\infty}^{\infty}$ of Whittaker-Someya-Shannon consists of orthonormal systems. The transform (ii) for the band-limited signal s is simply performed by the following integral transform:

$$\mu_k = \left(s, \frac{\sin \pi(t/h-k)}{h\pi(t/h-k)} \right)_{L_2} \tag{3.11}$$

$$= \int_{-\infty}^{\infty} s(t) \frac{\sin \pi(t/h-k)}{h\pi(t/h-k)} dt, \quad \mu_k = s(t_k), \quad k = 0, \pm 1, \pm 2, \cdots. \tag{3.12}$$

In this chapter, following the above analogy, the transform (ii) for a spline function $s \in {}^mS$ is formulated by functions $\left\{ {}^m_{[s^\bullet]}\psi_k \right\}_{k=-\infty}^{\infty}$ in the form of the following integral

transform:

$$\mu_k = \left(s, {}^m_{[s^\bullet]}\psi_k\right)_{L_2} \tag{3.13}$$

$$= \int_{-\infty}^{\infty} s(t)\overline{{}^m_{[s^\bullet]}\psi_k(t)}dt, \quad \mu_k = s(t_k), \quad k = 0, \pm 1, \pm 2, \cdots. \tag{3.14}$$

In the spline signal spaces, the sampling basis $\left\{{}^m_{[s]}\psi_k\right\}_{k=-\infty}^{\infty}$ does not consist of orthonormal systems except $m = 1$ and $m \to \infty$. Then functions $\left\{{}^m_{[s^\bullet]}\psi_k\right\}_{k=-\infty}^{\infty}$, $\left({}^m_{[s^\bullet]}\psi_k \in {}^mS\right)$ should be derived newly. This integral kernel is a biorthonormal basis[122, 123] for the sampling basis. From eq.(3.14), this biorthonormal basis characterizes the transform (ii) as its impulse response.

The above transforms (i) and (ii) construct a Fourier-like expansion formula using sampled values as the expansion coefficients. When a given signal $u \in L_2(\boldsymbol{R})$ is not in ${}^mS$, the function $s \in {}^mS$ which is given by

$$\mu_k = \int_{-\infty}^{\infty} u(t)\overline{{}^m_{[s^\bullet]}\psi_k(t)}dt, \quad k = 0, \pm 1, \pm 2, \cdots, \tag{3.15}$$

$$s(t) = \sum_{k=-\infty}^{\infty} \mu_k {}^m_{[s]}\psi_k(t) \tag{3.16}$$

is the least mean square approximation of u in ${}^mS$ [122, 123]. This means that ${}^m_{[s^\bullet]}\psi_k(t)$ performs like a delta function in ${}^mS$ with some continuous differentiability.

In this section, the sampling theorem in ${}^mS$ was formulated. To complete the sampling theorem, the biorthonormal basis is derived in the following sections.

3.4 Derivation of biorthonormal basis

In this section, the biorthonormal basis for the sampling basis is derived in the spline signal space ${}^{m}S$. First, the existence of the biorthonormal basis and its uniqueness are shown, and the biorthonormal basis is derived.

3.4.1 Existence of biorthonormal basis

In this subsection, the existence of the biorthonormal basis and its uniqueness are investigated.

To show its existence and uniqueness, a coordinate system ${}^{m}\varphi_{[s]}$ for the sampling basis, a mapping ${}^{m}\varphi_{[s^\bullet]}$ which gives inner products of signal and the sampling functions, and a coordinate transform operator ${}^{m}G$ from ${}^{m}\varphi_{[s]}$ to ${}^{m}\varphi_{[s^\bullet]}$, are introduced.

The coordinate system ${}^{m}\varphi_{[s]}$ for the sampling basis is defined as follows: Let $\boldsymbol{\mu}$ denote a vector which is obtained by sampling $s \in {}^{m}S$ at the sampling point $\{t_k\}_{k=-\infty}^{\infty}$, ($t_k \triangleq kh,\ k = 0, \pm 1, \pm 2, \cdots$), *i.e.*

$$\boldsymbol{\mu} \triangleq [\cdots, \mu_{-2}, \mu_{-1}, \mu_0, \mu_1, \mu_2, \cdots]^T, \quad \mu_k = s(t_k), \tag{3.17}$$

and let ${}^{m}K_{[s]}$ denote the totality of $\boldsymbol{\mu}$. Then the coordinate system for the sampling basis ${}^{m}\varphi_{[s]} : {}^{m}S \to {}^{m}K_{[s]}$ is defined as a mapping satisfying

$${}^{m}\varphi_{[s]}(s) \triangleq \boldsymbol{\mu}. \tag{3.18}$$

And the space ${}^{m}K_{[s]}$ becomes the Hilbert space

$$\ell_2 = \left\{ \boldsymbol{v} \middle| \sum_{k=-\infty}^{\infty} |v_k|^2 < +\infty \right\} \tag{3.19}$$

with the inner product

$$(\boldsymbol{v}, \boldsymbol{w})_{\ell_2} = \sum_{k=-\infty}^{\infty} v_k \overline{w_k}. \tag{3.20}$$

The coordinate system ${}^m\varphi_{[s]}$ is an isomorphic mapping between $s \in {}^mS$ which is bounded in the sense of L_2 norm and $\boldsymbol{\mu}$ which is bounded in the sense of ℓ_2 norm [114].

The mapping ${}^m\varphi_{[s^\bullet]}$ from signal $s \in {}^mS$ to the inner products of s and sampling functions ${}^m_{[s]}\psi_k$, $k = 0, \pm 1, \pm 2, \cdots$ is defined as follows: Let $\boldsymbol{\eta}$ denote a vector

$$\boldsymbol{\eta} \triangleq [\cdots, \eta_{-2}, \eta_{-1}, \eta_0, \eta_1, \eta_2, \cdots]^T \tag{3.21}$$

which is composed of inner products of $s \in {}^mS$ and ${}^m_{[s]}\psi_k$, *i.e.*

$$\eta_k = \left(s, {}^m_{[s]}\psi_k\right)_{L_2} = \int_{-\infty}^{\infty} s(t)\overline{{}^m_{[s]}\psi_k(t)}dt, \quad k = 0, \pm 1, \pm 2, \cdots, \tag{3.22}$$

and let ${}^mK_{[s^\bullet]}$ denote the totality of $\boldsymbol{\eta}$. Then ${}^m\varphi_{[s^\bullet]} : {}^mS \to {}^mK_{[s^\bullet]}$ is defined as a mapping which satisfying

$${}^m\varphi_{[s^\bullet]}(s) \triangleq \boldsymbol{\eta} \tag{3.23}$$

for any $s \in {}^mS$.

Next, the coordinate transform operator ${}^mG$ from ${}^m\varphi_{[s]}$ to ${}^m\varphi_{[s^\bullet]}$ is defined as follows:

$${}^mG \triangleq {}^m\varphi_{[s^\bullet]}{}^m\varphi_{[s]}{}^{-1}. \tag{3.24}$$

The coordinate transform operator ${}^mG : {}^mK_{[s]} \to {}^mK_{[s^\bullet]}$ is represented as a matrix of infinite dimension. The mutual relation among ${}^m\varphi_{[s]}$, ${}^m\varphi_{[s^\bullet]}$ and ${}^mG$ is illustrated in

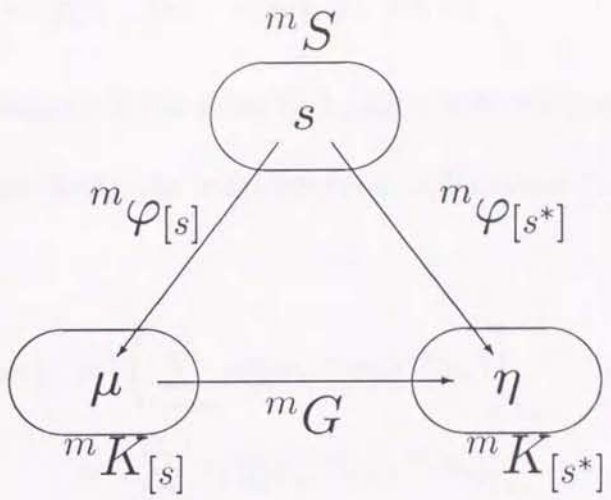

Figure 3.1: Mutual relation between $^{m}\varphi_{[s]}$, $^{m}\varphi_{[s^\bullet]}$ and ^{m}G.

Fig.3.1. In the following part, we investigate the existence of the biorthonormal basis and its uniqueness by using relations among $^{m}\varphi_{[s]}$, $^{m}\varphi_{[s^\bullet]}$ and ^{m}G.

The following lemma shows the sufficient condition for the existence of the biorthonormal basis and its uniqueness in terms of $^{m}\varphi_{[s^\bullet]}$.

Lemma 9 *if $^{m}\varphi_{[s^\bullet]}$ is an isomorphic mapping, the biorthonormal basis $\left\{ {}^{m}_{[s^\bullet]}\psi_k \right\}_{k=-\infty}^{\infty}$ exists uniquely and it is represented by*

$$ {}^{m}_{[s^\bullet]}\psi_k = {}^{m}\varphi_{[s^\bullet]}{}^{-1}(\boldsymbol{e}_k), \quad k = 0, \pm 1, \pm 2, \cdots, \tag{3.25} $$

where $\boldsymbol{e}_k$ is a column vector which has unit value at k-th components and zero's at other components.

(Proof) If the mapping $^{m}\varphi_{[s^\bullet]}$ is an isomorphic mapping, functions $\left\{ {}^{m}_{[s^\bullet]}\psi_k \right\}_{k=-\infty}^{\infty}$ defined by

$$ {}^{m}_{[s^{\bullet}]}\psi_k = {}^{m}\varphi_{[s^{\bullet}]}{}^{-1}(\boldsymbol{e}_k), \quad k = 0, \pm 1, \pm 2, \cdots \tag{3.26} $$

which are bounded in the sense of L_2 norm exist uniquely in ${}^{m}S$.

By using eq.(3.23), the inner products of functions ${}^{m}_{[s^{\bullet}]}\psi_k$ and $s \in {}^{m}S$ are evaluated as follows:

$$ \begin{aligned} \left(s, {}^{m}_{[s^{\bullet}]}\psi_k\right) &= \left(\sum_{\ell=-\infty}^{\infty} \mu_\ell {}^{m}_{[s]}\psi_k, {}^{m}\varphi_{[s^{\bullet}]}{}^{-1}(\boldsymbol{e}_k) \right)_{L_2} \\ &= \sum_{\ell=-\infty}^{\infty} \mu_\ell \left({}^{m}_{[s]}\psi_k, {}^{m}\varphi_{[s^{\bullet}]}{}^{-1}(\boldsymbol{e}_k) \right)_{L_2} \\ &= \sum_{\ell=-\infty}^{\infty} \mu_\ell \boldsymbol{e}_\ell^T \overline{\left({}^{m}\varphi_{[s^{\bullet}]} {}^{m}\varphi_{[s^{\bullet}]}{}^{-1}(\boldsymbol{e}_k) \right)} \\ &= \sum_{\ell=-\infty}^{\infty} \mu_\ell \boldsymbol{e}_\ell^T \boldsymbol{e}_k \\ &= \mu_k. \end{aligned} $$

Thus functions $\left\{ {}^{m}_{[s^{\bullet}]}\psi_k \right\}_{k=-\infty}^{\infty}$ construct the biorthonormal basis.

Assume that functions $\{\phi_k\}_{k=-\infty}^{\infty}$ other than $\left\{ {}^{m}_{[s^{\bullet}]}\psi_k \right\}_{k=-\infty}^{\infty}$ satisfy

$$ (s, \phi_k)_{L_2} = \mu_k, \quad \phi_k \in {}^{m}S, \quad k = 0, \pm 1, \pm 2, \cdots, \tag{3.27} $$

we have

$$ (s, \phi_k)_{L_2} - \left(s, {}^{m}_{[s^{\bullet}]}\psi_k\right)_{L_2} = 0 \tag{3.28} $$

$$ \left(s, \phi_k - {}^{m}_{[s^{\bullet}]}\psi_k\right)_{L_2} = 0, \tag{3.29} $$

for any $s \in {}^{m}S$ and

$$ \phi_k = {}^{m}_{[s^{\bullet}]}\psi_k, \quad k = 0, \pm 1, \pm 2, \cdots. \tag{3.30} $$

Therefore, the biorthonormal basis $\left\{ {}^{m}_{[s^{\bullet}]}\psi_k \right\}_{k=-\infty}^{\infty}$ exists uniquely.

■

From Lemma 9, ${}^m\varphi_{[s^*]}$ should be an isomorphic mapping for the existence of the biorthonormal basis and its uniqueness.

The following lemma shows the relation between ${}^m\varphi_{[s^*]}$ and ${}^mG$.

Lemma 10 *The following two conditions are equivalent:*

(i) *The mapping* ${}^m\varphi_{[s^*]}$ *is an isomorphic mapping,*

(ii) *The mapping* ${}^mG$ *is an isomorphic mapping.*

(Proof) (i) Assume that the mapping ${}^m\varphi_{[s^*]}$ is an isomorphic mapping. Then ${}^mG$ and ${}^mG^{-1}$ is represented by

$$
\begin{aligned}
{}^mG &= {}^m\varphi_{[s^*]}{}^m\varphi_{[s]}{}^{-1}, \\
{}^mG^{-1} &= {}^m\varphi_{[s]}{}^m\varphi_{[s^*]}{}^{-1},
\end{aligned}
$$

respectively. Now, the mapping ${}^m\varphi_{[s]}$ is an isomorphic mapping, then ${}^mG$ is also an isomorphic mapping.

(ii) Assume that ${}^mG$ is an isomorphic mapping. Then the mapping ${}^m\varphi_{[s^*]}$ and ${}^m\varphi_{[s]}{}^{-1}$ is represented by

$$
\begin{aligned}
{}^m\varphi_{[s^*]} &= {}^mG{}^m\varphi_{[s]}, \\
{}^m\varphi_{[s^*]}{}^{-1} &= {}^m\varphi_{[s]}{}^{-1}{}^mG^{-1},
\end{aligned}
$$

respectively. Now, the mapping ${}^m\varphi_{[s]}$ is an isomorphic mapping, ${}^m\varphi_{[s^*]}$ is also an isomorphic mapping.

■

The following proposition shows the necessary and sufficient condition for the existence of the biorthonormal basis and its uniqueness.

Proposition 7 *If the matrix ${}^{m}G$ is an isomorphic mapping, the biorthonormal basis* $\left\{ {}^{m}_{[s^{\bullet}]}\psi_k \right\}_{k=-\infty}^{\infty}$ *exists uniquely and it is represented by*

$$ {}^{m}_{[s^{\bullet}]}\psi_k = {}^{m}\varphi_{[s]}{}^{-1\,m}G^{-1}(\boldsymbol{e}_k), \quad k = 0, \pm 1, \pm 2, \cdots, \tag{3.31} $$

where $\boldsymbol{e}_k$ is a column vector which has unit value at k-th components and zero's at other components.

(Proof) From Lemma 9 and Lemma 10, Proposition 7 holds obviously.

■

The following lemma shows a frequency characteristics of ${}^{m}G$ to investigate whether ${}^{m}G$ is an isomorphic mapping or not.

Lemma 11 *The frequency characteristics ${}^{m}_{f}G(f)$ of the matrix ${}^{m}G$ is represented by*

$$ {}^{m}_{f}G(f) = \frac{1}{h} \sum_{q=-\infty}^{\infty} \left\{ \left(\frac{\sin \pi(fh+q)}{\pi(fh+q)} \right)^{2m} {}^{m}_{f}B(f+q/h)^2 \right\}. \tag{3.32} $$

(Proof) Since $s \in {}^{m}S$ is represented by

$$ s(t) = \sum_{k=-\infty}^{\infty} \mu_k {}^{m}_{[s]}\psi_k(t), \quad \mu_k = s(t_k), \quad k = 0, \pm 1, \pm 2, \cdots, \tag{3.33} $$

the ℓ-th component of $\boldsymbol{\eta} = {}^{m}\varphi_{[s^{\bullet}]}(s)$ is represented by

$$\begin{aligned}
\eta_\ell &= \left(s, {}^{m}_{[s]}\psi_\ell\right)_{L_2} \\
&= \left(\sum_{k=-\infty}^{\infty} \mu_k {}^{m}_{[s]}\psi_k, {}^{m}_{[s]}\psi_\ell\right)_{L_2} \\
&= \sum_{k=-\infty}^{\infty} \left({}^{m}_{[s]}\psi_k, {}^{m}_{[s]}\psi_\ell\right)_{L_2} \mu_k. \qquad (3.34)
\end{aligned}$$

The inner product $\left({}^{m}_{[s]}\psi_k, {}^{m}_{[s]}\psi_\ell\right)_{L_2}$ in eq.(3.34) is rearranged as follows:

$$\begin{aligned}
\left({}^{m}_{[s]}\psi_k, {}^{m}_{[s]}\psi_\ell\right)_{L_2} &= \int_{-\infty}^{\infty} {}^{m}_{[s]}\psi_k(t)\overline{{}^{m}_{[s]}\psi_\ell(t)}dt \\
&= \int_{-\infty}^{\infty} {}^{m}_{[s]}\psi_0(t-kh)\overline{{}^{m}_{[s]}\psi_0(t-\ell h)}dt \\
&= \int_{-\infty}^{\infty} {}^{m}_{[s]}\psi_0(t){}^{m}_{[s]}\psi_0((\ell-k)h-t)dt. \qquad (3.35)
\end{aligned}$$

Using Fourier transform of ${}^{m}_{[s]}\psi_0(t)$, i.e.

$$\begin{aligned}
{}^{m}_{[s]}\Psi(f) &= \int_{-\infty}^{\infty} {}^{m}_{[s]}\psi_0(t)e^{-j2\pi ft}dt \\
&= \left(\frac{\sin \pi fh}{\pi fh}\right)^{m} {}^{m}_{f}B(f),
\end{aligned}$$

eq.(3.35) is rearranged by the convolution theorem in Fourier transform as follows:

$$\begin{aligned}
\left({}^{m}_{[s]}\psi_k, {}^{m}_{[s]}\psi_\ell\right)_{L_2} &= \int_{-\infty}^{\infty} {}^{m}_{[s]}\Psi(f){}^{m}_{[s]}\Psi(f)e^{j2\pi f(\ell-k)h}df \\
&= \int_{-\infty}^{\infty} \left(\frac{\sin \pi fh}{\pi fh}\right)^{2m} {}^{m}_{f}B(f)^2 e^{j2\pi f(\ell-k)h}df. \qquad (3.36)
\end{aligned}$$

By substituting eq.(3.34) for η_ℓ, discrete Fourier transform $E(f)$ of $\boldsymbol{\eta}$, i.e.

$$E(f) = \sum_{\ell=-\infty}^{\infty} \eta_\ell e^{-j2\pi f\ell h} \qquad (3.37)$$

is evaluated as follows:

$$
\begin{aligned}
E(f) &= \sum_{\ell=-\infty}^{\infty} \left\{ \sum_{k=-\infty}^{\infty} \left({}^{m}_{[s]}\psi_k, {}^{m}_{[s]}\psi_\ell \right)_{L_2} \mu_k \right\} e^{-j2\pi f \ell h} \\
&= \sum_{\ell=-\infty}^{\infty} \sum_{k=-\infty}^{\infty} \left\{ \int_{-\infty}^{\infty} \left(\frac{\sin \pi f' h}{\pi f' h} \right)^{2m} {}^{m}_{f}B(f')^2 e^{j2\pi f'(\ell-k)h} df' \mu_k \right\} e^{-j2\pi f \ell h} \\
&= \left\{ \sum_{k=-\infty}^{\infty} \mu_k e^{-j2\pi f k h} \right\} \\
&\quad \left\{ \sum_{\ell=-\infty}^{\infty} \int_{-\infty}^{\infty} \left(\frac{\sin \pi f' h}{\pi f' h} \right)^{2m} {}^{m}_{f}B(f')^2 e^{j2\pi f'(\ell-k)h} df' \right\} e^{-j2\pi f(\ell-k)h} \\
&= M(f) \int_{-\infty}^{\infty} \left(\frac{\sin \pi f' h}{\pi f' h} \right)^{2m} {}^{m}_{f}B(f')^2 \left\{ \sum_{p=-\infty}^{\infty} e^{j2\pi(f'-f)ph} \right\} df', \quad (p = \ell - k),
\end{aligned}
$$

where $M(f)$ denote discrete Fourier transform $\boldsymbol{\mu}$, i.e.

$$
M(f) = \sum_{k=-\infty}^{\infty} \mu_k e^{-j2\pi f k h}. \tag{3.38}
$$

By using equality

$$
\sum_{p=-\infty}^{\infty} e^{j2\pi(f'-f)ph} = \frac{1}{h} \sum_{q=-\infty}^{\infty} \delta(f' - f - q/h) \tag{3.39}
$$

which is held in Fourier transform,

$$
\begin{aligned}
E(f) &= M(f) \int_{-\infty}^{\infty} \left(\frac{\sin \pi f' h}{\pi f' h} \right)^{2m} {}^{m}_{f}B(f')^2 \left\{ \frac{1}{h} \sum_{q=-\infty}^{\infty} \delta(f' - f - q/h) \right\} df' \\
&= M(f) \left\{ \frac{1}{h} \sum_{q=-\infty}^{\infty} \left(\frac{\sin \pi(fh+q)}{\pi(fh+q)} \right)^{2m} {}^{m}_{f}B(f + q/h)^2 \right\}.
\end{aligned}
$$

Therefore, the frequency characteristics ${}^{m}_{f}G$ of ${}^{m}G$ is represented by

$$
\begin{aligned}
{}^{m}_{f}G(f) &= E(f)/M(f) \\
&= \left\{ \frac{1}{h} \sum_{q=-\infty}^{\infty} \left(\frac{\sin \pi(fh+q)}{\pi(fh+q)} \right)^{2m} {}^{m}_{f}B(f + q/h)^2 \right\}.
\end{aligned}
$$

■

From Proposition 7 and Lemma 11, the existence of the biorthonormal basis and its uniqueness is shown by the following theorem.

Theorem 5 *In the spline signal space ${}^mS$, the biorthonormal basis $\left\{{}^m_{[s\bullet]}\psi_k\right\}_{k=-\infty}^{\infty}$ for the sampling basis exists uniquely.*

(Proof) Since the frequency characteristics ${}^m_fB(f+q/h)$ in eq.(3.32) is bounded from eq.(3.10) if m is bounded, ${}^m_fG(f)$ is bounded and non-zero for any f. Thus the mean square norms of the frequency characteristics for ${}^m_fG$

$$h\int_{-1/2h}^{1/2h}\left|{}^m_fG(f)\right|^2 df \tag{3.40}$$

and $1/{}^m_fG(f)$

$$h\int_{-1/2h}^{1/2h}\left|\frac{1}{{}^m_fG(f)}\right|^2 df \tag{3.41}$$

are bounded, respectively. And by the fact that

$$\begin{aligned} E(f) &= {}^m_fG(f)M(f) \\ M(f) &= E(f)/{}^m_fG(f) \end{aligned}$$

and that discrete Fourier transform preserves mean square norm, ${}^mG$ is bounded in the sense of ℓ_2 norm. Thus, ${}^mG$ is an isomorphic mapping.

Therefore, from Proposition 7, the biorthonormal basis exists in ${}^mS$.

■

In this subsection, the existence of the biorthonormal basis and its uniqueness were shown. The biorthonormal basis is derived by using the matrix ${}^mG$ in the next subsection.

3.4.2 Derivation of biorthonormal basis

In this subsection, the biorthonormal basis in ${}^mS$ is derived by using the matrix ${}^mG$.

The following lemma shows the operation of the matrix ${}^mG^{-1}$.

Lemma 12 *The matrix* ${}^mG^{-1}$ *maps* $\boldsymbol{\eta}$ *to* $\boldsymbol{\mu}$ *in the following manner:*

$$\mu_\ell = \sum_{k=-\infty}^{\infty} {}^m g_{\ell-k}\eta_k, \quad \boldsymbol{\mu} \in {}^mK_{[s]}, \quad \boldsymbol{\eta} \in {}^mK_{[s^\bullet]}, \ell = 0, \pm 1, \pm 2, \cdots, \tag{3.42}$$

where the coefficients $\{{}^m g_\ell\}_{\ell=-\infty}^{\infty}$ *are represented by*

$${}^m g_\ell = h\int_{-1/2h}^{1/2h} {}^m_f G^{-1} e^{j2\pi f\ell h} df, \quad \ell = 0, \pm 1, \pm 2, \cdots. \tag{3.43}$$

(Proof) The frequency characteristics $1/{}^m_f G(f)$ of ${}^mG^{-1}$ and discrete Fourier transforms $M(f) and E(f)$ of $\boldsymbol{\mu}$ and $\boldsymbol{\eta}$ hold the equation:

$$M(f) = {}^m_f G^{-1}(f)E(f). \tag{3.44}$$

By denoting inverse discrete Fourier transform of $1/{}^m_f G(f)$

$${}^m g_\ell = h\int_{-1/2h}^{1/2h} {}^m_f G^{-1}(f) e^{j2\pi f\ell h} df, \tag{3.45}$$

the convolution theorem in discrete Fourier transform leads that

$$\mu_\ell = \sum_{k=-\infty}^{\infty} {}^m g_{\ell-k}\eta_k. \tag{3.46}$$

■

By using ${}^m_f G^{-1}$ of Lemma 12, the biorthonormal basis in the spline signal space ${}^m S$ is given in the following theorem.

Theorem 6 *In the spline signal space ${}^m S$, the biorthonormal basis $\left\{ {}^m_{[s^\bullet]}\psi_k \right\}_{k=-\infty}^{\infty}$ for the sampling basis is represented by*

$$ {}^m_{[s^\bullet]}\psi_k(t) = \sum_{\ell=-\infty}^{\infty} {}^m g_{|\ell-k|} {}^m_{[s]}\psi_\ell(t). \tag{3.47} $$

(Proof) From eq.(3.31), $\left\{ {}^m_{[s^\bullet]}\psi_\ell \right\}_{\ell=-\infty}^{\infty}$ is represented by

$$ \begin{aligned} {}^m_{[s^\bullet]}\psi_\ell &= {}^m\varphi_{[s]} {}^{-1m}G^{-1}(\boldsymbol{e}_\ell) \\ &= \sum_{k=-\infty}^{\infty} \boldsymbol{e}_k^T \left({}^m G^{-1}(\boldsymbol{e}_\ell) \right) {}^m_{[s]}\psi_k. \end{aligned} $$

Therefore, by expanding ${}^m G^{-1}$ following eq.(3.42) in Lemma 12, ${}^m_{[s^\bullet]}\psi_\ell$ is represented by

$$ \begin{aligned} {}^m_{[s^\bullet]}\psi_\ell &= \sum_{k=-\infty}^{\infty} \left\{ \sum_{p=-\infty}^{\infty} {}^m g_{k-p} \boldsymbol{e}_p^T \boldsymbol{e}_\ell \right\} {}^m_{[s]}\psi_k \\ &= \sum_{k=-\infty}^{\infty} {}^m g_{k-\ell} {}^m_{[s]}\psi_k. \end{aligned} $$

■

Figure 3.2 shows examples of functions ${}^m_{[s^\bullet]}\psi_k$ composing the biorthonormal basis.

In this subsection, the biorthonormal basis for the sampling basis was derived in the spline signal space ${}^m S$. This basis characterizes the sampling operation in the spline signal space.

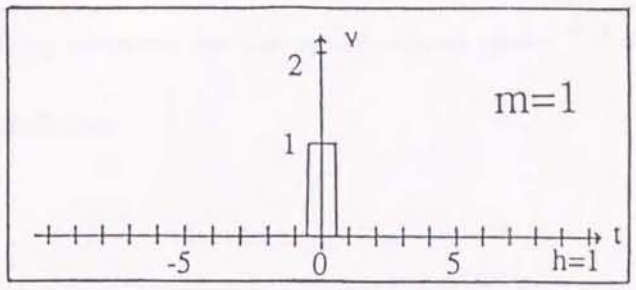

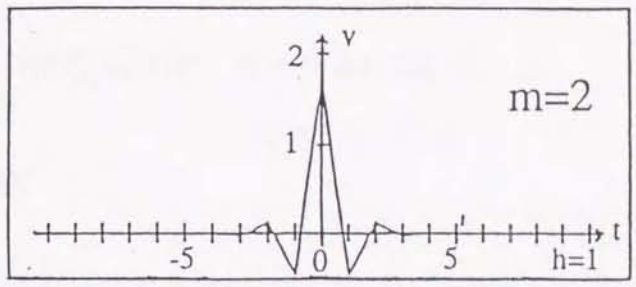

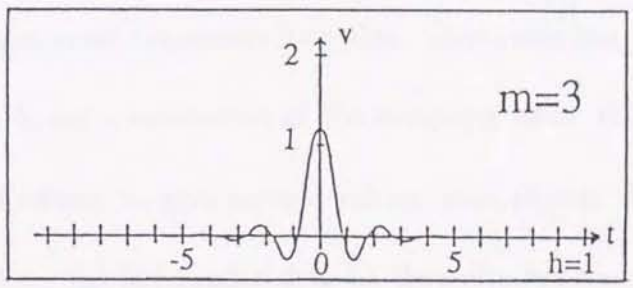

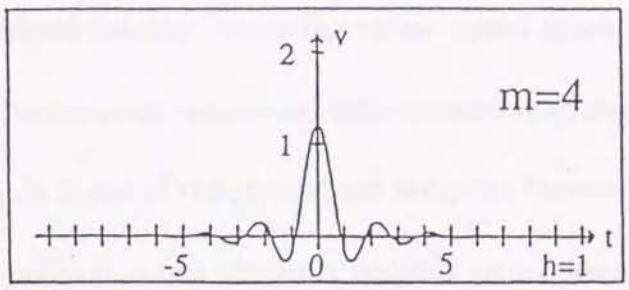

Figure 3.2: Examples of functions composing the biorthonormal basis for ${}^{m}S$ $\left(v = {}^{m}_{[s^{\bullet}]}\psi_0(t)\right)$.

The biorthonormal basis derived in this section and the sampling basis derived in [114] complete the sampling theorem for the spline signal space ${}^{m}S$ of degree $(m-1)$. They are summarized as follows:

For $s \in {}^{m}S$;

$$s(t) = \sum_{k=-\infty}^{\infty} \mu_k {}^{m}_{[s]}\psi_k(t), \quad \mu_k = s(t_k), \quad t_k = kh, \tag{3.48}$$

$$\mu_k = \int_{-\infty}^{\infty} s(t) \overline{{}^{m}_{[s^*]}\psi_k(t)} dt, \quad k = 0, \pm 1, \pm 2, \cdots. \tag{3.49}$$

3.5 Summary

In this chapter, the sampling theorem for the spline signal space was completed by deriving the biorthonormal expansion formulas. This sampling theorem consists of two transforms: (i) the linear combination of the sampling basis weighted by sample values, (ii) the integral transform to give sample values from signal. The biorthonormal basis constructing transform (ii) is considered to be the delta function at sampling point with some continuous differentiability. Since the spline signal space generalizes band-limited the signal space in the terms of continuous differentiability of signals, the derived Fourier-like expansion formula is one of the generalized sampling theorems to Whittaker-Someya-Shannon's. It is possible to select the most suitable signal space out of the spline signal spaces which connect the signal space of staircase functions and that of Fourier functions.

Part IV

Relations between Biorthonormal Functions and Delta Function

In Part IV, relations between biorthonormal functions and delta function are discussed in terms of the reproducing kernel for spline functions. The class of spline functions are limited to the infinite open domain.

In Chapter 4, a reproducing kernel for spline signal space is derived. The reproducing kernel is considered to be a delta function with some continuous differentiability in spline signal space. The uniform convergence of spline approximation is easily proven by using the reproducing kernel.

Chapter 4

Reproducing Kernel for Spline Functions

4.1 Introduction

In this chapter, we shall deal with the problem to derive cardinal spline $K(x,\xi)$, $s.t.\ K(\cdot,\xi) \in S_n$ for $\forall \xi \in \mathbf{R}$ and $K(x,\cdot) \in S_n$ for $\forall x \in \mathbf{R}$ which satisfies

$$\int_{-\infty}^{\infty} K(x,\xi)s(x)dx = s(\xi), \quad (\xi \in \mathbf{R}) \tag{4.1}$$

in function space S_n spanned by square-integrable cardinal spline s of degree n [105]. This integral kernel is a reproducing kernel for the function space S_n of cardinal splines. Authors derived an integral transform which transforms $s \in S_n$ to $\{s(k)\}_{k=-\infty}^{\infty} \in \ell^2$ in Ref.[5, 13, 12]. But the transform can perform like delta function for $\forall s \in S_n$ only at $(x = k,\ k \in \mathbf{Z})$. On the other hand, eq.(4.1) means that the reproducing kernel for S_n can perform like delta functions at any points.

Based on the theory of reproducing kernel [141], reproducing kernel has the meaning that the cardinal spline s of degree n which approximates $\forall y \in L_2(\mathbf{R})$ in the sense of least square error, *i.e.*,

$$\int_{-\infty}^{\infty} |y(x) - s(x)|^2 dx \to \min., \tag{4.2}$$

is given by

$$s(\xi) = \int_{-\infty}^{\infty} K(x,\xi) y(x) dx, \tag{4.3}$$

in the Hilbert space

$$L^2(\mathbf{R}) \triangleq \left\{ y \middle| \int_{-\infty}^{\infty} |y(x)|^2 dx < +\infty \right\}, \tag{4.4}$$

with inner product

$$(y,z)_{L^2} \triangleq \int_{-\infty}^{\infty} y(x)\overline{z(x)} dx. \tag{4.5}$$

In a function space composed of spline functions of degree $(2k-1)$ with knots $\{x_\ell\}_{\ell=0}^{I}, (a \leq x_1 < x_2 < \cdots < x_I \leq b; 1 \leq J \leq I)$ on $\mathbf{R}$, reproducing kernel was derived [107] with respect to inner product

$$(y,z) = \sum_{\ell=1}^{J} y(x_\ell) z(x_\ell) + \int_a^b y^{(J)}(x) z^{(J)}(x) dx. \tag{4.6}$$

However, in function space of cardinal splines, reproducing kernel has not been derived with respect to the most fundamental inner product $(\cdot,\cdot)_{L^2}$. This is the first approach to derive the reproducing kernel $K(x,\xi)$ for S_n as the solution of integral equation (4.1).

4.2 Preliminaries

The cardinal spline function space

$$S_n \triangleq \left\{ s \middle| s(x) = \sum_{k \in \mathbf{Z}} c_k B_n(x-k), \quad \{c_k\}_{k \in \mathbf{Z}} \in \ell^2 \right\} \tag{4.7}$$

generated by the B-spline function of degree n [105]

$$B_n(x) \triangleq \frac{1}{2\pi} \int_{-\infty}^{\infty} \left[\frac{2\sin(u/2)}{u} \right]^{n+1} e^{iux} du, \quad (n = 0, 1, 2, \cdots; x \in \mathbf{R}) \tag{4.8}$$

is a subspace of $L^2(\mathbf{R})$ [105, Lecture 4].

4.3 Reproducing kernel for cardinal splines

Theorem 7 *Reproducing kernel $K(x, \xi)$ satisfying*

$$\int_{-\infty}^{\infty} K(x, \xi) s(x) dx = s(\xi), \quad (\xi \in \mathbf{R}) \quad \textit{for} \ \ \forall s \in S_n \tag{4.9}$$

is given by

$$K(x, \xi) = \sum_{k \in \mathbf{Z}} \sum_{\ell \in \mathbf{Z}} v_{k-\ell} B_n(x-k) B_n(\xi - \ell), \tag{4.10}$$

where

$$v_r = \frac{1}{2\pi} \int_{-\pi}^{\pi} \frac{e^{iur}}{[2\sin(u/2)]^{2n+2} \sum_{q \in \mathbf{Z}} (u + 2\pi q)^{-(2n+2)}} du, \quad (r \in \mathbf{Z}). \tag{4.11}$$

Proof. Reproducing kernel $K(x, \xi)$ is represented in the form

$$K(x, \xi) \ = \ \sum_{k \in \mathbf{Z}} \sum_{\ell \in \mathbf{Z}} w_{k,\ell} B_n(x-k) B_n(\xi - \ell), \tag{4.12}$$

because reproducing kernel $K(x,\xi)$ should satisfy $K(\cdot,\xi) \in S_n$ and $K(x,\cdot) \in S_n$. Any function $s \in S_n$ is represented in the form $s(x) = \sum_{p\in\mathbf{Z}} \lambda_p B_n(x-p)$, $\{\lambda_p\}_{p=-\infty}^{\infty} \in \ell^2$. Substituting it for s in eq.(4.9), eq.(4.9) can be rearranged as follows:

$$\begin{aligned}
\int_{-\infty}^{\infty} \sum_{k\in\mathbf{Z}} \sum_{\ell\in\mathbf{Z}} w_{k,\ell} B_n(x-k) B_n(\xi-\ell) \sum_{p\in\mathbf{Z}} \lambda_p B_n(x-p) dx &= \sum_{p\in\mathbf{Z}} \lambda_p B_n(\xi-p), \\
\sum_{p\in\mathbf{Z}} \lambda_p \left[\sum_{k\in\mathbf{Z}} \sum_{\ell\in\mathbf{Z}} w_{k,\ell} \int_{-\infty}^{\infty} B_n(x-k) B_n(x-p) B_n(\xi-\ell) dx \right] &= \sum_{p\in\mathbf{Z}} \lambda_p B_n(\xi-p), \\
\sum_{p\in\mathbf{Z}} \lambda_p \left[\sum_{k\in\mathbf{Z}} \sum_{\ell\in\mathbf{Z}} w_{k,\ell} B_{2n+1}(p-k) B_n(\xi-\ell) \right] &= \sum_{p\in\mathbf{Z}} \lambda_p B_n(\xi-p).
\end{aligned}$$

Since $\{\lambda_p\}_{p=-\infty}^{\infty}$ is an arbitrary element in ℓ^2, we can further reduce it to the simultaneous equations

$$\sum_{k\in\mathbf{Z}} \sum_{\ell\in\mathbf{Z}} w_{k,\ell} B_{2n+1}(p-k) B_n(\xi-\ell) = B_n(\xi-p), \quad (p \in \mathbf{Z}). \tag{4.13}$$

The Fourier characteristic functions of the both sides of eq.(4.13) becomes

$$\begin{aligned}
\sum_{p\in\mathbf{Z}} \left[\sum_{k\in\mathbf{Z}} \sum_{\ell\in\mathbf{Z}} w_{k,\ell} B_{2n+1}(p-k) B_n(\xi-\ell) \right] e^{-iup} &= \sum_{p\in\mathbf{Z}} B_n(\xi-p) e^{-iup}, \\
\left[\sum_{q\in\mathbf{Z}} B_{2n+1}(q) e^{-iuq} \right] \left[\sum_{k\in\mathbf{Z}} \left\{ \sum_{\ell\in\mathbf{Z}} w_{k,\ell} B_n(\xi-\ell) \right\} e^{-iuk} \right] &= \sum_{p\in\mathbf{Z}} B_n(\xi-p) e^{-iup}.
\end{aligned}$$

Using the convolution theorem in Fourier transform, it holds good that

$$\begin{aligned}
\sum_{\ell\in\mathbf{Z}} w_{k,\ell} B_n(\xi-\ell) &= \frac{1}{2\pi} \int_{-\pi}^{\pi} \left[\frac{1}{\sum_{q\in\mathbf{Z}} B_{2n+1}(q) e^{-iuq}} \right] \left[\sum_{p\in\mathbf{Z}} B_n(\xi-p) e^{-iup} \right] e^{iuk} du, \quad (k \in \mathbf{Z}) \\
&= \sum_{\ell\in\mathbf{Z}} \left[\frac{1}{2\pi} \int_{-\pi}^{\pi} \frac{e^{iu(k-\ell)}}{\sum_{q\in\mathbf{Z}} B_{2n+1}(q) e^{-iuq}} du \right] \left[\frac{1}{2\pi} \int_{-\pi}^{\pi} \sum_{p\in\mathbf{Z}} B_n(\xi-p) e^{-iup} e^{iu\ell} du \right]. \quad (4.14)
\end{aligned}$$

Using Dirac's delta functions, it holds good that

$$\begin{aligned}
\frac{1}{2\pi}\int_{-\pi}^{\pi}\sum_{p\in\mathbf{Z}} B_n(\xi-p)e^{-iup}e^{iu\ell}du &= \frac{1}{2\pi}\int_{-\pi}^{\pi}\int_{-\infty}^{\infty} B_n(x)\left[\sum_{p\in\mathbf{Z}}\delta(x-\xi+p)\right]e^{iux}dx e^{-iu\xi}e^{iu\ell}du \\
&= \frac{1}{2\pi}\int_{-\infty}^{\infty} B_n(x)\left[\sum_{p\in\mathbf{Z}}\delta(x-\xi+p)\right]\int_{-\pi}^{\pi} e^{iu(x-\xi+\ell)}dxdu \\
&= \sum_{p\in\mathbf{Z}} B_n(\xi-p)\frac{1}{2\pi}\int_{-\pi}^{\pi} e^{iu(-p+\ell)}du \\
&= B_n(\xi-\ell). \qquad (4.15)
\end{aligned}$$

Substitute eq.(4.14) and eq.(4.15) for eq.(4.12). Then $K(x,\xi)$ is represented in the form

$$\begin{aligned}
K(x,\xi) &= \sum_{k\in\mathbf{Z}}\sum_{\ell\in\mathbf{Z}} w_{k,\ell}B_n(x-k)B_n(\xi-\ell) \\
&= \sum_{k\in\mathbf{Z}}\left[\sum_{\ell\in\mathbf{Z}}\left\{\frac{1}{2\pi}\int_{-\pi}^{\pi}\frac{e^{iu(k-\ell)}}{\sum_{q\in\mathbf{Z}} B_{2n+1}(q)e^{-iuq}}du\right\}B_n(\xi-\ell)\right]B_n(x-k) \\
&= \sum_{k\in\mathbf{Z}}\sum_{\ell\in\mathbf{Z}}\left[\frac{1}{2\pi}\int_{-\pi}^{\pi}\frac{e^{iu(k-\ell)}}{\sum_{q\in\mathbf{Z}} B_{2n+1}(q)e^{-iuq}}du\right]B_n(x-k)B_n(\xi-\ell).
\end{aligned}$$

This means that $w_{k,\ell}$ is represented in the form

$$\begin{aligned}
w_{k,\ell} &= \frac{1}{2\pi}\int_{-\pi}^{\pi}\frac{e^{iu(k-\ell)}}{\sum_{q\in\mathbf{Z}} B_{2n+1}(q)e^{-iuq}}du \\
&= \frac{1}{2\pi}\int_{-\pi}^{\pi}\frac{e^{iu(k-\ell)}}{\sum_{q\in\mathbf{Z}}\left[\frac{2\sin(u/2+\pi q)}{u+2\pi q}\right]^2}du \\
&= \frac{1}{2\pi}\int_{-\pi}^{\pi}\frac{e^{iu(k-\ell)}}{[2\sin(u/2)]^{2n+2}\sum_{q\in\mathbf{Z}}(u+2\pi q)^{-2n-2}}du.
\end{aligned}$$

Let v_r be coefficients defined as follows:

$$v_r = \frac{1}{2\pi}\int_{-\pi}^{\pi}\frac{e^{iur}}{[2\sin(u/2)]^{2n+2}\sum_{q\in\mathbf{Z}}(u+2\pi q)^{-2n-2}}du.$$

The coefficients v_r satisfy

$$w_{k,\ell} = v_{k-\ell}, \quad (k, \ell \in \mathbf{Z}).$$

■

That formula is similar to the cardinal function of E. T. Whittaker [101]. In function space

$$W \triangleq \left\{ w \middle| \int_{-\infty}^{\infty} w(x) e^{-iux} dx = 0 \ \text{ if} |u| \geq \pi, \ w \in L^2(\mathbf{R}) \right\}, \tag{4.16}$$

the cardinal expansion

$$\int_{-\infty}^{\infty} \frac{\sin \pi(x-\xi)}{\pi(x-\xi)} w(x) dx = w(\xi), \quad (\xi \in \mathbf{R}) \tag{4.17}$$

holds good for $\forall w \in W$. Equation (4.17) is a kind of generalization of eq.(4.9) because the cardinal spline space approaches the cardinal function space when the degree n tends to infinity [105, Lecture 3].

The following two theorems are followed by Theorem 7

Theorem 8 *Function space S_n is a reproducing kernel Hilbert space with reproducing kernel $K(x, \xi)$.*

Proof. The function space S_n is a Hilbert space with inner product $(\cdot, \cdot)_{L^2}$. By using $K_\xi \in S_n$ defined by

$$K_\xi(\cdot) \triangleq K(\cdot, \xi), \tag{4.18}$$

we have the relation

$$\begin{aligned}(K_\xi, s)_{L^2} &= \int_{-\infty}^{\infty} K_\xi(x)s(x)dx \\ &= \int_{-\infty}^{\infty} K(x,\xi)s(x)dx \\ &= s(\xi)\end{aligned}$$

for any $s \in S_n$.

■

Theorem 9 *For any $s \in S_n$, its approximation given by*

$$\sum_{k=-N}^{N} s(k)^m_{[s]}\psi_k(x) \tag{4.19}$$

converges s uniformly, where ${}^m_{[s]}\psi_k(x), k = 0, \pm 1, \pm 2, \cdots$ are sampling functions for S_n.

Proof. For any $s \in S_n$, $\sum_{k=-N}^{N} s(k)^m_{[s]}\psi_k$ converges s in the sense of mean square norm by Ref. [5, 13, 12], *i.e.*,

$$\left\| s - \sum_{k=-N}^{N} s(k)^m_{[s]}\psi_k \right\|_{L^2} \to 0, \quad (N \to \infty). \tag{4.20}$$

By using K_ξ defined by

$$K_\xi(\cdot) = K(\cdot, \xi), \tag{4.21}$$

we have

$$\left| s(x) - \sum_{k=-N}^{N} s(k)_{[s]}^{m} \psi_k(x) \right| = \left| \left(K_x, s - \sum_{k=-N}^{N} s(k)_{[s]}^{m} \psi_k \right)_{L^2} \right|$$
$$\leq \|K_x\|_{L^2} \left\| s - \sum_{k=-N}^{N} s(k)_{[s]}^{m} \psi_k \right\|_{L^2}.$$

Therefore the approximation converges uniformly, *i.e.*,

$$\left| s(x) - \sum_{k=-N}^{N} s(k)_{[s]}^{m} \psi_k(x) \right| \to 0, \quad (N \to \infty). \tag{4.22}$$

■

4.4 Summary

In this chapter, reproducing kernel for cardinal splines was derived. This reproducing kernel obtains function values of $s \in S_n$ at any point $\xi \in \mathbf{R}$, while the mapping from $s \in S_n$ to its function values $\{s(k)\}_{k=-\infty}^{\infty} \in \ell^2$ performs like delta function only at sampling points $(x = k,\ k \in \mathbf{Z})$ for $\forall s \in S_n$ in [5, 13, 12]. This means that the reproducing kernel $k(x, \xi)$ shall be called delta-like function.

Part V

Numerical Analysis Based on Biorthonormal Expansion Formulas of Spline Functions

In Part V, a real-time spline approximation method is proposed and analyzed. The class of spline functions are limited to the infinite open domain.

In Chapter 5, a real-time spline approximation based on the biorthonormal expansion formula is derived. The approximation error is estimated for the practical use of spline approximation for digital signal processing. An example of the real-time approximation shows the effectiveness of the approximation method in the implementation of flexible signal processing with spline functions.

Chapter 5

A Real-time Spline Approximation with Biorthonormal Expansion

5.1 Introduction

Approximation by spline functions has been widely utilized in the compression of the data volume for figures, medical images and other graphic images. The spline approximation problem has been discussed mostly in terms of the B-spline [119, 121, 110]. The approximation method using the B-spline functions requires to solve simultaneous equations after the whole input data was observed. This means that the approximation cannot be obtained in real-time. Therefore, approximation using the B-spline functions cannot be applied in the fields where the approximation result needs to be obtained in real-time for the input signal.

In this chapter, a spline approximation method is proposed, which can obtain the approximation result in real-time, based on the biorthonormal expansion formulas.

In the previous chapters, the Fourier-like expansion formulas composed of the sam-

pling basis and its biorthonormal basis were obtained for spline signal spaces, which constitute sampling theorems. In this chapter, by truncating the sampling basis and its biorthonormal basis with finite length, a least square approximation method which obtains approximation result in real-time is derived. By the truncation, an approximation error is caused. The relation between the truncation length and approximation error caused by the truncation is estimated. By referring to the relation, under some tolerable approximation error, the least square approximation by spline functions can be obtained in real-time.

5.2 Preliminaries

In this section, signal spaces composed of spline functions and the biorthonormal basis are prepared.

Generally, signals defined on the real axis are considered to be in the Hilbert space[140, 139]

$$L_2(\boldsymbol{R}) \triangleq \left\{ u \middle| \int_{-\infty}^{\infty} |u(t)|^2 dt < +\infty \right\} \tag{5.1}$$

with the inner product

$$(u, v)_{L_2} \triangleq \int_{-\infty}^{\infty} u(t)\overline{v(t)}dt, \tag{5.2}$$

where $\boldsymbol{R}$ denotes the totality of real numbers.

So we consider the signal space composed of spline functions [105] of degree $(m-1)$ as a subspace of $L_2(\boldsymbol{R})$. Let ${}^mS$ denote the signal space composed of spline function of

degree $(m-1)$ and be called a spline signal space of degree $(m-1)$. Then ${}^{m}S$ can be defined by

$$ {}^{m}S \triangleq \left[{}^{m}_{[b]}\psi_{\ell} \right]_{\ell=-\infty}^{\infty}, \quad {}^{m}S \subset L_2(\boldsymbol{R}) \tag{5.3} $$

based on the B-spline functions[105] of degree $(m-1)$

$$ {}^{m}_{[b]}\psi_{\ell}(t) \triangleq \int_{-\infty}^{\infty} \left(\frac{\sin \pi f h}{\pi f h} \right)^{m} e^{j2\pi f(t-\ell h)} df, \quad \ell = 0, \pm 1, \pm 2, \cdots. \tag{5.4} $$

The B-spline functions can be represented in the form of piecewise polynomials of degree $(m-1)$ as follows:

$$ {}^{m}_{[b]}\psi_{\ell}(t) = m h^{-m} \sum_{p=0}^{m} \frac{(-1)^p}{p!(m-p)!} (t - (\ell + m/2 - p)h)_{+}^{m-1} \tag{5.5} $$

$$ (t-a)_{+}^{m-1} \triangleq \begin{cases} (t-a)^{m-1}, & t > a \\ 0, & t \leq a \end{cases} \tag{5.6} $$

Which are $(m-2)$-times continuously differentiable. Here h is a positive constant which is the interval of each piecewise polynomial.

Let $\{t_k\}_{k=-\infty}^{\infty}, \quad t_k = kh, \quad k = 0, \pm 1, \pm 2, \cdots$ be sampling points on the time axis, then sampling basis $\left\{ {}^{m}_{[s]}\psi_k \right\}_{k=-\infty}^{\infty}$ and its biorthonormal basis in ${}^{m}S$ $\left\{ {}^{m}_{[s^{\bullet}]}\psi_k \right\}_{k=-\infty}^{\infty}$ are the functions which satisfy the following relations:

$$ s(t) = \sum_{k=-\infty}^{\infty} s(t_k) {}^{m}_{[s]}\psi_k, \quad \left({}^{m}_{[s]}\psi_k \in {}^{m}S \right) \tag{5.7} $$

$$ s(t_k) = \int_{-\infty}^{\infty} s(t) \overline{{}^{m}_{[s^{\bullet}]}\psi_k} dt, \quad \left({}^{m}_{[s^{\bullet}]}\psi_k \in {}^{m}S \right). \tag{5.8} $$

Equation (5.7) and eq.(5.8) consist of a biorthonormal expansion formulas for spline functions. The sampling basis and its biorthonormal basis were derived as follows [114, 5, 13,

12]:

$$
\begin{aligned}
{}^{m}_{[s]}\psi_k(t) &= \sum_{\ell=-\infty}^{\infty} {}^{m}\beta_{\ell-k}\, {}^{m}_{[b]}\psi_\ell, \quad k = 0, \pm 1, \pm 2, \cdots && (5.9)\\
{}^{m}_{[s^*]}\psi_k(t) &= \sum_{\ell=-\infty}^{\infty} {}^{m}g_{\ell-k}\, {}^{m}_{[s]}\psi_\ell, \quad k = 0, \pm 1, \pm 2, \cdots, && (5.10)
\end{aligned}
$$

where

$$
\begin{aligned}
{}^{m}\beta_p &= h\int_{-1/2h}^{1/2h} {}^{m}_{f}B(f)e^{j2\pi fph}df, \quad p = 0, \pm 1, \pm 2, \cdots && (5.11)\\
{}^{m}_{f}B(f) &= \frac{1}{\sum_{q=-\lceil (m-1)/2\rceil}^{\lceil (m-1)/2\rceil} {}^{m}_{[b]}\psi_0(qh)e^{-j2\pi fqh}} && (5.12)\\
{}^{m}g_p &= h\int_{-1/2h}^{1/2h} {}^{m}_{f}G(f)^{-1}e^{j2\pi fph}df, \quad p = 0, \pm 1, \pm 2, \cdots && (5.13)\\
{}^{m}_{f}G(f)^{-1} &= \frac{h}{\sum_{q=-\infty}^{\infty}\left(\frac{\sin\pi(fh+q)}{\pi(fh+q)}\right)^{2m} {}^{m}_{f}B(f+q/h)^2}. && (5.14)
\end{aligned}
$$

Here, $\lceil x \rceil$ means the maximum integer number which does not exceed x. The functions $\left\{ {}^{m}_{[s]}\psi_k \right\}_{k=-\infty}^{\infty}$ are called spline sampling basis and each function ${}^{m}_{[s]}\psi_k$ is called sampling function. And the functions $\left\{ {}^{m}_{[s^*]}\psi_k \right\}_{k=-\infty}^{\infty}$ are called spline biorthonormal functions and each function ${}^{m}_{[s]}\psi_k$ is called biorthonormal function. Figure 5.1 shows examples of the sampling functions and the biorthonormal functions.

In this section, the spline signal spaces were prepared, and the sampling basis as well as its biorthonormal basis in the signal spaces are introduced.

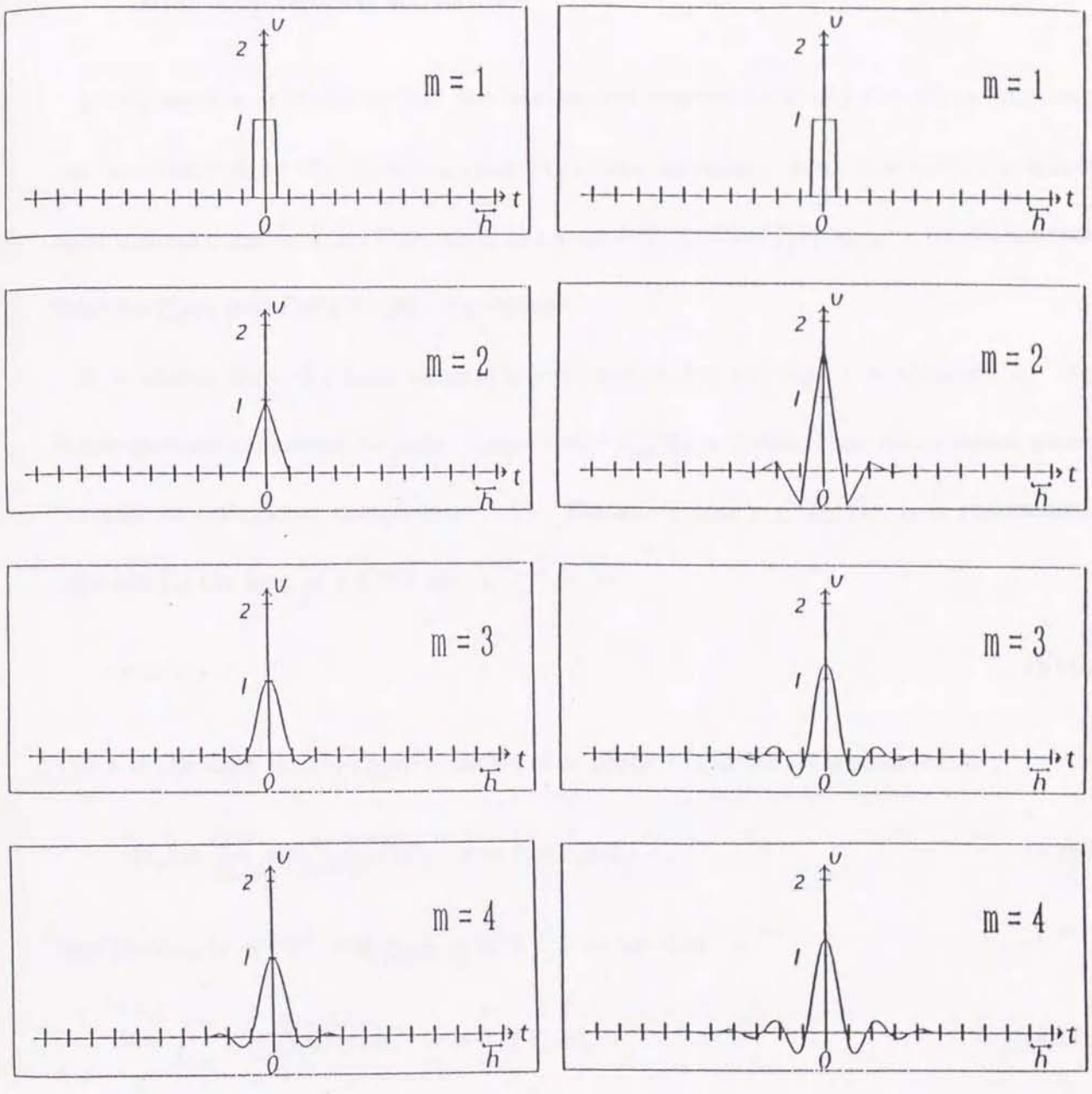

(a) Examples of sampling function

(b) Examples of biorthonormal function (h=1)

Figure 5.1: Examples of sampling functions and their biorthonormal functions.

5.3 Real-time spline approximation method based on biorthonormal expansion formulas

In this section, it is shown that the least square approximation by the spline functions can be obtained by the biorthonormal expansion formulas. Also, the real-time spline approximation method, by truncating the sampling function ${}^{m}_{[s]}\psi_0$ and its biorthonormal function ${}^{m}_{[s^\bullet]}\psi_0$ into finite length, is proposed.

It is shown that the least square approximation for any signal is obtained by the biorthonormal expansion formula. Signal space $L_2(\boldsymbol{R})$ is divided into spline signal space ${}^{m}S$ and its orthogonal complement ${}^{m}S^{\perp}$. For any signal $x \in L_2(\boldsymbol{R})$, it is represented uniquely by the sum of $s \in {}^{m}S$ and $s_c \in {}^{m}S^{\perp}$ as

$$x = s + s_c. \tag{5.15}$$

The s is the least square approximation of x. Since s is in ${}^{m}S$, it is sampled as

$$s(t_k) = \int_{-\infty}^{\infty} s(t)\overline{{}^{m}_{[s^\bullet]}\psi_k(t)}dt, \quad k = 0, \pm 1, \pm 2, \cdots. \tag{5.16}$$

And since s_c is in ${}^{m}S^{\perp}$ and ${}^{m}_{[s^\bullet]}\psi_k$ is in ${}^{m}S$, it holds that

$$0 = \int_{-\infty}^{\infty} s_c(t)\overline{{}^{m}_{[s^\bullet]}\psi_k(t)}dt, \quad k = 0, \pm 1, \pm 2, \cdots. \tag{5.17}$$

Then, by using

$$v_k = \int_{-\infty}^{\infty} x(t)\overline{{}^{m}_{[s^\bullet]}\psi_k(t)}dt, \quad k = 0, \pm 1, \pm 2, \cdots, \tag{5.18}$$

we have

$$v_k = s(t_k), \quad k = 0, \pm 1, \pm 2, \cdots. \tag{5.19}$$

Therefore the least square approximation s in ${}^mS$ for any signal $s \in L_2(\boldsymbol{R})$ is given by

$$v_k = \int_{-\infty}^{\infty} x(t) \overline{{}^m_{[s^\bullet]}\psi_k(t)} dt, \quad k = 0, \pm 1, \pm 2, \cdots \tag{5.20}$$

$$s(t) = \sum_{k=-\infty}^{\infty} v_k {}^m_{[s]}\psi_k(t). \tag{5.21}$$

Here, by eq.(5.9) and eq.(5.10), we have

$${}^m_{[s]}\psi_k(t) = {}^m_{[s]}\psi_0(t - kh) \tag{5.22}$$

$${}^m_{[s^\bullet]}\psi_k(t) = {}^m_{[s^\bullet]}\psi_0(t - kh). \tag{5.23}$$

Then eq.(5.20) and eq.(5.21) are rearranged as

$$v_k = \int_{-\infty}^{\infty} x(t) \overline{{}^m_{[s^\bullet]}\psi_0(t - kh)} dt, \quad k = 0, \pm 1, \pm 2, \cdots \tag{5.24}$$

$$s(t) = \sum_{k=-\infty}^{\infty} v_k {}^m_{[s]}\psi_0(t - kh). \tag{5.25}$$

These become the prototype of the real-time spline approximation method.

The real-time approximation method is obtained by truncating the sampling basis and its biorthonormal basis. For a positive constant H, the sampling function and the biorthonormal function truncated into $[-Hh, Hh]$ are represented as

$${}^m_{[s]}\tilde{\psi}_0(t) \triangleq \begin{cases} {}^m_{[s]}\psi_0(t), & |t| < Hh \\ 0, & |t| \geq Hh \end{cases} \tag{5.26}$$

$${}^m_{[s^\bullet]}\tilde{\psi}_0(t) \triangleq \begin{cases} {}^m_{[s^\bullet]}\psi_0(t), & |t| < Hh \\ 0, & |t| \geq Hh \end{cases}. \tag{5.27}$$

Then eq.(5.24) and eq.(5.25) can be approximated by

$$\tilde{v}_k = \int_{-\infty}^{\infty} x(\tau) \overline{{}^m_{[s^\bullet]}\tilde{\psi}_0(\tau - kh)} d\tau$$

$$= \int_{-Hh}^{Hh} x(\tau + kh)\overline{{}^{m}_{[s^*]}\tilde{\psi}_0(\tau)}d\tau, \quad k = 0, \pm 1, \pm 2, \cdots \tag{5.28}$$

$$\tilde{s}(t) = \sum_{k=-\infty}^{\infty} \tilde{v}_{k[s]}{}^{m}\tilde{\psi}_0(t - kh)$$

$$= \sum_{k=-\lfloor t/h+H \rfloor}^{\lceil t/h-H \rceil} \tilde{v}_{k[s]}{}^{m}\tilde{\psi}_0(t - kh), \tag{5.29}$$

where $\lceil x \rceil$ denotes the maximum integer number which is not greater x , and $\lfloor x \rfloor$ denotes the minimum integer number which is not less than x.

The above equations mean that $\tilde{s}(t)$ can be immediately calculated only by $x(\tau)$, $((\lceil t/h - H \rceil - H)h \leq \tau \leq (\lfloor t/h + H \rfloor + H)h)$.

For $s \in L_2(\boldsymbol{R})$, we evaluate the approximation error between s and $\tilde{s}$ in the sense of mean square norm. The error is represented as

$$\frac{\| \tilde{s} - s \|_{L_2}}{\| x \|_{L_2}} = \frac{\left[\int_{-\infty}^{\infty} |\tilde{s}(t) - s(t)|^2 dt\right]^{1/2}}{\left[\int_{-\infty}^{\infty} |x(t)|^2 dt\right]^{1/2}}. \tag{5.30}$$

In this section, the real-time spline approximation method was proposed. And the approximation error caused by truncation was defined. In the following section, the error represented in eq.(5.30) is estimated.

5.4 The relation between approximation error and truncation length

In this section, the relation between the truncation length of the sampling function and its biorthonormal function and the approximation error caused by the truncation is estimated. In the first subsection, the upper bound of the biorthonormal function is

derived to estimate the error. In the next subsection, the relation between truncation length and approximation error is estimated.

5.4.1 Upper bounds of sampling function and its biorthonormal function

In this subsection, the upper bound of the biorthonormal function is derived to estimate the error.

The upper bound of the sampling basis was derived by Ref. [117]. From Ref. [117], the following lemma shows one of the upper bounds of the sampling function.

Lemma 13

(i) *When* $m = 1$

$$ {}^{1}_{[s]}\psi_0(t) = \begin{cases} 1, & |t/h| < 1/2 \\ 0, & |t/h| \geq 1/2 \end{cases} . \tag{5.31} $$

(ii) *When* $m = 2$

$$ {}^{2}_{[s]}\psi_0(t) = \begin{cases} 1 - |t/h|, & |t/h| < 1 \\ 0, & |t/h| \geq 1 \end{cases} . \tag{5.32} $$

(iii) *When* $m \geq 3$, *there exist two constant* ${}^{m}U, {}^{m}u$ $(0 < {}^{m}U < \infty, 0 < {}^{m}u < 1)$ *s.t.*

$$ \left| {}^{m}_{[s]}\psi_0(t) \right| \leq {}^{m}U {}^{m}u^{|t|/h}. \tag{5.33} $$

To represent the upper bound of biorthonormal function, the following lemma shows the biorthonormal function in the form of linear combination of the B-spline functions.

Lemma 14 *The biorthonormal function* ${}^{m}_{[s^{\bullet}]}\psi_0(t)$ *is represented in the form of linear combination of the B-spline functions*

$$ {}^{m}_{[s^{\bullet}]}\psi_0(t) = \sum_{p=-\infty}^{\infty} {}^{m}d_{p\,{}^{m}_{[b]}}\psi_p(t), \tag{5.34} $$

where the coefficients $\{{}^{m}d_p\}_{p=-\infty}^{\infty}$ *is*

$$ {}^{m}d_p = h\int_{-1/2h}^{1/2h} \frac{{}^{2m}_{f}B(f)}{{}^{m}_{f}B(f)} e^{j2\pi fph}df, \quad p = 0, \pm 1, \pm 2, \cdots. \tag{5.35} $$

(Proof) Substituting ${}^{m}_{[s]}\psi_k(t)$ in eq.(5.9) for eq.(5.10), ${}^{m}_{[s^{\bullet}]}\psi_0(t)$ is represented in the form of linear combination of B-spline functions as follows:

$$ \begin{aligned} {}^{m}_{[s^{\bullet}]}\psi_0(t) &= \sum_{k=-\infty}^{\infty} {}^{m}g_{k\,{}^{m}_{[s]}}\psi_k(t) \\ &= \sum_{k=-\infty}^{\infty} {}^{m}g_k \sum_{p=-\infty}^{\infty} {}^{m}\beta_{p-k\,{}^{m}_{[b]}}\psi_p(t) \\ &= \sum_{p=-\infty}^{\infty} \left[\sum_{k=-\infty}^{\infty} {}^{m}g_k\,{}^{m}\beta_{p-k}\right] {}^{m}_{[b]}\psi_p(t). \end{aligned} $$

Let ${}^{m}d_p$ denote $\sum_{k=-\infty}^{\infty} {}^{m}g_k\,{}^{m}\beta_{p-k}$, then it is represented as

$$ \begin{aligned} {}^{m}d_p &= \sum_{k=-\infty}^{\infty} {}^{m}g_k\,{}^{m}\beta_{p-k} \\ &= h\int_{-1/2h}^{1/2h} {}^{m}_{f}G(f)^{-1}\,{}^{m}_{f}B(f)e^{j2\pi fph}df, \quad p = 0, \pm 1, \pm 2, \cdots \end{aligned} $$

by convolution theorem for discrete Fourier transform, eq.(5.9), and eq.(5.13).

Let $\delta(\cdot)$ denote delta function, ${}^{m}_{f}B(f)$ represented by eq.(5.12) becomes

$$ {}^{m}_{f}B(f) = \frac{1}{\sum_{q=-\lceil (m-1)/2\rceil}^{\lceil (m-1)/2\rceil} {}^{m}_{[b]}\psi_0(qh)e^{-j2\pi fqh}} $$

$$= \frac{1}{\sum_{q=-\infty}^{\infty} {}_{[b]}^{m}\psi_0(qh)e^{-j2\pi fqh}}$$

$$= \frac{1}{\sum_{q=-\infty}^{\infty} \int_{-\infty}^{\infty} {}_{[b]}^{m}\psi_0(t)e^{-j2\pi ft}\delta(t-qh)dt}$$

$$= \frac{1}{\int_{-\infty}^{\infty} {}_{[b]}^{m}\psi_0(t)\left[\sum_{q=-\infty}^{\infty}\delta(t-qh)\right]e^{-j2\pi ft}dt}.$$

By the convolution theorem for Fourier transform, we have

$${}_{f}^{m}B(f) = \frac{1}{\int_{-\infty}^{\infty}\left\{\int_{-\infty}^{\infty} {}_{[b]}^{m}\psi_0(t)e^{-j2\pi f't}dt\right\}\left\{\int_{-\infty}^{\infty}\left[\sum_{p=-\infty}^{\infty}\delta(t-ph)\right]e^{-j2\pi(f-f')t}dt\right\}df'}$$

$$= \frac{1}{\int_{-\infty}^{\infty}\left\{\int_{-\infty}^{\infty} {}_{[b]}^{m}\psi_0(t)e^{-j2\pi f't}dt\right\}\left\{\sum_{p=-\infty}^{\infty} e^{j2\pi(f'-f)ph}\right\}df'}.$$

From eq.(5.5) and the equation

$$\sum_{p=-\infty}^{\infty} e^{j2\pi(f'-f)ph} = \frac{1}{h}\sum_{p=-\infty}^{\infty}\delta(f'-f-p/h), \tag{5.36}$$

${}_{f}^{m}B(f)$ is rearranged as

$${}_{f}^{m}B(f) = \frac{1}{\int_{-\infty}^{\infty}\left(\frac{\sin\pi f'h}{\pi f'h}\right)^{m}\left[\frac{1}{h}\sum_{p=-\infty}^{\infty}\delta(f'-f-p/h)\right]df'}$$

$$= \frac{h}{\sum_{p=-\infty}^{\infty}\left(\frac{\sin\pi(fh+p)}{\pi(fh+p)}\right)^{m}}.$$

By using the above ${}_{f}^{m}B(f)$, ${}_{f}^{m}G(f)$ is represented by

$${}_{f}^{m}G(f) = \frac{1}{h}\sum_{q=-\infty}^{\infty}\left(\frac{\sin\pi(fh+q)}{\pi(fh+q)}\right)^{2m} {}_{f}^{m}B(f+q/h)^2$$

$$
\begin{aligned}
&= \frac{1}{h}\sum_{q=-\infty}^{\infty}\left(\frac{\sin\pi(fh+q)}{\pi(fh+q)}\right)^{2m}\left\{\frac{h}{\sum_{p=-\infty}^{\infty}\left(\frac{\sin\pi(fh+q+p)}{\pi(fh+q+p)}\right)^{m}}\right\}^{2} \\
&= \frac{1}{h}\sum_{q=-\infty}^{\infty}\left(\frac{\sin\pi(fh+q)}{\pi(fh+q)}\right)^{2m}\left\{\frac{h}{\sum_{r=-\infty}^{\infty}\left(\frac{\sin\pi(fh+r)}{\pi(fh+r)}\right)^{m}}\right\}^{2}, \quad (r=q+p) \\
&= \frac{{}_f^m B(f)^2}{{}_f^{2m}B(f)}.
\end{aligned}
$$

Then the coefficients $\{{}^m d_p\}_{p=-\infty}^{\infty}$ is represented as

$$
\begin{aligned}
{}^m d_p &= h\int_{-1/2h}^{1/2h} {}_f^m G(f)^{-1}\,{}_f^m B(f) e^{j2\pi fph}df \\
&= h\int_{-1/2h}^{1/2h} \frac{{}_f^{2m}B(f)}{{}_f^m B(f)} e^{j2\pi fph}df, \quad p=0,\pm1,\pm2,\cdots.
\end{aligned}
$$

■

The following lemma shows one of the upper bound of biorthonormal function.

Lemma 15

(i) *When* $m=1$,

$$
{}_{[s^\bullet]}^{1}\psi_0(t) = \begin{cases} 1, & |t/h| < 1/2 \\ 0, & |t/h| \geq 1/2 \end{cases}. \tag{5.37}
$$

(ii) *When* $m \geq 2$, *there exist two constants* ${}^m W, {}^m w$ $(0 < {}^m W < \infty, 0 < {}^m w < 1)$ *s.t.*

$$
\left|{}_{[s^\bullet]}^{m}\psi_0(t)\right| \leq {}^m W\,{}^m w^{|t|/h}. \tag{5.38}
$$

(Proof) (i) when $m=1$, coefficients $\{{}^m d_p\}_{p=-\infty}^{\infty}$ is represented as

$$ {}^{2}_{f}B(f){}^{1}_{f}B(f) = 1 \cdot 1 = 1, \quad (m = 1) \tag{5.39} $$

by eq.(5.5).

By substituting them for eq.(5.35), we have

$$ {}^{1}d_p = \begin{cases} 1, & p = 0, \\ 0, & p \neq 0 \end{cases} . $$

By substituting ${}^{1}d_p$ for eq.(5.34), we have

$$ {}^{1}_{[s\bullet]}\psi_0(t) = {}^{1}_{[s]}\psi_0(t) $$

From eq.(5.31), we have

$$ {}^{1}_{[s\bullet]}\psi_0(t) = \begin{cases} 1, & |t/h| < 1/2, \\ 0, & |t/h| \geq 1/2 \end{cases} . $$

(ii) When $m \geq 2$, by Lemma 1 and Lemma 2 in [117], coefficients $\left\{ {}^{2m}\beta_p \right\}_{p=-\infty}^{\infty}$ satisfies

$$ \left| {}^{2m}\beta_p \right| \leq {}^{2m}B({}^{2m}b)^{|p|}, \quad p = 0, \pm 1, \pm 2, \cdots \tag{5.40} $$

for certain constants $0 < {}^{2m}b < 1,\ 0 < {}^{2m}B < \infty$. From eq.(5.12), the inverse discrete Fourier transform of $1/{}^{m}_{f}B(f)$ becomes $\left\{ {}^{m}_{[b]}\psi_0(ph) \right\}_{p=-\infty}^{\infty}$. The coefficients $\{ {}^{m}d_p \}_{p=-\infty}^{\infty}$ is represented by the convolution of $\left\{ {}^{2m}\beta_p \right\}_{p=-\infty}^{\infty}$ and $\left\{ {}^{m}_{[b]}\psi_0(ph) \right\}_{p=-\infty}^{\infty}$. Using

$$ {}^{m}_{[b]}\psi_0(t) = 0, \quad |p| > \lceil (m-1)/2 \rceil \tag{5.41} $$

from eq.(5.5), the one of the upper bound of the amplitude is evaluated as

$$ \begin{aligned} |{}^{m}d_p| &= \left| \sum_{k=-\infty}^{\infty} {}^{2m}\beta_{p-k}\, {}^{m}_{[b]}\psi_0(kh) \right| \\ &= \left| \sum_{k=-\lceil (m-1)/2 \rceil}^{\lceil (m-1)/2 \rceil} {}^{2m}\beta_{p-k}\, {}^{m}_{[b]}\psi_0(kh) \right| \end{aligned} $$

$$
\begin{aligned}
&\leq \sum_{k=-\lceil (m-1)/2\rceil}^{\lceil (m-1)/2\rceil} \left|{}^{2m}\beta_{p-k}\right| \left|{}^{m}_{[b]}\psi_0(kh)\right| \\
&\leq \frac{1}{h} \sum_{k=-\lceil (m-1)/2\rceil}^{\lceil (m-1)/2\rceil} \left|{}^{2m}\beta_{p-k}\right| \\
&\leq \frac{1}{h} \sum_{k=-\lceil (m-1)/2\rceil}^{\lceil (m-1)/2\rceil} {}^{2m}B({}^{2m}b)^{|p-k|} \\
&= \frac{{}^{2m}B}{h}\left\{({}^{2m}b)^{|p|} + 2\sum_{k=1}^{\lceil (m-1)/2\rceil}({}^{2m}b)^{|p-k|}\right\} \\
&\leq \frac{{}^{2m}B}{h}\left\{({}^{2m}b)^{|p|} + 2\sum_{k=1}^{\lceil (m-1)/2\rceil}({}^{2m}b)^{|p|-|k|}\right\} \\
&= \left[\frac{{}^{2m}B}{h}\left\{1 + 2\sum_{k=1}^{\lceil (m-1)/2\rceil}({}^{2m}b)^{-k}\right\}\right]({}^{2m}b)^{|p|} \\
&= {}^{2m}B\frac{2({}^{2m}b)^{-\lceil (m-1)/2\rceil} - ({}^{2m}b) - 1}{h(1 - {}^{2m}b)}({}^{2m}b)^{|p|}, \quad p = 0, \pm 1, \pm 2, \cdots .
\end{aligned}
$$

Let ${}^{m}D$ and ${}^{m}d$ denote

$$
{}^{m}D = {}^{2m}B\frac{2({}^{2m}b)^{-\lceil (m-1)/2\rceil} - {}^{2m}b - 1}{h(1 - {}^{2m}b)}, \tag{5.42}
$$

$$
{}^{m}d = {}^{2m}b, \tag{5.43}
$$

respectively, we have

$$
|{}^{m}d_p| \leq {}^{m}D({}^{m}d)^{|p|}, \quad p = 0, \pm 1, \pm 2, \cdots, \quad (|{}^{m}d| < 1,\ 0 < {}^{m}D < \infty).
$$

Since the B-spline function is symmetry from eq.(5.10)

$$
{}^{m}_{[s\bullet]}\psi_0(t) = {}^{m}_{[s\bullet]}\psi_0(|t|), \tag{5.44}
$$

it is enough to consider only the case that $t \geq 0$ to show eq.(5.38). From eq.(5.5), we have

$$
0 < {}^{m}_{[b]}\psi_p(t) < 1/h, \quad |t/h - p| < m/2,
$$

$$ {}^{m}_{[b]}\psi_p(t) = 0, \quad |t/h - p| < m/2. $$

Then one of the upper bound of $\left|{}^{m}_{[s^*]}\psi_0(t)\right|$ is represented as follows:

$$\begin{aligned}
\left|{}^{m}_{[s^*]}\psi_0(t)\right| &= \left|\sum_{p=-\infty}^{\infty} {}^{m}d_p {}^{m}_{[b]}\psi_p(t)\right| \\
&= \left|\sum_{p=-\lfloor t/h-m/2\rfloor}^{\lceil t/h+m/2\rceil} {}^{m}d_p {}^{m}_{[b]}\psi_p(t)\right| \\
&\leq \sum_{p=-\lfloor t/h-m/2\rfloor}^{\lceil t/h+m/2\rceil} |{}^{m}d_p| \left|{}^{m}_{[b]}\psi_p(t)\right| \\
&\leq \frac{1}{h} \sum_{p=-\lfloor t/h-m/2\rfloor}^{\lceil t/h+m/2\rceil} |{}^{m}d_p| \\
&\leq \frac{1}{h} {}^{m}D \sum_{p=-\lfloor t/h-m/2\rfloor}^{\lceil t/h+m/2\rceil} {}^{m}d^{|p|}.
\end{aligned}$$

Using ${}^{m}d^{-1} > {}^{m}d$, it is rearranged as

$$\begin{aligned}
\left|{}^{m}_{[s^*]}\psi_0(t)\right| &\leq \frac{1}{h} {}^{m}D \sum_{p=-\lfloor t/h-m/2\rfloor}^{\lceil t/h+m/2\rceil} {}^{m}d^{|p|} \\
&= \frac{{}^{m}D({}^{m}d\lfloor t/h - m/2\rfloor - {}^{m}d\lceil t/h + m/2\rceil)}{h(1 - {}^{m}d)} \\
&= \frac{{}^{m}D {}^{m}d\lfloor t/h - m/2\rfloor}{h(1 - {}^{m}d)}.
\end{aligned}$$

Thus, we have

$$\begin{aligned}
\left|{}^{m}_{[s^*]}\psi_0(t)\right| &\leq \frac{{}^{m}D {}^{m}d\lfloor t/h - m/2\rfloor}{h(1 - {}^{m}d)} \\
&\leq \frac{{}^{m}D {}^{m}d|t/h| - m/2}{h(1 - {}^{m}d)} \\
&= \frac{{}^{m}D {}^{m}d-m/2 {}^{m}d^{|t|/h}}{h(1 - {}^{m}d)}.
\end{aligned}$$

Here, by introducing

$$\begin{aligned}
{}^{m}W &= \frac{{}^{m}D^{-m/2}d}{h(1 - {}^{m}d)} \\
{}^{m}w &= {}^{m}d,
\end{aligned}$$

m	2	3	4	5	6	7	8	9	10
${}^{m}U$	1.0000	1.2589	1.3335	1.2589	1.1481	1.1350	1.1220	1.1092	1.0965
${}^{m}u$	0.3679	0.1715	0.2679	0.3758	0.4266	0.4623	0.5309	0.5559	0.5754
${}^{m}W$	1.8011	1.3530	1.2861	1.1555	1.1501	1.1409	1.1320	1.1252	1.1135
${}^{m}w$	0.2777	0.4650	0.5755	0.6380	1.1409	0.7644	0.7843	0.8032	0.8062

Table 5.1: Attenuation parameters of sampling functions and their biorthonormal functions.

eq.(5.38) holds. ■

From Lemma 15, the biorthonormal function ${}^{m}_{[s\bullet]}\psi_0$ is a time limited function when $m = 1$. Thus there is no need to truncate the biorthonormal function when $m = 1$. And when $m \geq 2$, the amplitude of ${}^{m}_{[s\bullet]}\psi_0$ at time t decreases exponentially depending on $|t|$. From Lemma 13 and Lemma 15, the amplitude of the sampling function and its biorthonormal function decrease exponentially, then it is expected that the approximation error caused by the truncation rapidly diminishes.

Table 5.1 shows the numerical evaluation of ${}^{m}W$ and ${}^{m}w$ for ${}^{m}_{[s\bullet]}\psi_0$. Table 5.1 shows the numerical evaluation of ${}^{m}U$ and ${}^{m}u$ for ${}^{m}_{[s]}\psi_0$ from [117]. From Table 5.1, there is a tendency that larger $(m-1)$ decreases the attenuation speed.

Figure 5.2 shows the upper bounds of the sampling function and its biorthonormal function in logarithmic scale. From Fig. 5.2, the derived upper bounds are good.

In this subsection, it was shown that the upper bounds of the sampling function and its biorthonormal function attenuate exponentially. In the next section, the relation between approximation error and the truncation length is estimated by using the upper bounds.

5.4.2 The relation between approximation error and truncation length

In this subsection, the relation between approximation error and the truncation length is estimated by using the upper bounds.

The following lemma shows the upper bound of error in coefficients $v_k, \quad k = 0, \pm 1, \pm 2, \cdots$ caused by truncation of the biorthonormal function.

Proposition 8 *When* $m \geq 2$,

$$\left(\frac{\| \tilde{\boldsymbol{v}} - \boldsymbol{v} \|_{\ell_2}}{\| x \|_{L_2}} \right)^2 \leq \frac{2^m w^2}{(1 - {}^m w)^2} {}^m w^{2(H+1)}. \tag{5.45}$$

(Proof) From eq.(5.24) and eq.(5.28), we have

$$\begin{aligned}
\| \tilde{\boldsymbol{v}} - \boldsymbol{v} \|_{\ell_2}^2 &= \sum_{k=-\infty}^{\infty} |\tilde{v}_k - v_k|^2 \\
&= \sum_{k=-\infty}^{\infty} \left| \int_{-\infty}^{\infty} x(t) \overline{{}^m_{[s^\bullet]} \tilde{\psi}_0(t - kh)} dt - \int_{-\infty}^{\infty} x(t) \overline{{}^m_{[s^\bullet]} \psi_0(t - kh)} dt \right|^2 \\
&= \sum_{k=-\infty}^{\infty} \left| \int_{-\infty}^{\infty} x(t) \left\{ \overline{{}^m_{[s^\bullet]} \tilde{\psi}_0(t - kh)} - \overline{{}^m_{[s^\bullet]} \psi_0(t - kh)} \right\} dt \right|^2 \\
&\leq \sum_{k=-\infty}^{\infty} \int_{-\infty}^{\infty} |x(t)|^2 \left| \overline{{}^m_{[s^\bullet]} \tilde{\psi}_0(t - kh)} - \overline{{}^m_{[s^\bullet]} \psi_0(t - kh)} \right|^2 dt \\
&= \int_{-\infty}^{\infty} |x(t)|^2 \left\{ \sum_{k=-\infty}^{\infty} \left| \overline{{}^m_{[s^\bullet]} \tilde{\psi}_0(t - kh)} - \overline{{}^m_{[s^\bullet]} \psi_0(t - kh)} \right|^2 \right\} dt
\end{aligned}$$

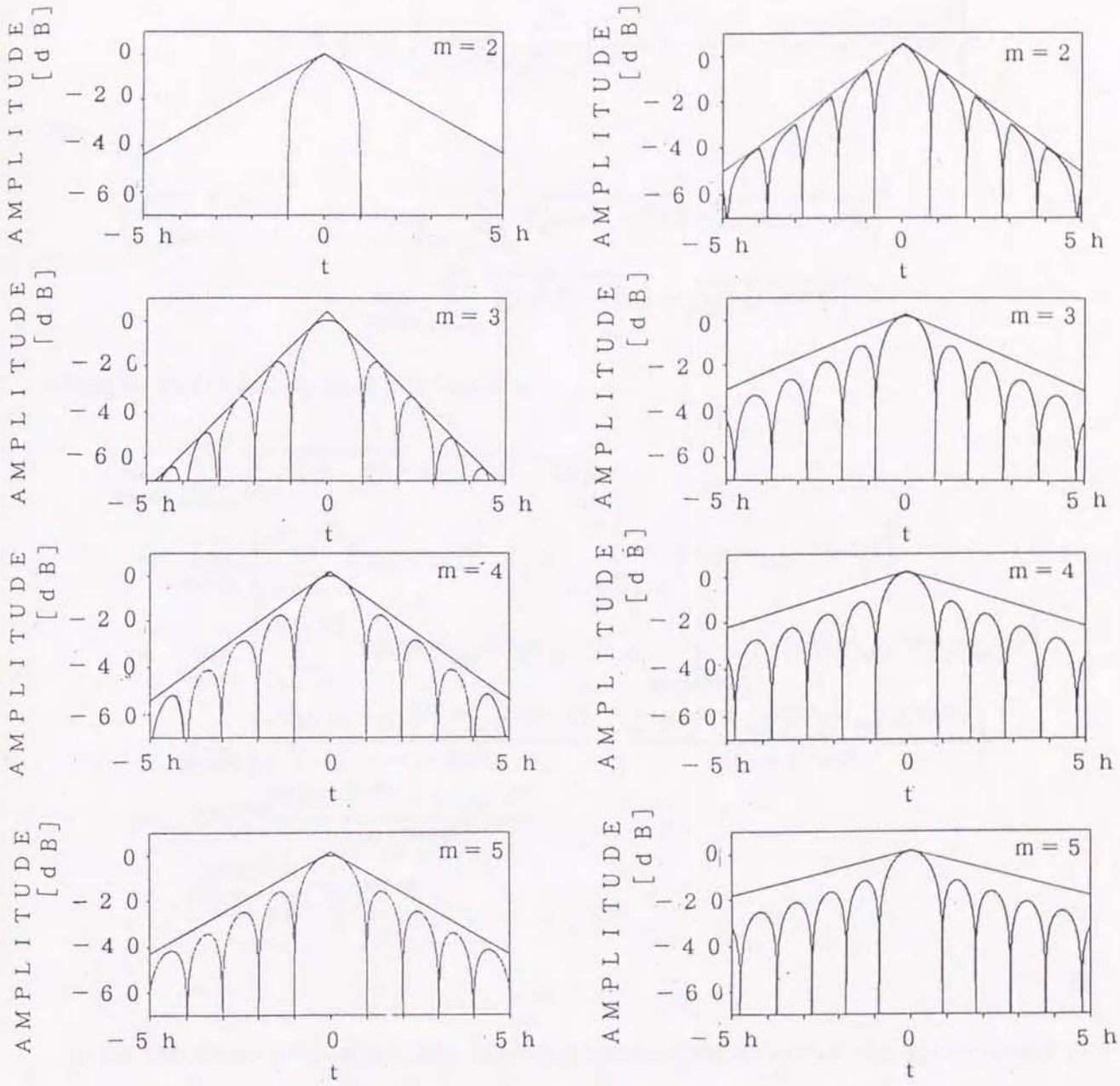

(a) Upper bound of sampling function

(b) Upper bound of biorthonormal function

Figure 5.2: Upper bounds of sampling functions and their biorthonormal functions.

$$\leq \int_{-\infty}^{\infty} |x(t)|^2 dt \left\{ \sup_{-\infty<t<\infty} \sum_{k=-\infty}^{\infty} \left| \overline{{}^m_{[s^\bullet]}\tilde{\psi}_0(t-kh)} - \overline{{}^m_{[s^\bullet]}\psi_0(t-kh)} \right|^2 \right\}$$

$$= \| \boldsymbol{x} \|_{L_2}^2 \left\{ \sup_{-\infty<t<\infty} \sum_{k=-\infty}^{\infty} \left| \overline{{}^m_{[s^\bullet]}\tilde{\psi}_0(t-kh)} - \overline{{}^m_{[s^\bullet]}\psi_0(t-kh)} \right|^2 \right\},$$

and

$$\left(\frac{\| \tilde{\boldsymbol{v}} - \boldsymbol{v} \|_{\ell_2}}{\| \boldsymbol{x} \|_{L_2}} \right)^2 \leq \sup_{-\infty<t<\infty} \sum_{k=-\infty}^{\infty} \left| \overline{{}^m_{[s^\bullet]}\tilde{\psi}_0(t-kh)} - \overline{{}^m_{[s^\bullet]}\psi_0(t-kh)} \right|^2$$

$$= \sup_{0\leq t<h} \sum_{k=-\infty}^{\infty} \left| \overline{{}^m_{[s^\bullet]}\tilde{\psi}_0(t-kh)} - \overline{{}^m_{[s^\bullet]}\psi_0(t-kh)} \right|^2.$$

Using eq.(5.27) and eq.(5.38), it becomes

$$\sup_{0\leq t<h} \sum_{k=-\infty}^{\infty} \left| \overline{{}^m_{[s^\bullet]}\tilde{\psi}_0(t-kh)} - \overline{{}^m_{[s^\bullet]}\psi_0(t-kh)} \right|^2$$

$$\leq \sup_{0\leq t<h} \left\{ \sum_{k=-\infty}^{\lceil t/h-H \rceil} \left| {}^mW({}^mw)^{t/h-k} \right|^2 + \sum_{k=\lfloor t/h+H \rfloor}^{\infty} \left| {}^mW({}^mw)^{-t/h+k} \right|^2 \right\}$$

$$= \sup_{0\leq t<h} \left\{ \sum_{k=-\infty}^{\lceil t/h-H \rceil} ({}^mW)^2({}^mw)^{2t/h}({}^mw)^{-2k} + \sum_{k=\lfloor t/h+H \rfloor}^{\infty} ({}^mW)^2({}^mw)^{-2t/h}({}^mw)^{2k} \right\}$$

$$= \sup_{0\leq t<h} \left\{ \frac{({}^mW)^2({}^mw)^{2t/h}({}^mw)^{2\lceil t/h-H \rceil}}{1-({}^mw)^2} + \frac{({}^mW)^2({}^mw)^{-2t/h}({}^mw)^{2\lfloor t/h+H \rfloor}}{1-({}^mw)^2} \right\}$$

$$= ({}^mW)^2 \frac{({}^mw)^{-2\lceil -H \rceil} + ({}^mw)^{2\lfloor H \rfloor}}{1-({}^mw)^2}$$

$$= \frac{2({}^mW)^2}{1-({}^mw)^2}({}^mw)^{2H+2}.$$

■

From the above proposition, the following theorem shows one of the upper bound of the error $\| \tilde{s} - s \| / \| x \|$ in eq.(5.30).

Theorem 10 *When* $m \geq 2$,

$$\left(\frac{\| \tilde{s} - s \|_{L_2}}{\| x \|_{L_2}} \right)^2 \leq \frac{2h({}^mW{}^mU{}^mw)^2}{(1-{}^mw^2)\log {}^mu} ({}^mw{}^mu)^{2H}$$

$$-\frac{2h({}^{m}W{}^{m}U)wm^2}{(1-{}^{m}w^2)\log{}^{m}u}({}^{m}w)^{2H}$$
$$-\frac{h^{m}U^4({}^{m}u^2+1)}{(1-{}^{m}u^2)\log{}^{m}u}({}^{m}u)^{2H}. \tag{5.46}$$

(Proof) From eq.(5.25) and eq.(5.29), we have

$$\begin{aligned}
&\| \tilde{s}-s \|_{L_2} \\
&= \int_{-\infty}^{\infty}\left|\sum_{k=-\infty}^{\infty}\tilde{v}_{k}{}^{m}_{[s]}\tilde{\psi}_0(t-kh)-\sum_{k=-\infty}^{\infty}v_{k}{}^{m}_{[s]}\psi_0(t-kh)\right|^2 dt \\
&= \int_{-\infty}^{\infty}\left|\sum_{k=-\infty}^{\infty}\left[\tilde{v}_{k}{}^{m}_{[s]}\tilde{\psi}_0(t-kh)-v_{k}{}^{m}_{[s]}\psi_0(t-kh)\right]\right|^2 dt \\
&\leq \int_{-\infty}^{\infty}\sum_{k=-\infty}^{\infty}\left|\tilde{v}_{k}{}^{m}_{[s]}\tilde{\psi}_0(t-kh)-v_{k}{}^{m}_{[s]}\psi_0(t-kh)\right|^2 dt \\
&= \int_{-\infty}^{\infty}\sum_{k=-\infty}^{\infty}\left|\tilde{v}_{k}{}^{m}_{[s]}\tilde{\psi}_0(t-kh)-v_{k}{}^{m}_{[s]}\tilde{\psi}_0(t-kh)\right. \\
&\quad \left.+v_{k}{}^{m}_{[s]}\tilde{\psi}_0(t-kh)-v_{k}{}^{m}_{[s]}\psi_0(t-kh)\right|^2 dt \\
&\leq \int_{-\infty}^{\infty}\sum_{k=-\infty}^{\infty}\left|\tilde{v}_{k}{}^{m}_{[s]}\tilde{\psi}_0(t-kh)-v_{k}{}^{m}_{[s]}\tilde{\psi}_0(t-kh)\right|^2 dt \\
&\quad +\int_{-\infty}^{\infty}\sum_{k=-\infty}^{\infty}\left|v_{k}{}^{m}_{[s]}\tilde{\psi}_0(t-kh)-v_{k}{}^{m}_{[s]}\psi_0(t-kh)\right|^2 dt \\
&\leq \int_{-\infty}^{\infty}|\tilde{v}_k-v_k|^2\sum_{k=-\infty}^{\infty}\left|{}^{m}_{[s]}\tilde{\psi}_0(t-kh)\right|^2 dt \\
&\quad +\int_{-\infty}^{\infty}|v_k|^2\sum_{k=-\infty}^{\infty}\left|{}^{m}_{[s]}\tilde{\psi}_0(t-kh)-{}^{m}_{[s]}\psi_0(t-kh)\right|^2 dt \\
&= \| \tilde{\boldsymbol{v}}-\boldsymbol{v} \|^2_{\ell_2}\| {}^{m}_{[s]}\tilde{\psi}_0 \|^2_{L_2}+\| \boldsymbol{v} \|^2_{\ell_2}\| {}^{m}_{[s]}\tilde{\psi}_0-{}^{m}_{[s]}\psi_0 \|^2_{L_2}.
\end{aligned} \tag{5.47}$$

using Lemma 13, one of the upper bounds of $\| {}^{m}_{[s\bullet]}\tilde{\psi}_0(t) \|^2_{L_2}$ is represented as

$$\| {}^{m}_{[s]}\tilde{\psi}_0 \|_{L_2} = \int_{-\infty}^{\infty}\left|{}^{m}_{[s]}\tilde{\psi}_0(t)\right|^2 dt$$

$$
\begin{aligned}
&\leq \int_{-Hh}^{Hh} |{}^{m}U({}^{m}u)^{|t|/h}|^2 dt \\
&= \int_{-Hh}^{Hh} {}^{m}U^2({}^{m}u)^{2|t|/h} dt \\
&= 2\int_{0}^{Hh} {}^{m}U^2({}^{m}u)^{2t/h} dt \\
&= \frac{h({}^{m}U)^2}{\log {}^{m}u}\left\{({}^{m}u)^{2H}-1\right\}. \qquad (5.48)
\end{aligned}
$$

From eq.(5.24), one of the upper bounds of $\| \boldsymbol{x} \|_{\ell_2}^2$ is represented as

$$
\begin{aligned}
\| \boldsymbol{v} \|_{\ell_2}^2 &= \sum_{k=-\infty}^{\infty} |v_k|^2 \\
&= \sum_{k=-\infty}^{\infty} \left| \int_{-\infty}^{\infty} x(t)\overline{{}^{m}_{[s^\bullet]}\psi_0(t-kh)}dt \right|^2 \\
&\leq \sum_{k=-\infty}^{\infty} \int_{-\infty}^{\infty} |x(t)|^2 \left|\overline{{}^{m}_{[s^\bullet]}\psi_0(t-kh)}\right|^2 dt \\
&= \int_{-\infty}^{\infty} |x(t)|^2 \left\{ \sum_{k=-\infty}^{\infty} \left|\overline{{}^{m}_{[s^\bullet]}\psi_0(t-kh)}\right|^2 \right\} dt \\
&\leq \int_{-\infty}^{\infty} |x(t)|^2 \, dt \left\{ \sup_{-\infty<t<\infty} \sum_{k=-\infty}^{\infty} \left|\overline{{}^{m}_{[s^\bullet]}\psi_0(t-kh)}\right|^2 \right\} \\
&\leq \| x \|_{L_2}^2 \left\{ \sup_{-\infty<t<\infty} \sum_{k=-\infty}^{\infty} \left|{}^{m}U({}^{m}u)^{|t-kh|/h}\right|^2 \right\} \\
&= \| x \|_{L_2}^2 \left\{ \sup_{-\infty<t<\infty} \sum_{k=-\infty}^{\infty} ({}^{m}U)^2({}^{m}u)^{2|t-kh|/h} \right\} \\
&= \| x \|_{L_2}^2 \left\{ \sup_{-\infty<t<\infty} \left[\sum_{k=-\infty}^{\lceil t/h \rceil} ({}^{m}U)^2({}^{m}u)^{2(t/h-k)} + \sum_{k=-\lceil t/h \rceil+1}^{\infty} ({}^{m}U)^2({}^{m}u)^{2(t/h-k)} \right] \right\} \\
&= \| x \|_{L_2}^2 \frac{({}^{m}U)^2}{1-({}^{m}u)^2} \left\{ \sup_{-\infty<t<\infty} \left[({}^{m}u)^{2(t/h-\lceil t/h \rceil)} + ({}^{m}u)^{2-(t/h-\lceil t/h \rceil-1)} \right] \right\} \\
&= \| x \|_{L_2}^2 \frac{({}^{m}U)^2}{1-({}^{m}u)^2} \left\{ ({}^{m}u)^2 + 1 \right\}. \qquad (5.49)
\end{aligned}
$$

From Lemma 13, one of the upper bounds of $\| {}^{m}_{[s]}\psi_0(t) - {}^{m}_{[s]}\tilde{\psi}_0(t) \|_{L_2}^2$ is represented as

$$
\| {}^{m}_{[s]}\tilde{\psi}_0 - {}^{m}_{[s]}\psi_0 \|_{L_2}^2 = \int_{-\infty}^{\infty} \left| {}^{m}_{[s]}\tilde{\psi}_0(t) - {}^{m}_{[s]}\psi_0(t) \right|^2 dt
$$

$$
\begin{aligned}
&= \int_{-\infty}^{-Hh} \left|{}^{m}_{[s]}\psi_0(t)\right|^2 dt + \int_{Hh}^{\infty} \left|{}^{m}_{[s]}\psi_0(t)\right|^2 dt \\
&\leq \int_{-\infty}^{-Hh} \left|{}^{m}U({}^{m}u)^{|t|/h}\right|^2 dt + \int_{Hh}^{\infty} \left|{}^{m}U({}^{m}u)^{|t|/h}\right|^2 dt \\
&= \int_{-\infty}^{-Hh} {}^{m}U^2({}^{m}u)^{-2t/h} dt + \int_{Hh}^{\infty} {}^{m}U^2({}^{m}u)^{2t/h} dt \\
&= \frac{-h({}^{m}u)^2}{\log {}^{m}u}({}^{m}u)^{2H}. \qquad (5.50)
\end{aligned}
$$

By substituting eq.(5.48), eq.(5.49) and eq.(5.50) for eq.(5.47) and using Proposition 8, we have

$$
\begin{aligned}
\| \tilde{s} - s \|_{L_2}^2 &= \| \hat{\boldsymbol{v}} - \boldsymbol{v} \|_{\ell_2}^2 \| {}^{m}_{[s]}\tilde{\psi}_0 \|_{L_2}^2 + \| \boldsymbol{v} \|_{\ell_2}^2 \| {}^{m}_{[s]}\tilde{\psi}_0 - {}^{m}_{[s]}\psi_0 \|_{L_2}^2 \\
&\leq \frac{2({}^{m}W)^2({}^{m}w)^2}{1-({}^{m}w)^2}({}^{m}w)^{2H} \| x \|_{L_2}^2 \frac{h({}^{m}U)^2}{\log {}^{m}u}\left\{({}^{m}u)^{2H} - 1\right\} \\
&\quad + \| x \|_{L_2}^2 \frac{({}^{m}U)^2}{1-({}^{m}u)^2}\left\{({}^{m}u)^2 + 1\right\}\frac{-h({}^{m}u)^2}{\log {}^{m}u}({}^{m}u)^{2H},
\end{aligned}
$$

and the upper bound of approximation error becomes

$$
\begin{aligned}
\left(\frac{\| \tilde{s} - s \|_{L_2}}{\| x \|_{L_2}}\right)^2 &\leq \frac{2({}^{m}W)^2({}^{m}w)^2}{1-({}^{m}w)^2}({}^{m}w)^{2H}\frac{h({}^{m}U)^2}{\log {}^{m}u}\left\{({}^{m}u)^{2H} - 1\right\} \\
&\quad + \frac{({}^{m}U)^2}{1-({}^{m}u)^2}\left\{({}^{m}u)^2 + 1\right\}\frac{-h({}^{m}u)^2}{\log {}^{m}u}({}^{m}u)^{2H} \\
&= \frac{2h({}^{m}W{}^{m}U{}^{m}w)^2}{(1-{}^{m}w^2)\log {}^{m}u}({}^{m}w{}^{m}u)^{2H} \\
&\quad - \frac{2h({}^{m}W{}^{m}U{}^{m}w)^2}{(1-{}^{m}w^2)\log {}^{m}u}({}^{m}w)^{2H} \\
&\quad - \frac{h{}^{m}U^4({}^{m}u^2+1)}{(1-{}^{m}u^2)\log {}^{m}u}({}^{m}u)^{2H}.
\end{aligned}
$$

■

From the theorem, the suitable truncation length H is determined by eq.(5.46) when the tolerable approximation error $\| \tilde{s} - s \| / \| x \|$ is given. From eq.(5.46), the upper

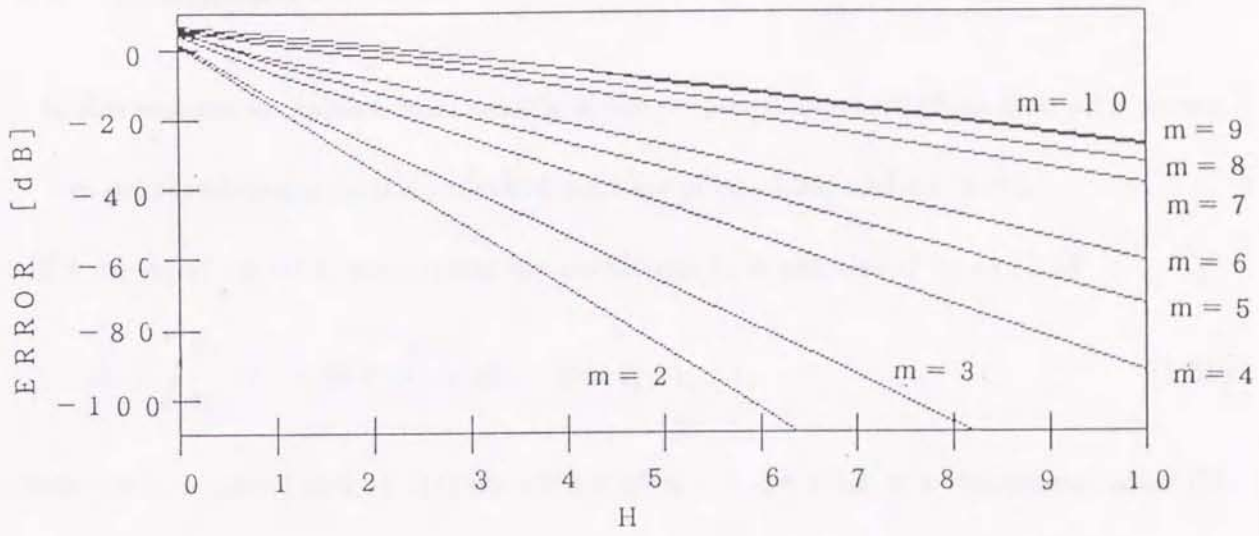

Figure 5.3: Rélation between truncation width (H) and upper bound of error.

bound of the approximation error caused by the truncation of the sampling function and its biorthonormal function attenuates exponentially according to H.

Figure 5.3 shows the relation between H and the upper bound of error from eq.(5.46). Considering the frequently used cases of $m = 3$ and $m = 4$, it is enough to truncate within $H = 5$ and $H = 7$, respectively, to keep the truncation error within -60dB. From these cases, there is no need for the truncation length to be long.

In this subsection, the relation between approximation error and the truncation length was estimated by using the upper bounds. By using the relation, the suitable truncation length for given tolerable error can be determined.

In this section, the real-time spline approximation method was characterized.

5.5 Examples

In this section, an application example of the proposed approximation method is shown.

The proposed approximation method consists of eq.(5.28) and eq.(5.29).

For an input signal x, approximation coefficient $\tilde{v}_k$ is calculated by eq.(5.28

$$\tilde{v}_k = \int_{-Hh}^{Hh} x(\tau + kh)\overline{{}^{m}_{[s^*]}\tilde{\psi}_0(\tau)}d\tau, \quad k = 0, \pm 1, \pm 2, \cdots. \tag{5.51}$$

Since the $\tilde{v}_k$ is calculated by $x(t)$ on $-Hh + kh \leq t \leq Hh + kh$, it is determined after Hh from $t_k = kh$.

The output $\tilde{s}(t)$ at t is calculated by eq.(5.29)

$$\tilde{s}(t) = \sum_{k=-\lfloor t/h+H \rfloor}^{\lceil t/h-H \rceil} \tilde{v}_k {}^{m}_{[s]}\tilde{\psi}_0(t - kh). \tag{5.52}$$

Since the $\tilde{s}(t)$ at t is calculated by $\{\tilde{v}_k\}_{k=\lceil t/h-H \rceil}^{\lfloor t/h+H \rfloor}$, it is determined after Hh from t.

Therefore, the approximation $\tilde{s}(t)$ of input signal $x(t)$ at t is determined after $2Hh$ from $x(t)$.

Figure 5.4 shows an example: (a) input signal $x(t) = 1 + 0.5\sin(\frac{2\pi t}{36h}) + 0.4\cos(\frac{8\pi t}{36h}) + 0.1\cos(\frac{20\pi t}{36h})$, (b) approximation result $\tilde{s}(t)$ by the proposed method, (c) approximation result $s(t)$ by the conventional method using the B-spline functions.

The approximation result $s(t)$ by the conventional method using the B-spline functions was calculated after the input signal was observed whole the finite observation interval. In the proposed method, in order that the approximation error is less than -60dB on $m = 3$, the truncation length becomes $H = 5$. The integral was evaluated discretely on t

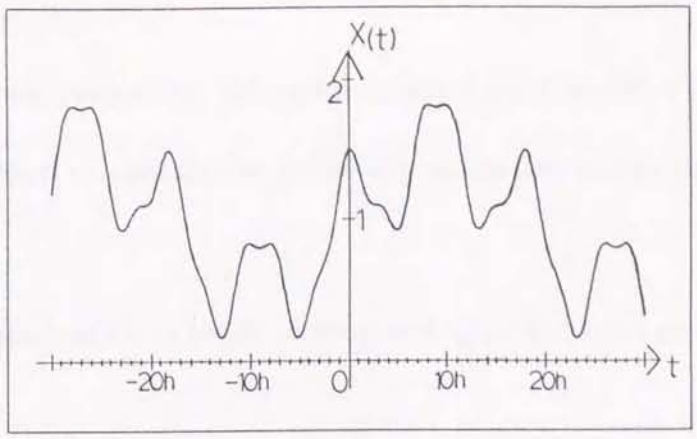

(a)Original signal x(t) to be approximated

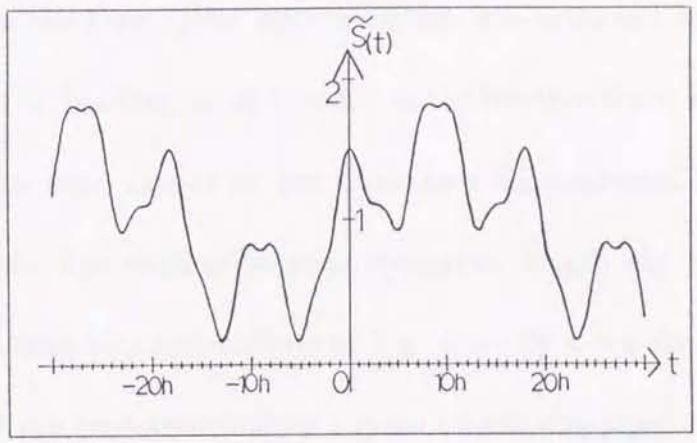

(b)Approximation of x(t) by this method

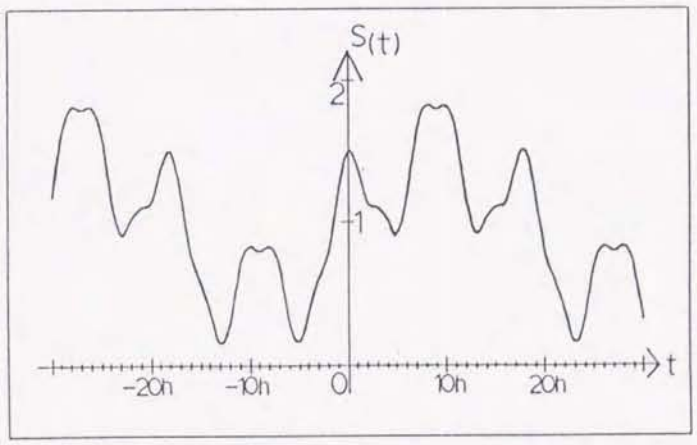

(c)Approximation of x(t) by the method with B-spline functions

Figure 5.4: Example of approximation.

with $h/16$. By numerical evaluation, the approximation error is -86.4 dB. It was shown that the proposed method can obtain the spline approximation within the given tolerable error.

In this section, an application example of proposed approximation method was shown.

5.6 Summary

In this chapter, the real-time spline approximation was proposed by truncating the sampling function and its biorthonormal function in the biorthonormal expansion formulas. The approximation error caused by the truncation was evaluated for the proposed approximation method. The relation between truncation length and the upper bound of the approximation error was summarized in Fig. 5.3. By using the figure, the suitable truncation length can be determined for a given tolerable approximation error. This makes the proposed method practical. One of the further researches is the application to data compression.

Part VI

FIR Filter Design Method using Spline Approximation

In Part VI, a design method of the linear phase FIR filter is proposed. The FIR filters take advantages that it can exactly implement linear phase filters and stable ones. The design methods of FIR filter are classified into three methods as follows: (i) windowing method, (ii) frequency sampling method and (iii) optimal filter design method. The Remez exchange method is one of the optimization method to approximate functions in the sense of equi-ripple error.

In Chapter 6, a design technique of the linear phase FIR filters using spline functions is presented. The filters are represented by C-spline functions. The method is based on Remez exchange method to approximate frequency characteristics in the sense of equi-ripple error.

In Chapter 7, computational complexity of polynomial interpolation for the Remez exchange method is evaluated. This approximation method is widely utilized for filter design techniques. It is found that the Newton's polynomial interpolation is two times faster than the conventional polynomial interpolation.

Chapter 6

Linear Phase FIR Filter Design Method Based on Weighted Equi-ripple Spline Approximation by Remez Exchange Method

6.1 Introduction

The FIR filters have advantages that they can implement linear phase characteristics exactly, and that they are always stable. On the other hand, the FIR filters have a defect that the dimension of the filter becomes large to have good frequency characteristics. For a given frequency characteristics, it is important to design FIR filters with smaller dimension than what the conventional design methods require.

In this chapter, a design method is proposed for the linear phase FIR filters based on equi-ripple spline approximation using the Remez exchange method. The impulse responses of the designed filters are represented by C-spline functions which are piecewise polynomials in the time domain and are non-rational functions in the frequency domain.

The frequency characteristics are approximated in the frequency domain in the sense of equi-ripple error criteria using Remez exchange method. Some design examples are shown. Based on the design examples, experimental relations among some parameters of filter are investigated.

The proposed design method can obtain the FIR filters with smaller dimension than what conventional design methods require. And the proposed method can obtain the FIR filters which cannot be obtained by the conventional design methods.

6.2 Preliminaries

This section prepares some formulas of C-spline functions to represent FIR filters.

The C-spline function is represented by linear combination of finite number of B-spline functions which have local support. Then, the C-spline function representing the FIR filter $s(t)$ is a time-limited real-valued function as follows:

$$s(t) = 0, \quad (|t| \geq T/2). \tag{6.1}$$

To design the linear phase FIR filters, the condition

$$s(t) = s(-t) \tag{6.2}$$

is used. Then, the linear phase FIR filter $s(t)$ of dimension n is uniquely represented as

$$s(t) = \begin{cases} \lambda_0 {}^m_{[b]}\psi_{(n-1)/2}(t) + \displaystyle\sum_{r=1}^{(n-1)/2} \lambda_r \left\{ {}^m_{[b]}\psi_{(n-1)/2-r}(t) + {}^m_{[b]}\psi_{(n-1)/2+r}(t) \right\}, \\ \qquad\qquad\qquad\qquad\qquad\qquad\qquad\qquad n \text{ is odd}, \\ \displaystyle\sum_{r=0}^{(n-2)/2} \lambda_r \left\{ {}^m_{[b]}\psi_{(n-2)/2-r}(t) + {}^m_{[b]}\psi_{n/2+r}(t) \right\}, \\ \qquad\qquad\qquad\qquad\qquad\qquad\qquad\qquad n \text{ is even}; \quad \lambda_r \in \boldsymbol{R}. \end{cases} \tag{6.3}$$

by using the B-spline functions, *i.e.* $\left\{ {}^{m}_{[b]}\psi_\ell(t) \right\}_{\ell=0}^{n-1}$

$$ {}^{m}_{[b]}\psi_\ell(t) = mh^{-m} \sum_{k=0}^{m} \frac{(-1)^k}{k!(m-k)!} (t - (\ell - (m+n-1)/2 + k)h)_+^{m-1}, \tag{6.4} $$

$$ \ell = 0, 1, 2, \cdots, n-1, $$

$$ m = 1, 2, 3, \cdots, $$

$$ h = T/(m+n-1), \tag{6.5} $$

$$ (t-a)_+^{m-1} = \begin{cases} (t-a)^{m-1}, & (t > a), \\ 0, & (t \leq a), \end{cases} \tag{6.6} $$

where $\boldsymbol{R}$ is a set of real numbers. The function $s(t)$ is a piecewise polynomial of degree $(m-1)$. The number m is called order.

The frequency characteristics of the linear phase FIR filter $s(t)$ is represented by the Fourier transform [124]

$$ \begin{aligned} S(f) &= \int_{-\infty}^{\infty} s(t) e^{j2\pi ft} dt \\ &= \left[\frac{\sin \pi fh}{\pi fh} \right]^m P(f), \end{aligned} \tag{6.7} $$

where $P(f)$ is a cosine polynomial

$$ P(f) = \begin{cases} \lambda_0 + 2 \sum_{r=1}^{(n-1)/2} \lambda_r \cos(2\pi rfh), & n \text{ is odd}, \\ 2 \sum_{r=0}^{(n-2)/2} \lambda_r \cos(\pi(2r+1)fh), & n \text{ is even}. \end{cases} \tag{6.8} $$

When dimension n and order m are given, the parameters determining $s(t)$ are coefficients $\{\lambda_r\}_{r=0}^{\lceil (n-1)/2 \rceil}$, where $\lceil x \rceil$ means the maximum integer number which is not grater than x.

In the next section, a design method is proposed to determine the parameters $\{\lambda_r\}_{r=0}^{\lceil (n-1)/2 \rceil}$.

6.3 Design Method

In this section, a design method of the linear phase FIR filters represented by C-spline function is discussed. In subsection 6.3.1, the approximation criteria is discussed. In subsection 6.3.2, a method to determine the parameters according to the criteria is proposed. Finally, in subsection 6.3.3, a design example is shown, and the feature of the proposed design method is discussed.

6.3.1 Discussion of design criteria

In this subsection, the approximation criteria is discussed.

We suppose that the target frequency characteristics are given as follows:

$$A(f),\ 0 \leq f \leq 1/2h. \tag{6.9}$$

To minimize the maximum errors, the weighted equi-ripple error criteria is adopted as an approximation criteria. Then, the design method should find an approximation $S(f)$ for $A(f)$ under the weighted equi-ripple error criteria.

From eq.(6.7) and eq.(6.8), $S(f)$ is a multiplication of even function $P(f)$ with period $1/h$ and $\left[\frac{\sin \pi fh}{\pi fh}\right]^m$. The frequency characteristics $S(f)$ in the interval $\{f|-\infty < f < \infty\}$ follows $S(f)$ in $\{f|0 \leq f \leq 1/2h\}$. Then, the frequency interval to be concerned with is limited into $\{f|0 \leq f \leq 1/2h\}$. The maximum frequency $1/2h$ can be increased by the dimension n for fixed T.

The weighted equi-ripple approximation $S(f)$ for $A(f)$ should satisfy

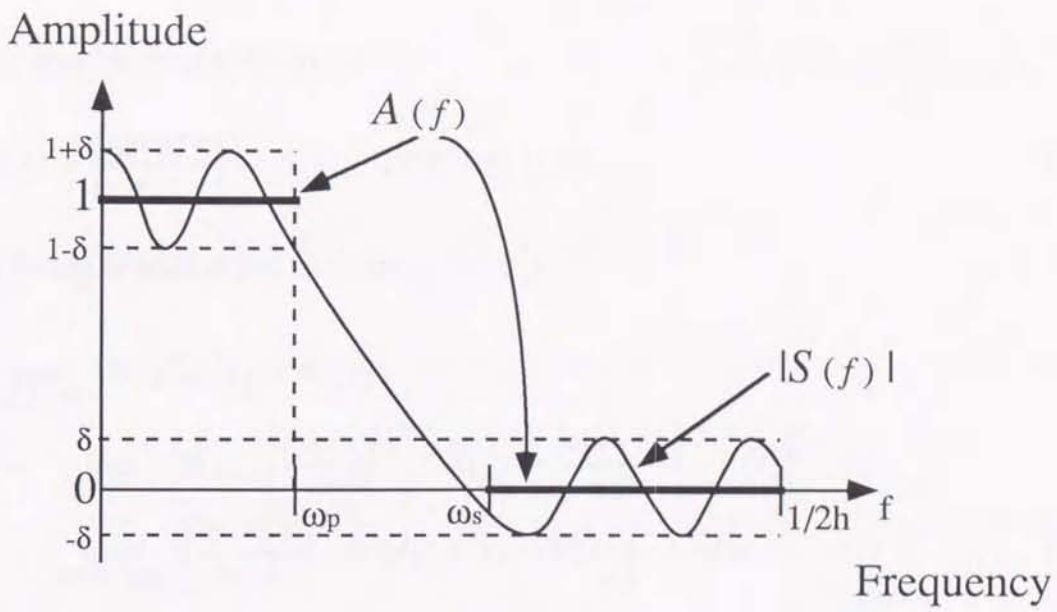

Figure 6.1: Relation between $A(f)$ and $S(f)$.

$$\max_{0 \le f \le 1/2h} |W(f)[A(f) - S(f)]| \rightarrow \min . \tag{6.10}$$

Figure 6.1 shows the relation between the target frequency characteristics $A(f)$ and its weighted equi-ripple approximation $S(f)$ with respect to the amplitude in the case of low-pass filter. Following the approximation criteria (6.10), parameters of linear phase FIR filters are determined in the next subsection.

6.3.2 Decision of parameters

In this subsection, a method to determine the parameters is proposed.

The equi-ripple approximation by cosine polynomial $P(f)$ is performed by the Remez exchange method proposed in [126, 128, 129]. The approximation $S(f)$ for $A(f)$ should be translated into the equi-ripple approximation problem by $P(f)$. Let $\tilde{A}(f)$ denote a

weighted amplitude characteristics

$$\tilde{A}(f) = \left[\frac{\sin \pi f h}{\pi f h}\right]^{-m} A(f), \quad (0 \le f \le 1/2h), \tag{6.11}$$

then eq.(6.10) is rearranged as follows:

$$\begin{aligned} &\max_{0\le f\le 1/2h} |W(f)[A(f) - S(f)]| \\ &= \max_{0\le f\le 1/2h} \left| W(f) \left[\left[\frac{\sin \pi f h}{\pi f h}\right]^{m} \tilde{A}(f) - \left[\frac{\sin \pi f h}{\pi f h}\right]^{m} P(f) \right] \right| \\ &= \max_{0\le f\le 1/2h} \left| \left[\frac{\sin \pi f h}{\pi f h}\right]^{m} W(f) \left[\tilde{A}(f) - P(f)\right] \right| \to \min . \end{aligned} \tag{6.12}$$

From eq.(6.12), the equi-ripple approximation $S(f)$ for $A(f)$ with weight $W(f)$ is translated into the equi-ripple approximation $P(f)$ for $\tilde{A}(f)$ with weight

$$\hat{W}(f) = \left[\frac{\sin \pi f h}{\pi f h}\right]^{m} W(f). \tag{6.13}$$

Here, $W(f)$ is an arbitrary positive-valued function, which can control the envelop of pass band and stop band. Following the above formulation, the function $P(f)$ is determined by the Remez exchange method.

The coefficients $\{\lambda_r\}_{r=0}^{\lceil (n-1)/2 \rceil}$ is determined by $P(f)$ as follows:

$$\lambda_r = \begin{cases} h \int_{-1/2h}^{1/2h} P(f) \cos(2\pi r f h) df, & n \text{ is odd}, \\ h \int_{-1/2h}^{1/2h} P(f) \cos(\pi (2r+1) f h) df, & n \text{ is even}. \end{cases} \tag{6.14}$$

Equation (6.14) is derived based on the fact that functions $\{\cos(2\pi r f h)\}_{r=0}^{(n-1)/2}$ in $[-1/2h, 1/2h]$ constitutes an orthogonal system, *i.e.*

$$2h \int_{-1/2h}^{1/2h} \cos(2\pi r f h) \cos(2\pi v f h) df = \begin{cases} 2, & (r = v = 0), \\ 1, & (r = v \text{ and } r \ne 0), \\ 0, & (r \ne v), \end{cases} \tag{6.15}$$

and functions $\{\cos(\pi(2r+1)fh)\}_{r=0}^{(n-2)/2}$ in $[-1/2h, 1/2h]$ constitutes orthogonal system, *i.e.*

$$2h\int_{-1/2h}^{1/2h}\cos(\pi(2r+1)fh)\cos(\pi(2v+1)fh)df = \begin{cases} 1, & (r=v), \\ 0, & (r\neq v). \end{cases} \tag{6.16}$$

From the above discussions, the coefficients $\{\lambda_r\}_{r=0}^{\lceil(n-1)/2\rceil}$ of the weighted equi-ripple approximation $S(f)$ for $A(f)$ is determined. The algorithm is shown in Fig.6.2.

In Fig.6.2, the input parameters are the target frequency characteristics described by the edge frequencies and amplitudes of pass-bands and stop-bands, weight $W(f)$, dimension n, and order m. And the output parameters are the coefficients $\{\lambda_r\}_{r=0}^{\lceil(n-1)/2\rceil}$. First, the weight $\hat{W}(f)$ is determined by eq.(6.13). Then, the approximation $S(f)$ for $A(f)$ is translated into the approximation $P(f)$ for $\tilde{A}(f)$. The cosine polynomial $P(f)$ is derived as the approximation for $\tilde{A}(f)$ by the Remez exchange method with weight $\hat{W}(f)$. The algorithm was shown in [126, 128, 129]. Finally, from the cosine polynomial $P(f)$, coefficients $\{\lambda_r\}_{r=0}^{\lceil(n-1)/2\rceil}$ is determined. By substituting coefficients $\{\lambda_r\}_{r=0}^{\lceil(n-1)/2\rceil}$ for eq.(6.3), the linear phase FIR filter $s(t)$ is determined.

6.3.3 Design examples and Discussions

In this subsection, an example designed by the proposed method is shown. The feature and effectiveness of the proposed design method are also discussed.

As a design example, a typical low-pass filter is designed. The specification of design example is in Table 6.1, and is shown in Fig. 6.3.

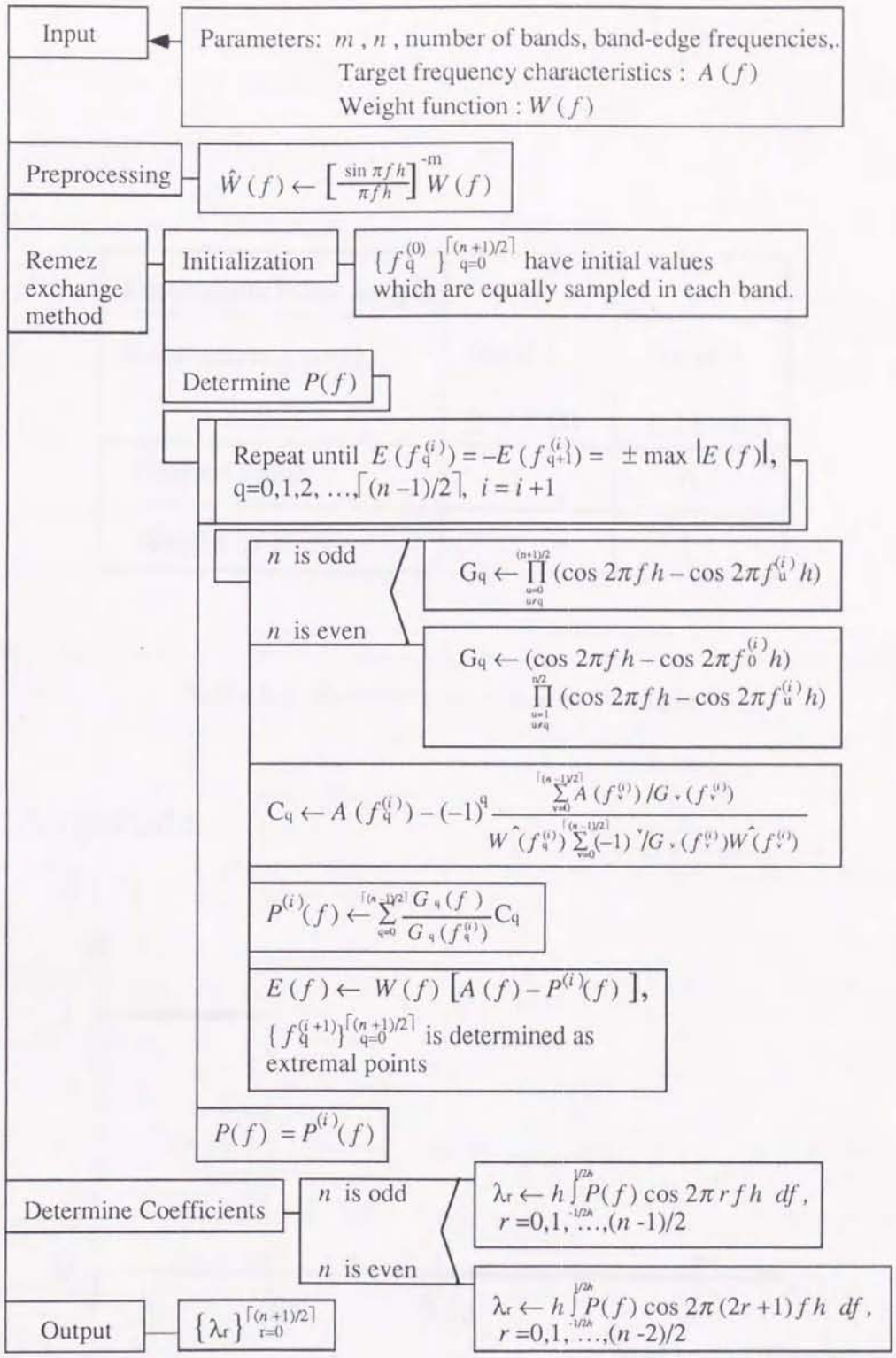

Figure 6.2: A flowchart of a method to determine $\{\lambda_r\}_{r=0}^{\lceil (n-1)/2 \rceil}$.

Dimension(Filter length)	24	
Band-edges (h=1)	Band 1 0 - 0.08	Band 2 0.16 - 0.5
Desired value	1	0
Weight of error	1	1

Table 6.1: Specification of design example.

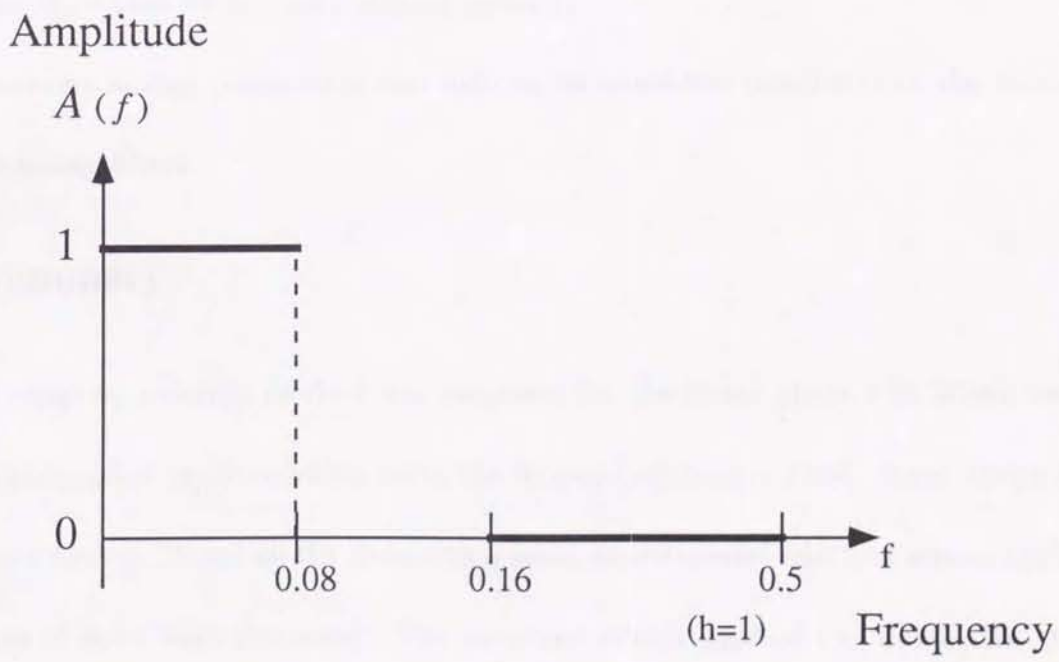

Figure 6.3: Amplitude characteristics of target filter.

Figure 6.4(a) shows an example designed by the proposed method, and Fig. 6.4(b) shows that by the conventional method[129]. From those figures, the filter in Fig. 6.4(a) has better attenuation in stop band than that in Fig. 6.4(b).

Figure 6.5 shows a relation between the deviation in each band and dimension. The deviation becomes small as the dimension becomes large. When the dimension is same, the deviations of the examples by the proposed method are smaller than that by the conventional method.

Figure 6.6 shows a relation between the deviation in each band and the transition band width. The deviation becomes small as the transition band width becomes wide. When the transition band width is same, the deviations of the examples by the proposed method are smaller than that by the conventional method.

The relations among parameters can help to estimate the possibility of the method before designing filters.

6.4 Summary

In this chapter, a design method was proposed for the linear phase FIR filters based on equi-ripple spline approximation using the Remez exchange method. Some design examples were shown. Based on the design examples, experimental relations among typical parameters of filter were discussed. The proposed design method can obtain the suitable FIR filters with smaller dimension than what conventional design methods require. And the proposed method can obtain the FIR filters which cannot be obtained by the

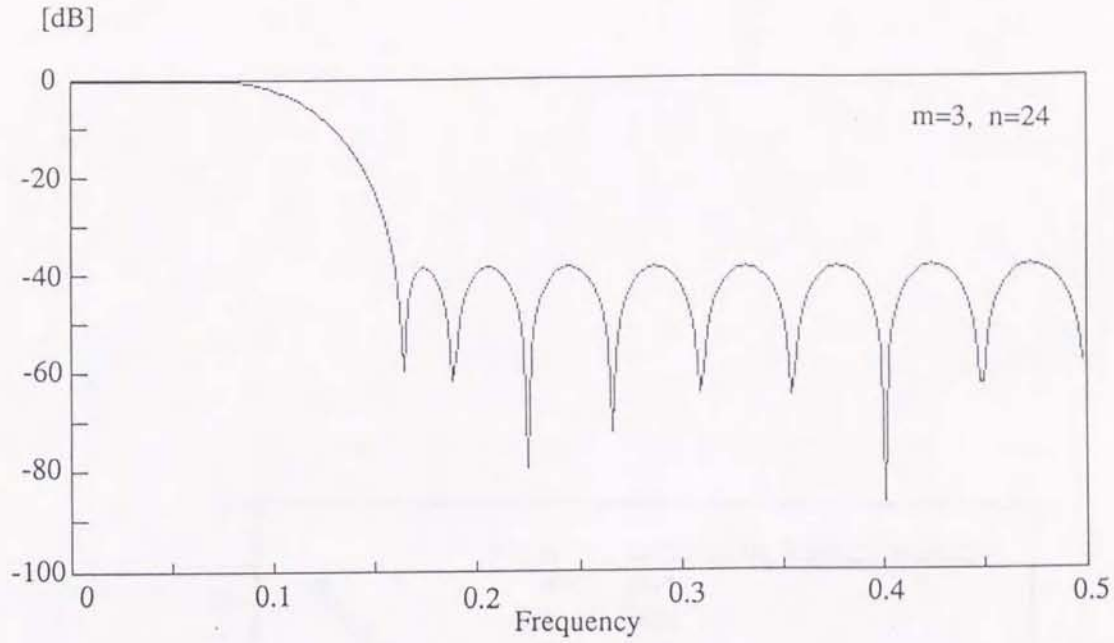

(a) Design example by the proposed method.

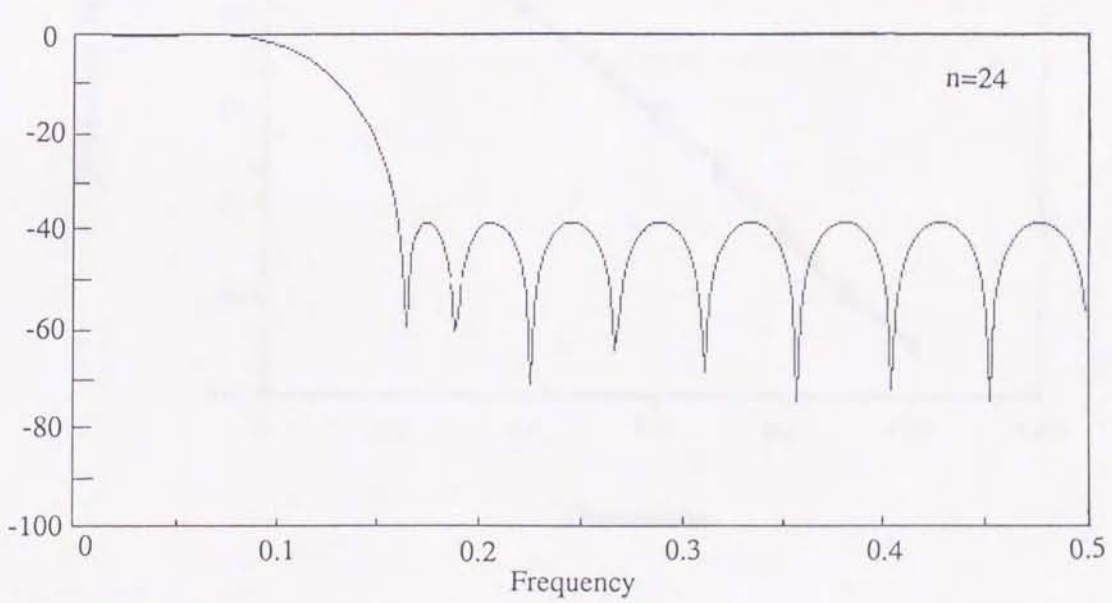

(b) Design example by the conventional method.

Figure 6.4: Design examples by the proposed method and the conventional method [129].

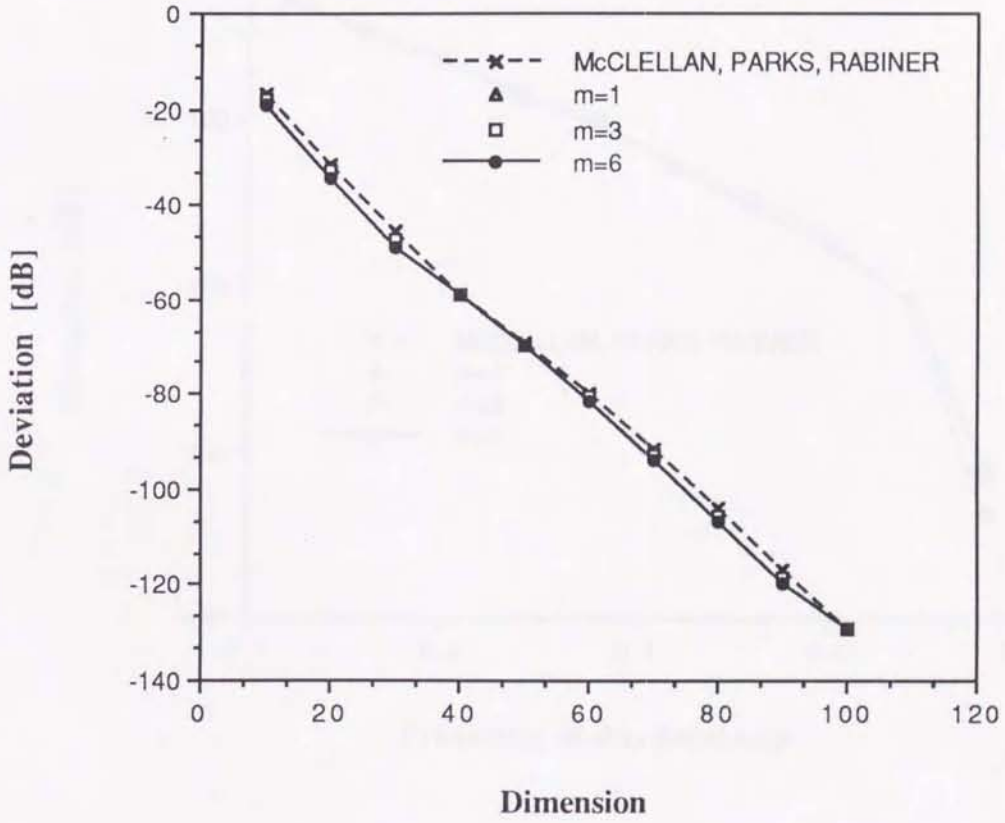

Figure 6.5: Relations between deviation and dimension.

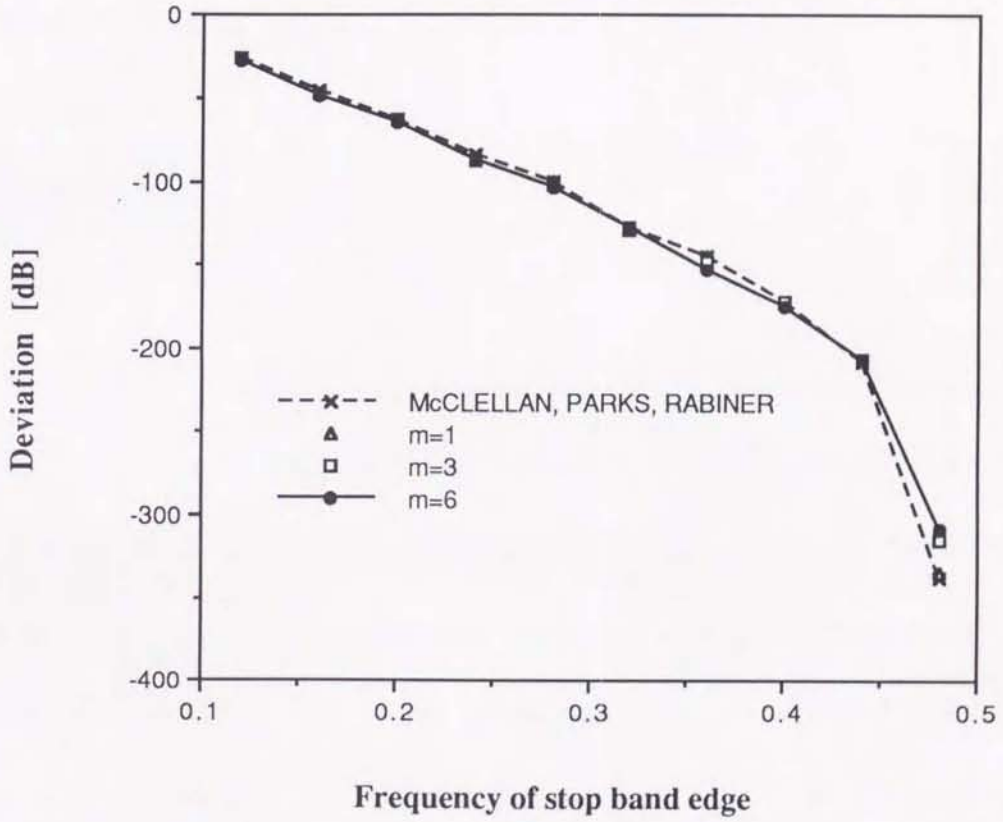

Figure 6.6: Relations between deviation and transition band width.

conventional design methods.

Chapter 7

Fast Polynomial Interpolation for Remez Exchange Method

7.1 Introduction

Abstract:

In this chapter, we shall analyze computational complexity of polynomial interpolations to find out the most suitable interpolation polynomial for the Remez exchange method.

The Remez exchange method[130] has been widely utilized for the design of linear phase Chebyshev digital filters. The Remez exchange method is necessary to have many iterations of polynomial interpolation for unequispaced data. The iterations are constructed by derivation of interpolating polynomials for many sets of interpolation data and evaluation of many values of each interpolating polynomial. This means that a computational complexity of the Remez exchange method depends on a computational complexity of the polynomial interpolation [130].

7.2 Preliminaries

The algorithms for obtaining an interpolation polynomial for unequispaced data are prepared in this section.

Let $g(x)$ denote the interpolation polynomial of degree $(N-1)$ for the data $\{(x_i, y_i)\}_{i=0}^{N-1}$; i.e. $g(x_i) = y_i, (i = 0, 1, 2, \cdots, N-1)$. The polynomial $g(x)$ is obtained from one of the following four methods.

Algorithm (A): Solving simultaneous equations

The interpolation polynomial $g(x)$ is assumed to be expressed with

$$g(x) = \sum_{j=0}^{N-1} a_j x^j,$$

where coefficients $\{a_j\}_{j=0}^{N-1}$ are the solution of

$$\sum_{j=0}^{N-1} a_j x_i^j = y_i, \quad i = 0, 1, 2, \cdots, N-1.$$

Algorithm (B): Lagrange's interpolation algorithm

The interpolation polynomial $g(x)$ is expressed with

$$g(x) = \sum_{i=0}^{N-1} y_i L_i(x),$$

where

$$L_i(x) = \prod_{\substack{j=0 \\ j \neq i}}^{N-1} \frac{x - x_j}{x_i - x_j}, \quad i = 0, 1, 2, \cdots, N-1.$$

Algorithm (C): Lagrange's interpolation algorithm in the barycentric form[132]

The interpolation polynomial $g(x)$ is expressed with

$$g(x) = \frac{\sum_{i=0}^{N-1} \frac{c_i}{x - x_i} y_i}{\sum_{i=0}^{N-1} \frac{c_i}{x - x_i}},$$

where

$$c_i = \prod_{\substack{j=0 \\ j \neq i}}^{N-1} \frac{1}{x_i - x_j}, \quad i = 0, 1, 2, \cdots, N-1.$$

Algorithm (D): Newton's interpolation algorithm

The interpolation polynomial $g(x)$ is expressed with

$$g(x) = f[x_0] + \sum_{i=1}^{N-1} f[x_0, x_1, \cdots, x_i] \left\{ \prod_{j=0}^{i-1} (x - x_j) \right\},$$

where $f[\cdot]$ is defined by the following recursive equation

$$f[x_i] = y_i$$

$$f[x_0, x_1, \cdots, x_k, x] = \frac{f[x_1, x_2, \cdots, x_k, x] - f[x_0, x_1, \cdots, x_k]}{x - x_0}.$$

7.3 Computational complexity

Figure 7.1 illustrates the flow charts of the above algorithms for obtaining K values of the interpolating polynomial of degree $(N-1)$ from N data. Figure 7.2 illustrates boxes used in Fig.7.1. Figure 7.2(a) means that the variable x gets the value a. Figure 7.2(b) means that the shaded branch A is iterated N times while i increases from 1 to N by 1. Figure 7.2(c) means that the shaded branch B is executed if and only if the condition is true. The other algorithms are evaluated in the same way. In the algorithm (A), Gaussian elimination is employed in solving simultaneous equations. In the algorithm (D), An

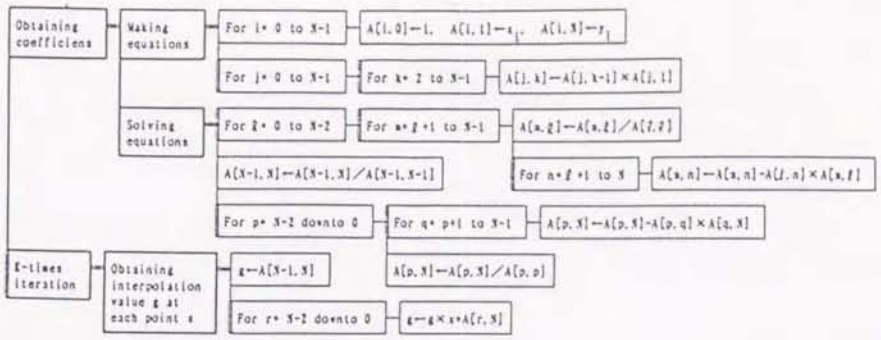

(a)Solving simultaneous equations:Algorithm(A)

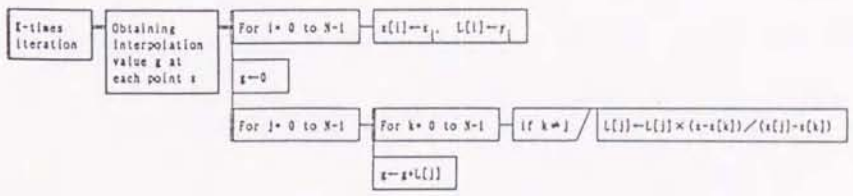

(b)Lagrange's interpolation:Algorithm(B)

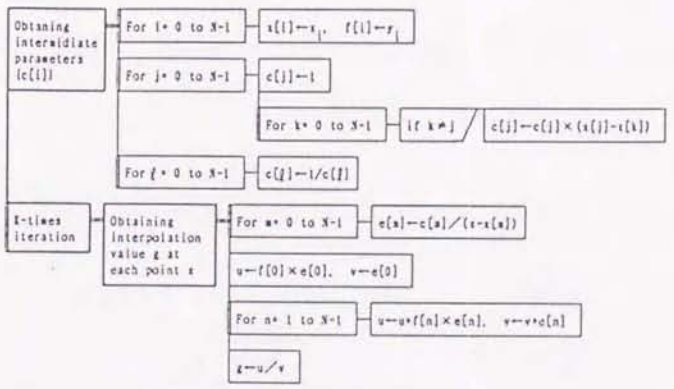

(c)Lagrange's interpolation in the barycentric form: Algorithm(C)

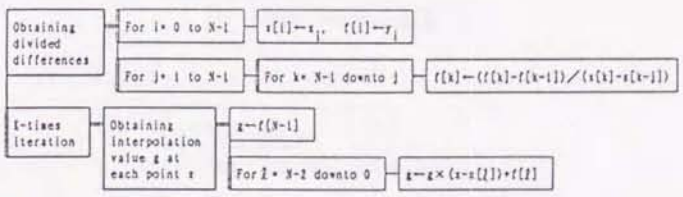

(d)Newton's interpolation:Algorithm(D)

Figure 7.1: Flow charts of interpolation algorithm.

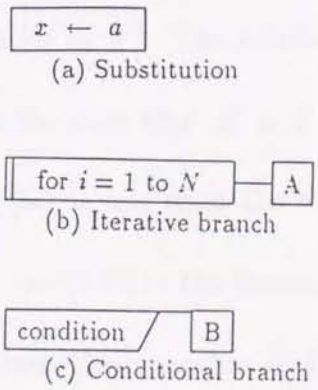

(a) Substitution

(b) Iterative branch

(c) Conditional branch

Figure 7.2: Boxes used in Fig.1.

efficient algorithm[131] for calculating the divided differences is employed. Computational complexity is evaluated in the flow chart. At first, the number of operations in each box is evaluated. If a box is in an iterative branch, the number of operations in the box is multiplied by the number of iterations. If a box is in a conditional branch, the number of operations in the box is counted on the condition. The number of the whole operations is obtained by calculating the numbers for all the boxes. Recent computers are very fast in register-register arithmetic operations so that memory-register transfer takes a considerable part of the whole computation. Since reference to arrays requires memory-register transfer, number of references to array elements shall be evaluated as well as arithmetic operations. The computational complexity of each flow chart is listed in Table 7.1.

In Table 7.1, we can see computational complexity with N and K. The number of operations for the algorithm (A) is less than other algorithms in the case that K is very much larger than N as in the order of N^2. The number of operations for algorithm (B) is less than other algorithms in the case that K is a very small number. The number of operations for the algorithm (C) is less than the algorithm (A) for $K \geq 2$. That is why the algorithm (C) has been used[130] in the Remez exchange method which needs to examine many interpolation values (their number K is almost proportional to N). But the algorithm (D) is faster than the algorithm (C) in the case that $K \geq N$. Besides, the number of divisions with the algorithm (D) is constant for any K. Therefore, If we employ the algorithm (D) for interpolation, the computation speed in the Remez exchange

	Number of operations to obtain K interpolation values			
	Add/Subtract	Multiplication	Division	Reference to array
Algorithm (A)	$(N^3-4N)/3+1$ $+K(N-1)$	$(N^3+3N^2-10N)/3$ $+K(N-1)$	N^2-N+1	$(8N^3+27N^2-56N+39)/6$ $+K(N-1)$
Algorithm (B)	$K(2N^2-N)$	$K(N^2-N)$	$K(N^2-N)$	$K(5N^2-2N)$
Algorithm (C)	N^2-N $+K(3N-2)$	N^2-N $+KN$	N $+K(N+1)$	$4N^2+N$ $+K(6N)$
Algorithm (D)	N^2-N $+K(2N-2)$	$K(N-1)$	$(N^2-N)/2$	$(5N^2-N)/2$ $+K(2N-1)$

Table 7.1: Computational complexity of algorithms for polynomial interpolation.

method becomes faster.

7.4 Summary

The Newton's algorithm for polynomial interpolation works faster in the Remez exchange method than the Lagrange's one in the barycentric form.

Part VII

Conclusions

The fluency functions, which were proposed and referred to by the wisdom systems laboratory[113], provide a powerful procedure for flexible signal processing and analysis of complex systems. Application of the fluency functions has already been attempted to digital signal processing [119, 120, 121, 124]. In a fluency signal space representing a continuous-time signal space with a fluency function, a signal is expressed in the form of linear combination of the sampling basis with the sample values of the signal as the coefficients, the sequence of which corresponds to a signal in a discrete-time signal space. The sampling theorem describes the mutual transformation method between the fluency signal space and the discrete-time signal space. In this study, the spline functions, which are very useful for interpolation and approximation of signals, were analyzed for fundamental characterization of the fluency functions in the spline signal spaces. The sampling theorem for the spline signal spaces was completed in the form of biorthonormal expansion formula and the reproducing kernel was derived for the spaces. The spline functions as fluency function were applied to the real-time approximation method and the FIR filter design method.

In part II, the sampling theorem was accomplished for the spline signal space with periodic quadratic functions. The sampling basis for this signal space was previously described [112]. The biorthonormal basis for the sampling basis was derived in this study, leading to the completion of the sampling theorem in the form of biorthonormal expansion formula. This expansion formula approximates signals in the sense of the least square error with periodic quadratic spline functions on the finite closed domain with periodicity. The

sampling theorem was extended to arbitrary degrees, making it possible to correspond the spline signal spaces respectively to the signal spaces from stepwise functions to the Fourier's band-limited functions. The periodic signal spaces are thus derived for every degree. This correspondence will furnish to a classification method of periodic signals based on their differentiability.

In Part III, the sampling theorem was completed for non-periodic spline functions of arbitrary degrees. For the sampling basis[114] in non-periodic signal spaces, the biorthonormal basis was derived in the similar manner for periodic signal spaces. The input signals on the infinite open domain can thus be approximated with non-periodic spline functions in the sense of the least square error. The correspondence of non-periodic signal spaces to the spline signal spaces of appropriate degrees will provide a classification method of non-periodic signals based on their differentiability. The functions consisting of the biorthonormal basis enable to obtain the sample values of the spline signals at every sampling point, indicating their property similar to a delta function.

In part IV, the reproducing kernels to obtain the sample values of the spline signals at every point in the domain were derived for the non-periodic spline signal spaces. The reproducing kernel performs like a delta function with some differentiability in the spline signal spaces. The of a reproducing kernel as a delta function makes numerical solution possible for some kinds of differential equations. The uniform convergence of spline approximation followed from a property of the kernel, suggesting the effectiveness of the real-time approximation based on the truncation of the support of the functions consisting

of the sampling basis and its biorthonormal basis.

In parts V and VI, a real-time approximation method was proposed as one of the implementation components for signal processing with the fluency functions, and the sampling theorem derived was applied for the FIR filter design method by which the FIR filters better than conventional ones were designed. On a real-time approximation method, the error in implementation of the biorthonormal expansion formulas was analyzed for this method. The hardware equipments will be feasible based on this method and error analysis. Next, on the FIR filter design method, the Remez exchange method, which is widely utilized for the filter design method, was also numerically analyzed. More efficient approximation methods like relaxation method would be useful for the design method.

This study aims to establish some key steps in the theoretical and experimental investigation of digital signal processing based on the fluency functions. It is demonstrated from this study and the works of the wisdom systems laboratory that the fluency functions are applicable to more complex systems. The author hopes to continue the work on this direction in the near future.

Acknowledgments

The author wishes to express his gratitude to the persons who have directed his research and who have gave him valuable comments, advice, and hospitality. His special gratitude is due to Professor Kazuo TORAICHI Ph.D. of the Institute of Information Sciences and Electronics at University of Tsukuba for his perceptive direction, kindness, sincere supervision and encouragement. He owes Professor Naoto SAKAMOTO Ph.D. of the Institute particular thanks for the valuable comments and advice in the mathematical aspects and encouragement. He is also most obliged to Professor Syuichi ITAHASHI Ph.D. of the Institute for his guidance and valuable advice. To Professor Yoshihiko EBIHARA Ph.D. of the Institute he also owes a debt for his valuable comments and advice. He is also very grateful to Professor Yukio ISHIBASHI Ph.D. of the Institute for his valuable comments and advice.

He is also grateful very indebted to the following: Assistant Professor Naohisa OTSUKA Ph.D. in the Institute for the valuable advice; Associate Professor Masaru KAMADA Ph.D. in the Swiss Federal Institute of Technology Zurich for valuable comments and advice concerning dual sampling base window function; Professor Taizo IIJIMA Ph.D. of the Japan Advanced Institute of Science and Technology for his valuable comments and encouragement; Professor Rokuya ISHII Ph.D of the Yokohama National University for his advice, especially in the research of window functions. Finally, the author would like to express sincere thanks to all the former and present members of Wisdom Systems Laboratory at the Institute of Information Sciences and Electronics for the many helpful

discussions and kindnesses.

The Author's Work

[1] K. Toraichi and M. Iwaki: "Periodic sampling basis and its biorthonormal basis for the signal space of piecewise polynomials," *Trans. IEICE Japan*, Vol.J75-A, No.6, pp.1003-1012 (1992), (in Japanese).

[2] K. Toraichi, M. Iwaki, M. Kamada, R. Ishii and R. Kawamoto: "A design method of windows by spline functions based on weighted equiripple approximation," *Trans. IEE Japan*, Vol.113-C, No.4, pp.254-260 (1993), (in Japanese).

[3] K. Toraichi, R. Kawamoto, M. Kamada, M. Iwaki and R. Ishii: "Method of designing windows based on spline approximation," *International Journal of Systems Science*, Vol.24, No.8, pp.1539-1549 (1993).

[4] M. Iwaki, R. Ishii and K. Toraichi: "Polynomial interpolation for Remez exchange method," *Electronics Letters*, Vol.28, No.20, pp.1900-1902 (1992).

[5] K. Toraichi, M. Iwaki and M. Kamada: "Biorthonormal expansion in signal spaces composed of spline functions," *Proceedings of IEEE International Conference on Acoustics, Speech, and Signal Processing*, Vol.2, pp.1119-1122 (1989).

[6] K. Toraichi, S. Ishiuchi and M. Iwaki: "A Method of improving image quality for medical video hardcopy," *Proceedings of IEEE International Conference on Acoustics, Speech, and Signal Processing*, Vol.3, pp.1500-1503 (1989).

[7] M. Iwaki and K. Toraichi: "On pseudo high vision system using time-varying two variate splines," *Proceedings of the 11th International Symposium on Biotelemetry*, pp.263-267 (1990).

[8] N. Nakamura, K. Toraichi, M. Kamada and M. Iwaki: "Contribution of ultrasound to tone quality," *Proceedings of International Symposium on Musical Acoustics*, pp.137-140 (1992).

[9] M. Iwaki, K. Toraichi and R. Ishii: "A fast polynomial interpolation for Remez exchange method," *Proceedings of IEEE Pacific Rim Conference on Computers, Communications, and Signal Processing*, Vol.2, pp.411-414 (1993).

[10] B. Sridadi, K. Toraichi, M. Iwaki and H. Inaba: "A series of discrete-time models of a continuous-time system based on fluency-signal approximation," *Proceedings of IEEE Pacific Rim Conference on Computers, Communications, and Signal Processing*, Vol.2, pp.493-496 (1993).

[11] K. Toraichi, M. Kamada, M. Iwaki and R. Mori: "Derivation of dual sampling bases for spline functions", *Paper of Tech. Group*, PRU88-22, (1988).

[12] M. Iwaki and K. Toraichi: "Sampling theorem for spline signal space of arbitrary degree," *IEICE Trans. Fundamentals*, (in press).

[13] K. Toraichi, M. Iwaki, R. E. Kalman and M. Kamada: "Biorthonormal functions for cardinal Lagrange splines," (submitted to *Numerische Mathematik*).

The Other References

[101] E. T. Whittaker: "On the functions which are represented by the expansions of interpolation theory," *Proc. Royal Soc.* Edinbergh, Vol.35, pp.181-194 (1915).

[102] I. Someya: "Wave transmission," Syukyou-Sya (1949), (in Japanese).

[103] C. E. Shannon: "Communication in the presence of noise," *Proc. IRE*, Vol.37, pp.10-21 (1949).

[104] Goldman, S., "Information Theory," Prentice-Hall (1953).

[105] I. J. Schoenberg: "Contribution to the problem of approximation of equidistant data by analytic functions," *Quart. Appl. Math.*, Vol.4, Part A, pp.45-99; Part B, pp.112-141 (1946).

[106] H.B. Curry and I.J. Schoenberg: "On polya frequency functions IV. The fundamental spline functions and their limits," *J. d'Analyse Math.*, Vol.17, pp.71-107 (1966).

[107] C. de Boor and R. E. Lynch: "On splines and their minimum properties," *J. Math. Mech.*, Vol.15, pp.953-969 (1966).

[108] T. N. E. Greville: "Spline functions and applications," MRC Orientation Lecture Series, University of Wisconsin, Madison, Wisconsin, (1971).

[109] I. J. Schoenberg: "Cardinal spline interpolation," SIAM, Philadelphia, (1973).

[110] C. de Boor: "A practical guide to splines," Springer-Verlag, (1978).

[111] K. Toraichi, H. Ogawa and A. Igarashi: "A note on several orthogonal bases for digital signal processing," *Trans. IECE Japan*, Vol.J60-A, No.2, pp.139-146 (1977), (in Japanese).

[112] K. Toraichi, M. Kamada and R. Mori: "Properties of interpolation by periodic spline functions of degree 2," *Trans. IEE Japan*, Vol.E106, No.11/12, pp.183-190 (1986).

[113] M. Kamada, K. Toraichi and R. Mori: "Periodic spline orthonormal bases," *J. Approx. Theory*, Vol.55, pp.27-38 (1988).

[114] M. Kamada, K. Toraichi and R. Mori: "Sampling bases for the signal spaces composed of spline functions," *Trans. IEICE Japan*, Vol.J71-A, No.3, pp.875-881 (1988), (in Japanese).

[115] K. Toraichi and M. Kamada: "Characterization of periodic spline functions in comparison with Fourier series," *Trans. IEICE Japan*, Vol.E72, No.6, pp.702-709 (1989).

[116] K. Toraichi and M. Kamada: "A note on connection between spline signal spaces and band-limited signal spaces," *Trans. IEICE Japan*, Vol.J73-A, No.9, pp.1501-1508 (1990), (in Japanese).

[117] M. Kamada, K. Toraichi and Y. Ikebe: "A note on error estimation for spline interpolation with sampling bases," *Trans. IEICE Japan*, Vol.J73-A, No.8, pp.1415-1422 (1990), (in Japanese).

[118] K. Toraichi: "Biorthonormal expansion in the signal space composed of periodic quadratic spline functions," *Trans. IEICE Japan*, Vol.J73-A, No.11, pp.1815-1822 (1990), (in Japanese).

[119] K.Toraichi, I. Sekita and R. Mori: "On automatic compression of fonts of high quality characters," *IEICE Japan*, Vol.J70-D, No.6, pp.1169-1172 (1987), (in Japanese).

[120] K. Toraichi, M. Kamada, S. Itahashi, and R. Mori: "Window functions obtained by convolution integrals of rectangular windows," *Int. J. Systems Sci.*, Vol.19, No.12, pp.2491-2506 (1988).

[121] K. Toraichi, T. Horiuchi, F. Nagasaki and Y. Matsumoto: "A method of compressing data volume of left ventricular cineangiograms for their digital database system," *Trans. IEE Japan*, Vol.110-C, No.8, pp.490-499 (1990), (in Japanese).

[122] Y. Isomichi: "Generalized sampling theorem," *Trans. IECE Japan*, Vol.J52-C, No.2, pp.79-85 (1969), (in Japanese).

[123] T. Iijima: "Information analysis," Asakura-Syoten, (1988), (in Japanese).

[124] K. Toraichi, R. Kawamoto, M. Kamada and R. Ishii: "A design method of window functions by spline approximation," *Trans. IEICE Japan*, Vol.J73-A, No.11, pp.1808-1814 (1990), (in Japanese).

[125] H. Imai: "Digital signal processing," Sangyo-Syuppan, (1980), (in Japanese).

[126] M. Maeda and R. Ishii: "A method of designing a window function with an arbitraly sidelobe decrease characteristic," *Trans. IEICE Japan*, Vol.J72-A, No.9, pp.1400-1407 (1989),

[127] F. J. Harris: "On the use of windows for harmonic analysis with the discrete Fourier transform," *Proc. IEEE*, Vol.66, No.1, pp.51-83 (1978).

[128] E. Ya. Remez: "General communication methods of Chebyshev approximation," Kiev, USSR: Atomic Energy Translation 4491, pp.1-85 (1957).

[129] L. R. Rabiner, J. H. McClellan and T. W. Parks: "FIR digital filter design techniques using weighted Chebyshev approximation," *Proc. IEEE*, Vol.63, pp.595-610 (1975).

[130] T. W. Parks and J. H. McClellan: "Chebyshev approximation for nonrecursive digital filters with linear phase," *IEEE Trans. Circuit Theory*, Vol.CT-19, No.2, pp.189-194 (1972).

[131] S. D. Conte and C. de Boor: "Elementary numerical analysis: an algorithmic approach," , 2nd ed., McGrow-Hill, New York, (1972).

[132] W. J. Taylor: "Method of Lagrangean curvilinear interpolation," *J. Research Nat'l. Bur., Standards*, Vol.35, pp.151-155 (1945).

[133] N. I. Akhiezer: "Theory of approximation," New York, Unger, (1956).

[134] R. B. Blackman, and J. W. Tukey: "The measurement of power spectra," New York, Dover, (1958).

[135] F. R. Gantmacher: "The theory of matrices," Chelsea Publishing, New York, N. Y., (1960).

[136] E. Parzen: "Mathematical consideration in the estimation of spectra," *Theenometrics*, Vol.3, pp.167-190 (1961).

[137] J.F. Kaiser: "Digital filters," *Ch.7 in System Analysis by Digital Computer*, F.F. Kuo and J.F.Kaiser, Eds., Johon Wiley & Sons, New York (1966).

[138] A. V. Oppenheim and R. V. Shafer: "Digital signal processing," Prentice-Hall, (1975).

[139] S. Arimoto: "Digital processing of signals and images," Sangyou-Tosho, (1980), (in Japanese).

[140] H. Umegaki and M. Ohya: "Statistical entropy," Kyouritsu-Shuppan, (1983), (in Japanese).

[141] T. Ando: "Reproducing Kernel Spaces and Quadratic Inequality," Lecture note at Hokkaido University, (1987).

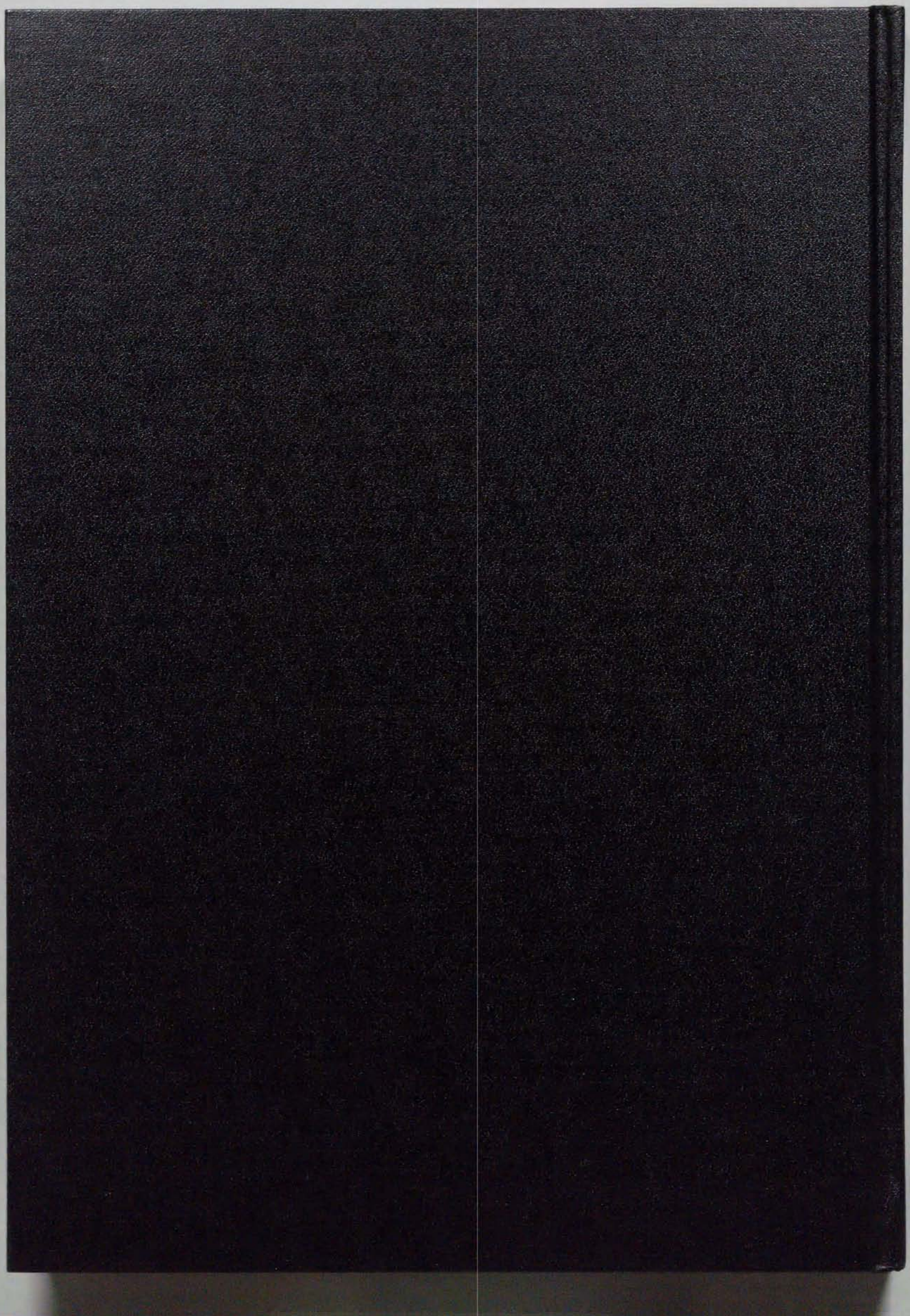

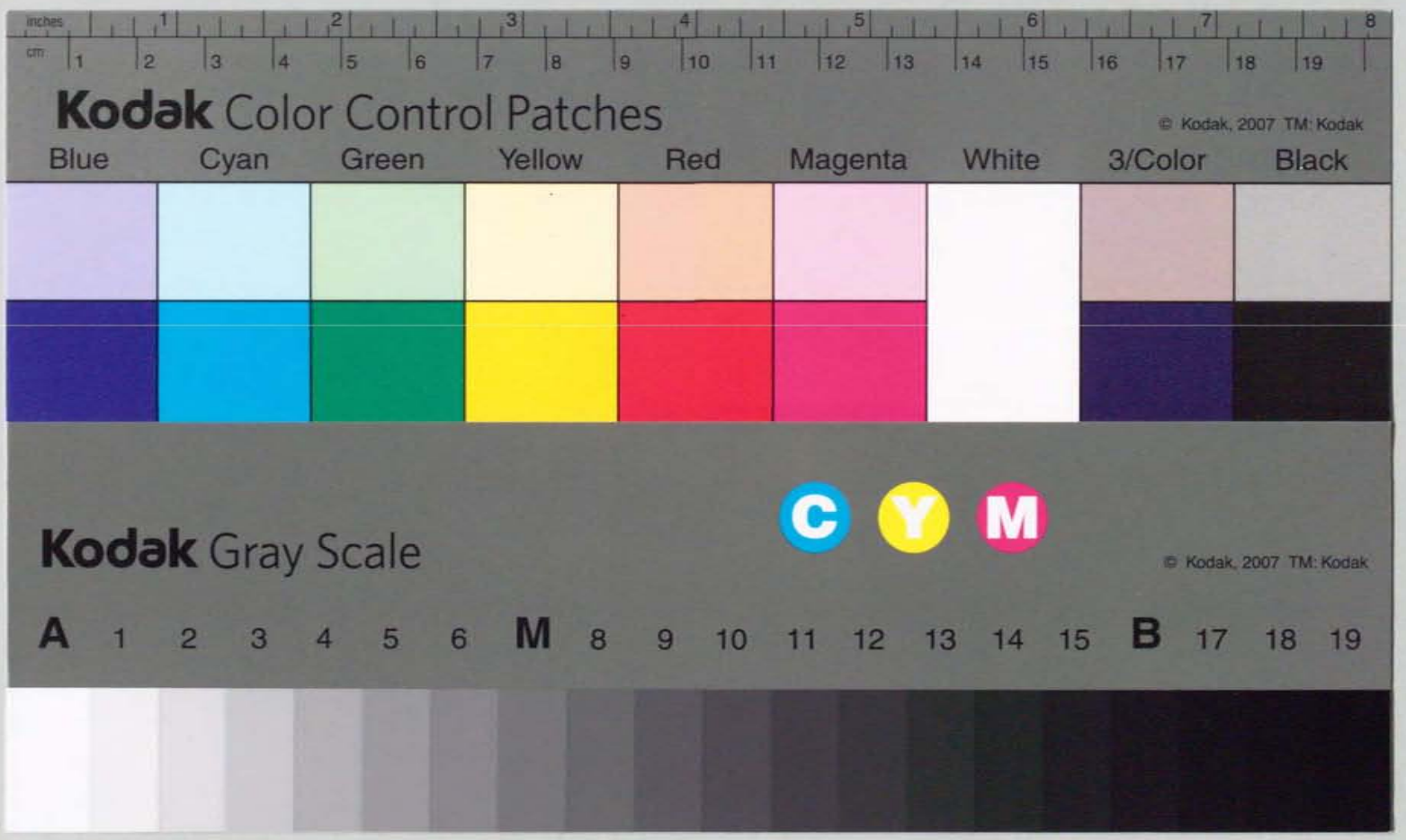
inches
cm
Kodak Color Control Patches
© Kodak, 2007 TM: Kodak
Blue
Cyan
Green
Yellow
Red
Magenta
White
3/Color
Black
Kodak Gray Scale
C
Y
M
© Kodak, 2007 TM: Kodak
A 1 2 3 4 5 6 M 8 9 10 11 12 13 14 15 B 17 18 19